CHEMICAL REVIEWS

Review

pubs.acs.org/CR

Photochemistry of Transition Metal Hydrides

Robin N. Perutz* and Barbara Procacci*

Department of Chemistry, University of York, York YO10 5DD, United Kingdom

ABSTRACT: Photochemical reactivity associated with metal−hydrogen bonds is widespread among metal hydride complexes and has played a critical part in opening up C−H bond activation. It has been exploited to design different types of photocatalytic reactions and to obtain NMR spectra of dilute solutions with a single pulse of an NMR spectrometer. Because photolysis can be performed on fast time scales and at low temperature, metal-hydride photochemistry has enabled determination of the molecular structure and rates of reaction of highly reactive intermediates. We identify five characteristic photoprocesses of metal monohydride complexes associated with the M−H bond, of which the most widespread are M−H homolysis and R−H reductive elimination. For metal dihydride complexes, the dominant photoprocess is reductive elimination of H_2. Dihydrogen complexes typically lose H_2 photochemically. The majority of photochemical reactions are likely to be dissociative, but hydride complexes may be designed with equilibrated excited states that undergo different photochemical reactions, including proton transfer or hydride transfer. The photochemical mechanisms of a few reactions have been analyzed by computational methods, including quantum dynamics. A section on specialist methods (time-resolved spectroscopy, matrix isolation, NMR, and computational methods) and a survey of transition metal hydride photochemistry organized by transition metal group complete the Review.

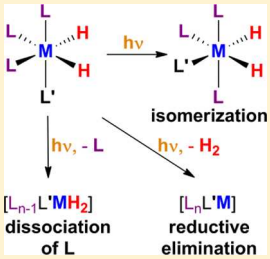

CONTENTS

Special Issue: Metal Hydrides

Received: March 30, 2016
Published: July 6, 2016

DOI: 10.1021/acs.chemrev.6b00204
Chem. Rev. 2016, 116, 8506−8544

1. INTRODUCTION

Molecular transition metal hydride complexes play roles in innumerable chemical reactions and catalytic processes. They illustrate the formation of simple covalent bonds with transition metals and vary in character from acidic to hydridic. Furthermore, a large proportion of metal hydride complexes exhibit photochemical reactivity associated with the M−H bond(s). Although many examples of photochemical reactivity have long been known and have opened up new fields of research, we are not aware of any wide-ranging reviews of this subject. It was first reported by two groups independently in 1972 that metal dihydride complexes may undergo photochemical reductive elimination of H_2. Camus, Cocevar, and Mestroni reported that cationic cobalt dihydrides $[Co(H)_2(NN)(PR_3)_2]^+$ (NN = 2,2′-bipyridine *or* 1,10-phenanthroline, R_3 = Bu_3, Pr_3, Et_3, Et_2Ph) exhibit photoinduced reductive elimination of H_2 under vacuum; the reaction is reversed thermally by restoring a hydrogen atmosphere.[1] In the same year, Giannotti and Green communicated that a tungsten dihydride, $Cp_2W(H)_2$ (Cp = η^5-C_5H_5), loses H_2 photochemically and undergoes insertion of the metal into the C−H bonds of benzene.[2] Since then, a variety of photoprocesses have been observed that involve the metal−hydrogen bond(s) directly: dissociation of hydrogen atoms, reductive elimination of H_2 or RH (R = alkyl, silyl, etc.), hydrogen transfer, isomerization, and electron transfer. In addition, there may be photoprocesses involving other ligands. It is now clear that the majority of transition metal *cis*-dihydride complexes undergo photodissociation of H_2, provided that the relevant absorption bands are not obscured by other transitions with much higher absorption coefficients. The photoprocesses for monohydride complexes often involve M−H homolysis, but new photoprocesses are still being discovered.

Photochemical reactions of metal dihydrides have played a critical role in opening up C−H bond activation of arenes and especially of alkanes.[3−5] The ability to initiate reactions photochemically provides a route to the synthesis of labile products because the photochemistry may be performed at low temperature. It also offers the opportunity to study fast reaction kinetics and reaction intermediates by time-resolved spectroscopy (especially laser flash photolysis) and by low-temperature matrix isolation. These techniques have all been applied to the C−H activation problem. Photochemistry is also a synthetic tool, sometimes with no alternative route, as in the synthesis of decamethylrhenocene by M−H homolysis.[6]

Most recently, photochemistry has been used to generate metal dihydride complexes in selected nuclear spin states formed synchronously with a pulsed laser[7] and to study reaction intermediates in nitrogenase.[8] Another important development is the recognition that equilibrated excited states of metal hydride polypyridine complexes can act as both strong acids and strong hydride donors, opening up new photocatalytic reactions.[9,10] The past few years have also seen important progress in the photochemistry of complexes with bridging hydrides.[11,12]

The production of hydrogen by photocatalytic methods is of enormous current interest, but the vast majority of approaches involve neither photochemical reaction of metal hydride complexes directly nor formation of excited states of metal hydride complexes by photosensitization. The involvement of hydrides in the photocatalytic splitting of water, typically by protonation of an intermediate, is reviewed elsewhere,[13−17] and a very different approach will be taken here. There are exceptions, however, that involve metal hydrides directly that will concern us here.[18,19] In addition, we will review examples in which photocatalysis with metal hydrides has been used for dehydrogenation of alkanes and alcohols, borylation of arenes, and other C−H functionalization reactions.

This Review starts with a section that surveys key photoprocesses separating the complexes into monohydrides, dihydrides, polyhydrides, bridging hydrides, and dihydrogen complexes. This part incorporates the theory of photodissociation and also includes a subsection for photocatalysis. It is intended that the organization of this section should enable readers to identify photoprocesses relevant to their hydride complexes without difficulty. In the succeeding section, we examine specialist methods for studying mechanisms of photochemistry of metal hydride complexes, concentrating on time-resolved spectroscopy, matrix isolation, NMR methods, and computational methods. Here, we also assess the significance of photochemistry in studying reactive intermediates. In the next part, we present a systematic survey organized by transition metal group that follows the pattern of section 2 in addressing monohydrides, followed by dihydrides and polyhydrides. A concluding section completes the Review. For an up-to-date introduction to photochemical principles, the reader is referred to the recent book by Balzani, Ceroni, and Juris.[20] Although we have not found any wide-ranging reviews of the photochemistry of metal hydrides, there are several relevant reviews of narrower areas that include some metal hydride photochemistry.[3−5,16,17,21−25]

2. PHOTOCHEMICAL PROCESSES

In this section, we review the major photoprocesses observed for transition metal hydrides, providing one or two key examples of each photoprocess. Metal hydride complexes typically show absorption bands in the UV region, often with somewhat indistinct maxima, leading to difficulties in measurement of quantum yields. There is some evidence of wavelength dependence of relative quantum yields for different pathways. We will highlight examples with useful information on electronic spectra, quantum yields, and wavelength-dependent photochemistry in this section. The available evidence, albeit limited in extent, points to dissociative photochemical mechanisms for the vast majority of the reactions. Some decisive exceptions concern the metal hydride polypyridine complexes in which equilibrated excited states are formed before reaction. The isomerization of square-planar platinum complexes is also likely to be completely intramolecular. The majority of the examples here involve mononuclear complexes, since there is little recent research on photochemistry of metal hydride clusters. However, we single out complexes with bridging hydride ligands, because of the principles they illustrate.

2.1. Metal Monohydride Complexes

Several photochemical pathways are known for monohydrides involving the M−H bond: metal−hydrogen bond homolysis, reductive elimination of R−H (R = alkyl or silyl), isomerization,

DOI: 10.1021/acs.chemrev.6b00204
Chem. Rev. 2016, 116, 8506−8544

proton transfer, and hydride transfer. These pathways may compete with photodissociation of other ligands such as CO or with partial decoordination of cyclopentadienyl ligands (Scheme 1).

Scheme 1. Photoprocesses of Metal Monohydride Complexes

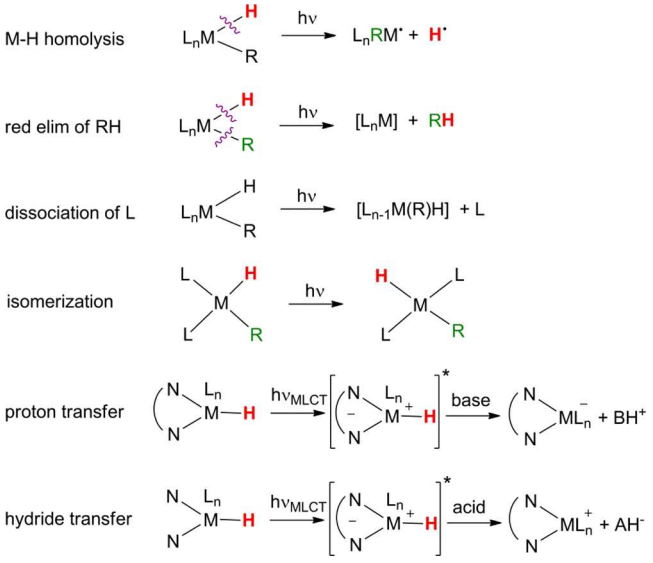

2.1.1. Homolytic Splitting of M−H Bond. The homolytic splitting of the metal−hydrogen bond may occur photochemically without the requirement for any radical initiators. An excellent example is provided by the near-UV and visible ($\lambda > 290$ nm) photolysis of Cp^*_2ReH ($Cp^* = \eta^5$-C_5Me_5) in pentane solution leading to the formation of decamethylrhenocene in 60% isolated yield.[6] There is no evidence for any competing photoprocess, and this remains the only known access route to decamethylrhenocene (eq 1). Often, M−H homolysis competes

$$Cp_2^*ReH \longrightarrow Cp_2^*Re + H \quad (1)$$

with photodissociation of other ligands: $MnH(CO)_5$ acts as a prototypical example. Initial matrix-isolation studies of $MnH(CO)_5$ revealed only CO loss,[26] but later the dissociation of H atoms was demonstrated by trapping the hydrogen atom with CO as the formyl radical, allowing the square pyramidal structure of $[Mn(CO)_5]$ to be demonstrated by IR spectroscopy.[27] Use of EPR spectroscopy for detection following photolysis (254 nm) of $MnH(CO)_5$ in argon matrices allowed the structure of $[Mn(CO)_5]$ to be confirmed independently, the electron distribution of the SOMO to be determined, and the H atom to be detected.[28] The amount of $[Mn(CO)_5]$ produced was increased by use of 193 nm irradiation in Ar matrices such that $[Mn(CO)_5]$ became the dominant product detected by IR spectroscopy.[29] The electronic spectrum of $MnH(CO)_5$ has been reported experimentally[30] and reinvestigated by more modern computational methods with complete active space self-consistent field (CASSCF) methods[31] with and without spin−orbit coupling.[32]

The theoretical basis of the photochemistry of $MnH(CO)_5$ has also been investigated extensively. Early calculations[33] have been superseded by calculations using CASSCF methods[34] that led to the conclusion that 193 nm irradiation causes excitation to the C^1E state ($d\pi \rightarrow \pi^*$), which undergoes intersystem crossing and internal conversion to the a^3A_1 ($\sigma \rightarrow \sigma^*$ Mn−H) state. This state lies on the potential energy surface for H−Mn homolysis. Irradiation at 229 nm generates the B^1E state ($d\pi \rightarrow \sigma^*$), which undergoes Mn−CO bond lengthening, ultimately yielding Mn−CO cleavage and formation of an excited state of $[MnH(CO)_4]$. This calculation rationalizes the observation of increased yield of $[Mn(CO)_5]$ at short wavelength irradiation. An ab initio study with CASSCF/multireference configuration interaction (MRCI) and complete active space second-order perturbation theory (CASPT2) reinvestigated the electronic structure of $MnH(CO)_5$ and identified that population of the A^1E and B^1E states results in CO dissociation, but it did not identify the mechanism of Mn−H homolysis unambiguously.[31] The most recent calculations place the C^1E state at 46 820 cm^{-1} (214 nm) and indicate that it has 63% $d\pi \rightarrow \sigma^*$ Mn−H character.[32] It is important to emphasize that such calculations suggest that there is a high density of states at the energies that are irradiated and that the photochemistry must be considered in terms of electronic states, not just population in terms of antibonding orbitals. Moreover, complex crossing between potential energy surfaces is often involved. Nevertheless, dissociation does occur on an M−H antibonding surface.

2.1.2. Reductive Elimination of RH (R = Me, $SiEt_3$, OEt, etc.). While thermal reductive elimination of alkanes from metal alkyl hydride complexes is commonplace, the corresponding photochemical reactions are relatively rare. Irradiation of $Cp^*_2ZrH(R)$ (R = alkyl) results in alkane reductive elimination. Crossover and isotopic labeling demonstrated that the reductive elimination occurs by an intramolecular mechanism (eq 2).[35]

$$Cp^*_2ZrH(alkyl) \longrightarrow [Cp^*_2Zr] + H\text{-}alkyl \quad (2)$$

The photochemical reaction of *cis-mer*-$[MH(SiEt_3)(CO)_3(PPh_3)]$ (M = Fe, Ru) in alkane glasses at 100 K reveals formation of both CO (40%) and $SiHEt_3$ (60%) as primary photoproducts—only these two photoprocesses are significant. Photochemical reductive elimination can be used to exchange coordinated silyl groups (eq 3) at room temperature in solution

$$MH(SiEt_3)(CO)(PPh_3) + HSiPh_3 \longrightarrow MH(SiPh_3)(CO)(PPh_3) + HSiEt_3 \quad (3)$$

with a quantum yield of 0.6 ± 0.1 at 313 nm. However, loss of CO remains a competing process.[36] The alkoxide hydride $Cp^*IrH(OEt)(PPh_3)$ undergoes reductive elimination of EtOH on irradiation.[37]

2.1.3. Photoisomerization. Square-planar platinum complexes are well-known to undergo photochemical *cis*−*trans* isomerization, and platinum hydrides are no exception. Examples are provided by *cis*-$[PtH(SiR_2R')(PCy_3)_2]$ (R, R′ = H, alkyl, aryl), which undergo quantitative isomerization on UV irradiation at room temperature (section 4.7). It is likely that this is an intramolecular process proceeding via a tetrahedral transition state as has been postulated for other platinum complexes.[38] Photoisomerization may also occur in other ways: the octahedral complex $[IrH(tpy)(ppy)]^+$ (tpy = 2,2′:6′,2″-terpyridine, ppy = 2-phenylpyridine) changes configuration,[39] while $IrH(triphos)(C_2H_4)$ (triphos = $MeC(CH_2PPh_2)_3$) undergoes oxidative C−H cleavage to form the vinyl dihydride $IrH_2(CH{=}CH_2)(triphos)$.[40]

2.1.4. Photochemical Proton Transfer and Hydride Transfer. There are two further photoprocesses that have been discovered much more recently: transfer of a proton from an excited state and transfer of a hydride from an excited state. In each case, we are concerned with metal hydride polypyridine

DOI: 10.1021/acs.chemrev.6b00204
Chem. Rev. 2016, 116, 8506−8544

Scheme 2. Photochemical Proton and Hydride Transfer from Excited Triplet State for $[Cp^*IrH(bpy)]^+$ (Reproduced with Permission from Ref 9; Copyright 2014 American Chemical Society)

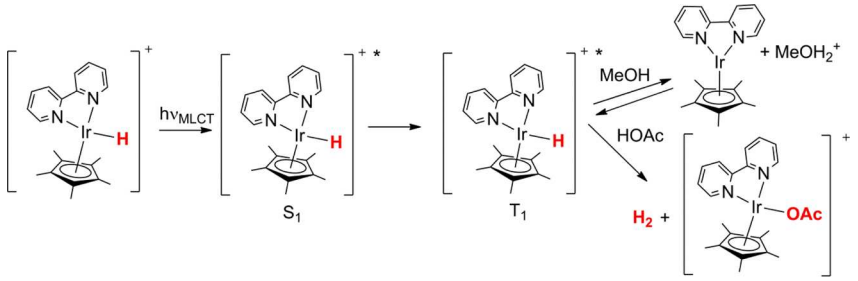

complexes that have equilibrated excited states, as opposed to the dissociative excited states of metal hydrides that are usually formed. As with many polypyridine complexes, $[Cp^*IrH(bpy)]^+$ (bpy = 2,2′-bipyridine) forms an equilibrated excited state that is emissive. (λ_{em} 708 nm).[9,41,42] This cation forms a transient when irradiated in methanol (λ_{ex} 430 nm) that is readily identified as $[Cp^*Ir(bpy)]$ and that regenerates the precursor by second-order kinetics.[10] The solvent kinetic isotope effect for the regeneration step is remarkably large at 8.2 when methanol is replaced by methanol-d_1. Ultrafast laser experiments (excited at 355 nm) show that the rate of formation of the triplet metal-to-ligand charge-transfer (MLCT) state (1.4×10^{10} s^{-1}) is ca. 18 times faster than its rate of deprotonation (8.1×10^8 s^{-1}).[10] The ground-state pK_a is measured as 23.3 in CH_3CN compared to the excited state value pK_a* of −12, estimated from the emission spectra, confirming that it can protonate methanol.[9] Remarkably, this complex is also predicted to be a very strong hydride donor, stronger than $[HBEt_3]^-$, resulting from the transfer of charge to bpy in the excited state. Experimentally, $[Cp^*IrH(bpy)]^+$ transfers hydride to several acids in CD_3CN, forming H_2; the weakest of these acids is acetic acid (pK_a = 23.5), where the other product is $[Cp^*Ir(OAc)(bpy)]^+$ (Scheme 2). Photoreaction with methylnicotinamide iodide yields the products of single-hydride transfer or double-hydride transfer according to the conditions.[9] The full mechanism of hydride transfer is not yet known and may involve either direct hydride transfer in the excited state or a sequence of reactions resulting in net hydride transfer. Thus, the ability to act both as a strong excited-state acid and hydride donor may be compared to the ability of metal polypyridine complexes to act as both strong oxidizers and strong reducers. Several photocatalytic reactions are associated with $[Cp^*IrH(bpy)]^+$ (section 2.6).

2.2. Metal Dihydride Complexes

The photoinduced reductive elimination of H_2 from dihydride complexes is by far the most common photochemical pathway for metal hydrides and competes effectively with the photodissociation of other ligands such as phosphine or CO. All of the evidence points to this reaction as a concerted cleavage of the two M−H bonds with concomitant formation of the H−H bond. Three other pathways have been identified: photoinduced electron transfer, photoisomerization, and hydrogen migration (Scheme 3). In contrast to the monohydrides, there is no convincing evidence for homolytic cleavage of an M−H bond generating hydrogen atoms. In addition, there are a few examples of formation of charge-transfer complexes that exhibit different photochemical pathways. In the examples given in section 2.2.1, photoelimination is the sole process, but this is not generally true; see the case of $Ru(H)_2(PMe_3)_4$ for an example.[43]

Scheme 3. Photoprocesses of Metal Dihydride Complexes

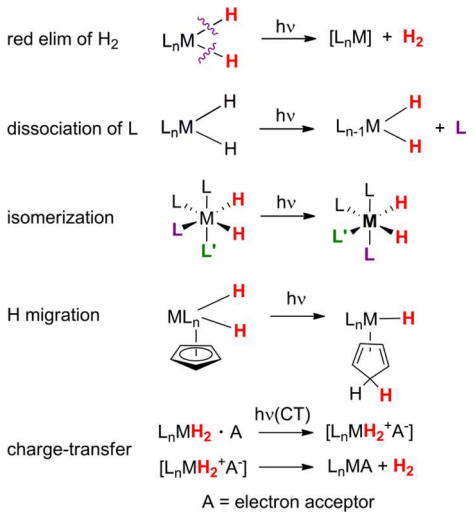

2.2.1. Reductive Elimination of H_2. Irradiation of $Cp_2W(H)_2$ in solution causes loss of H_2 and insertion of $[Cp_2W]$ into C−H, C−S, S−H, or O−H bonds.[2,44−48] The discoveries of the insertion reactions into the C−H bonds of benzene and tetramethylsilane were significant landmarks in the development of C−H bond activation. The complex $Cp_2W(H)_2$ has a clear absorption maximum in hexane solution at 270 nm (ε = 5000 dm^3 mol^{-1} cm^{-1}) with a shoulder at 325 nm tailing into the visible region; the gas-phase absorption spectrum has also been reported.[49] The photoreaction occurs with a lower limiting quantum yield of ca. 0.01 upon irradiation at 366 nm.[50] Matrix isolation experiments revealed tungstenocene as the primary photoproduct and showed via IR, UV−vis, laser-induced fluorescence, and magnetic circular dichroism that it has a parallel sandwich structure with a $^3E_{2g}$ ground state. These early experiments are summarized in reviews.[23,51] Since then, the matrix photochemistry has been investigated in more detail.[52−54] Additional reports have added the photochemical reactions of $Cp_2W(H)_2$ in solution with $HSiCl_3$, $HSiMe_2Cl$, and $HSiMe_3$ to make the corresponding $Cp_2WH(SiR_3)$ complexes.[55,56] Co-irradiation of $Cp_2W(H)_2$ and metal−metal-bonded carbonyl complexes such as $[CpNi(CO)]_2$ or $[CpRu(CO)_2]_2$ have been used to generate heterodinuclear complexes. In these reactions with two metal complexes, there is no control of which complex undergoes photochemical reactions, and it is likely that both contribute.[57] The solution photoreactions of $Cp_2W(H)_2$ are shown in Scheme 4; these reactions cannot be achieved by heating $Cp_2W(H)_2$, but many are accessible if $Cp_2WH(CH_3)$ is used as a thermal source of $[Cp_2W]$. The corresponding photochemistry of $Cp_2Mo(H)_2$ is described in section 4.3.2.

DOI: 10.1021/acs.chemrev.6b00204
Chem. Rev. 2016, 116, 8506−8544

Scheme 4. Solution Photochemistry of $Cp_2W(H)_2$

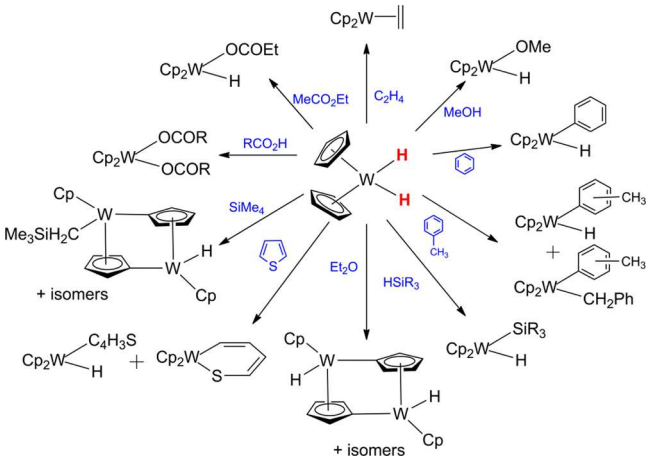

Scheme 5. Solution Photochemistry of $Ru(H)_2(dmpe)_2$

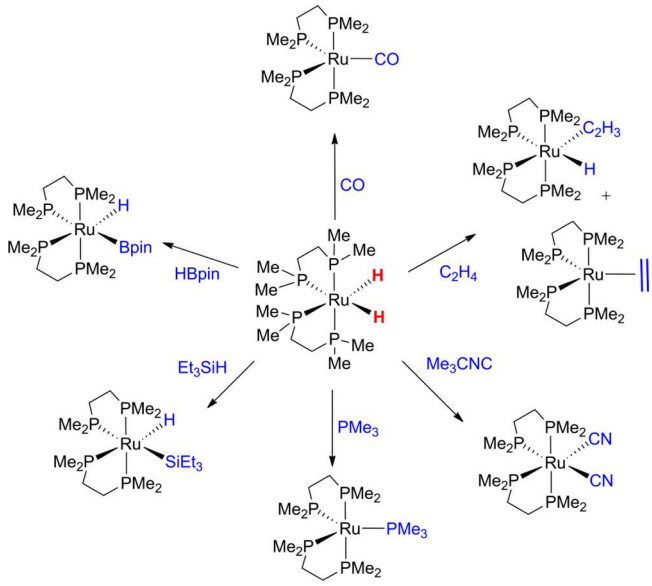

The first report of the solution photochemistry of $Ru(H)_2(dmpe)_2$ and $Ru(H)_2(dppe)_2$ (dmpe = $Me_2PCH_2CH_2PMe_2$, dppe = $Ph_2PCH_2CH_2PPh_2$) in toluene-d_8 employed mass spectrometry to demonstrate that the dominant photoprocess in these complexes is loss of H_2, revealing H_2 with only ca. 3% HD. A similar quantity of HD is formed in a crossover experiment where $Ru(H)_2(dmpe)_2$ and $Ru(D)_2(dmpe)_2$ are irradiated together (313 nm) in solution.[58] Photolysis in an EPR spectrometer at low temperature in the presence of a spin trap also failed to generate a hydrogen spin adduct. Irradiation in benzene solution in the presence of carbon monoxide or ethylene led to loss of H_2 and the formation of the corresponding complexes $Ru(dmpe)_2L$ or $Ru(dppe)_2L$ (L = CO, C_2H_4). In the absence of substrate, the products were identified as $Ru_2(dmpe)_5$ and $RuH(C_6H_4PPhCH_2CH_2PPh_2)(dppe)$, respectively.[58] In understanding these reactions, it is important to note that the *cis*-dihydride isomers dominate over the trans isomers ($Ru(H)_2(dmpe)_2$ ca. 13:1, $Ru(H)_2(dppe)_2$ ca. 20:1) and that there is probably a slow equilibrium between the isomers. Further photochemical reactions of $Ru(H)_2(dmpe)_2$ were reported in later studies including C−H, Si−H, and B−H activation reactions (Scheme 5).[59,60] Notably, reinvestigation of the reaction with ethylene showed formation of *cis*-[RuH(CH=CH_2)$(dmpe)_2$] in addition to $Ru(dmpe)_2(C_2H_4)$. The UV absorption spectrum of $Ru(H)_2(dmpe)_2$ (colorless when pure) shows a maximum at 210 nm (ε = 4900 dm^3 mol^{-1} cm^{-1}) in pentane solution and a shoulder at 260 nm. The quantum yield at 308 nm has been determined by transient actinometry as 0.85 ± 0.1.[61]

The photochemical reactions of $Ru(H)_2(dmpe)_2$ have been investigated by both matrix isolation and laser flash photolysis (time-resolved absorption spectroscopy).[59] UV photolysis in argon or methane matrices causes depletion of the ν(RuH) bands of $Ru(H)_2(dmpe)_2$ in the IR spectrum and growth of characteristic UV−vis absorption bands for [$Ru(dmpe)_2$], including long-wavelength absorptions at 460, 543, and 743 nm (values for Ar matrix). The reactions can be partially reversed by long-wavelength irradiation. There is no evidence for activation of methane; introduction of 1.5% CO results in photochemical conversion of $Ru(H)_2(dmpe)_2$ to $Ru(dmpe)_2(CO)$.

Laser flash photolysis is simplest for a reaction that is driven forward photochemically and reverses thermally. Such a degenerate reaction is indeed set up by adding subatmospheric pressures of H_2 to a solution of $Ru(H)_2(dmpe)_2$ in cyclohexane (eq 4). The resulting transient absorption spectrum measured 400 ns after the 308 nm flash at 300 K shows a striking match to

$$RuH_2(dmpe)_2 \underset{k}{\overset{h\nu}{\rightleftharpoons}} [Ru(dmpe)_2] + H_2 \qquad (4)$$

the spectra observed in methane matrix at 12 K. The transient decays with pseudo-first-order kinetics allowing the second-order rate constant to be determined as (6.8 ± 0.3) × 10^9 dm^3 mol^{-1} s^{-1} by varying the partial pressure of H_2. The kinetic isotope effect for H_2 readdition is measured as k_H/k_D = 1.20 ± 0.08. The rate constant is very close to the diffusion limit and still represents the fastest recorded rate constant for reaction of H_2 at a transition metal center.[59]

When laser flash photolysis is performed under an argon atmosphere, the reaction is still largely reversible leading to second order kinetics. Flash photolysis in the presence of a variety of substrates resulting in quenching behavior, allowing second-order rate constants for reaction with [$Ru(dmpe)_2$] to be determined. The rate constants follow the order H_2 > CO > HBpin > *t*-BuNC > PMe_3 > C_2H_4 ≈ $HSiEt_3$ > cyclopentene and span a factor of ca. 2000. Activation parameters for several reactions of group 8 [MP_4] complexes, among them [$Ru(dmpe)_2$], are listed in Table 1. When the corresponding experiments are carried out in the absence of substrate, second-order kinetics are observed, consistent with recombination with H_2 as the major reaction. Indirect evidence for some reaction of [$Ru(dmpe)_2$] with itself or with $Ru(H)_2(dmpe)_2$ comes from anomalous behavior at higher concentrations and the nonzero intercept in the quenching plots.[59,60] The rise-time of [$Ru(dmpe)_2$] following irradiation (300 nm) of $Ru(H)_2(dmpe)_2$ under H_2 has been probed by picosecond transient absorption methods and shown to be <16 ps, the instrumental response (Figure 1). These experiments revealed partial decay of the transient with a rate constant ca. 100 times faster than observed in the nanosecond experiments (k_{obs} = 3 × 10^9 s^{-1}), perhaps due to geminate recombination.[62] The recent increases in sensitivity and time resolution would allow improvements to these measurements (section 3.1.1).

When a laser flash is employed to irradiate $Ru(H)_2(dmpe)_2$ under argon and the heat deposition is measured by photo-

DOI: 10.1021/acs.chemrev.6b00204
Chem. Rev. 2016, 116, 8506−8544

Table 1. Activation Parameters for Reactions of Group 8 [MP_4] Complexes Determined by Transient Absorption Spectroscopy

	$\Delta H^{\ddagger}$, kJ/mol	$\Delta S^{\ddagger}$, J/mol/K	$\Delta G^{\ddagger}_{298}$, kJ/mol	reference
[**Fe**$(dmpe)_2$] + $HSiEt_3$	22 ± 2	−87 ± 6	48 ± 3	63
[**Ru**$(dmpe)_2$] + $HSiEt_3$	9 ± 1	−53 ± 4	25 ± 2	59
[**Ru**$(depe)_2$] + $HSiEt_3$	11 ± 3	−112 ± 4	44 ± 1	64
[**Ru**$(dmpm)_2$] + $HSiEt_3$	11 ± 2	−40 ± 5	23 ± 2	65
[**Ru**(PP_3)] + $HSiEt_3$	35 ± 2	−18 ± 6	40 ± 4	66
[**Ru**(etp)(CO)] + $HSiEt_3$	11 ± 1	−49 ± 4	25.7 ± 0.1	67
[**Os**(PP_3)] + $HSiEt_3$	31 ± 5	−27 ± 12	39 ± 6	66
[**Ru**(PP_3)] + C_6H_6	39 ± 4	+1 ± 13	38 ± 6	66
[**Os**(PP_3)] + C_6H_6	38 ± 3	−7 ± 9	40 ± 4	66
[**Os**(PP_3)] + pentane	27 ± 1	−59 ± 4	45 ± 2	66

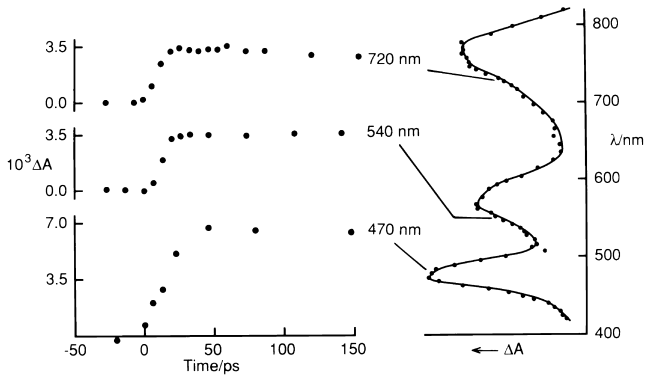

Figure 1. Transient absorption signals following laser flash photolysis of $Ru(H)_2(dmpe)_2$ in cyclohexane solution under 1 atm of H_2 at 300 K monitored at 470, 540, and 720 nm over a 150 ps time scale (left). The signals rise within the response time of 16 ps. The detection wavelengths for the traces (left) are mapped onto the transient UV−vis spectrum of [$Ru(dmpe)_2$] obtained by ns-laser flash photolysis. Reproduced from ref 62. Copyright 1994 American Chemical Society.

acoustic calorimetry, the enthalpy of reaction of [$Ru(dmpe)_2$] and H_2 to form $Ru(H)_2(dmpe)_2$ may be determined (eq 4, back reaction), yielding a value of $\Delta H = -22.7$ kcal/mol and allowing the Ru−H bond dissociation enthalpy to be estimated as 63.5 ± 2.0 kcal/mol. The same method can be used with CO and N_2 atmospheres to determine the Ru−CO and Ru−N_2 bond enthalpies as 43 ± 2.0 and 18.8 ± 2.0 kcal/mol, respectively.[61]

Fast kinetic methods have also been used to investigate the photochemistry of $Ru(H)_2(dppe)_2$, showing that transient [$Ru(dppe)_2$] may be generated in a similar way to that described for [$Ru(dmpe)_2$]. Replacement of the phosphine methyl substituents by phenyl groups leads to a reduction in the rate constants by a factor of 260 for H_2, rising to a factor of 3700 for ethylene, indicating a great increase in selectivity.[60,64] The transient absorption spectrum of [$Ru(dppe)_2$] resembles that of [$Ru(dmpe)_2$].

In a new method development (see section 3.2), the photochemistry of $Ru(H)_2(dppe)_2$ has been investigated in laser pump−NMR probe experiments in which a single pulse of a laser (355 nm) initiates dissociation of H_2 and a single radio frequency (*rf*) pulse serves to detect the resulting magnetization.[7] In these experiments, *para*-H_2 replaces the usual H_2 atmosphere, resulting in the formation of $Ru(H)_2(dppe)_2$ in selected nuclear spin states, greatly increasing the sensitivity of NMR detection. When the delay time between the laser pulse and the *rf* pulse is varied, oscillations in the magnetization are revealed with an oscillation frequency corresponding to the difference between the two spin−spin coupling constants $|J_{PHtrans} - J_{PHcis}|$. This laser pump−NMR probe method paves the way for studying millisecond or microsecond reaction kinetics with the benefits of highly resolved NMR spectra to identify species unambiguously.

The origin of the rich absorption spectrum of d^8 [$Ru(dmpe)_2$] has been traced to a square-planar (D_{2h}) structure with a singlet ground state. This characteristic pattern is found in other unconstrained [RuP_4] and [OsP_4] species[64,68] but is very different from that of constrained species that cannot adopt a square-planar structure[66,69] such as [$Ru(PP_3)$] (PP_3 = P-$(CH_2CH_2PPh_2)_3$). It also contrasts with that of [$Fe(dmpe)_2$], which adopts a triplet ground state.[63] The low-energy band of [$Ru(dmpe)_2$] is assigned to a $4d_z^2 \rightarrow 5p_z$ transition.

The initial photodissociation of H_2 from *cis*-[$Ru(H)_2(dmpe)_2$] has been modeled with *cis*-[$Ru(H)_2(PH_3)_4$] and time-dependent density functional theory (DFT) calculations.[70] The absorption band is identified with the HOMO-1 to LUMO transition to the S_2 state ($d_{xz} \rightarrow$ combination of $d_{x^2-z^2}$, d_{z^2}, and σ_g of H_2 fragment; C_2 axis defined as *y*). Elimination of H_2 is found to be exothermic and dissociative in both the S_1 and S_2 excited states. Wave-packet analysis shows that elimination of H_2 occurs via an avoided crossing on a time scale of 100 fs if the wave packet is allowed to propagate on the potential energy surface after relaxation to the geometry corresponding to the H_2 elimination barrier. This relaxation may itself take a few hundred femtoseconds.

Density functional calculations have also been reported on [$Ru(PH_3)_4$] as a model for [$Ru(dmpe)_2$], making extensive comparisons to [$Fe(PH_3)_4$] and [$Rh(PH_3)_4$]$^+$.[71] The singlet state of [$Ru(PH_3)_4$] was calculated to be more stable than the triplet state by ca. 12 kcal/mol and the triplet state was calculated to adopt a D_{2d} geometry with P−Ru−P angles of 159°. (There is an interesting comparison to the Ru^0 complex $Ru(CO)_2(Pt\text{-}Bu_2Me)_2$ that has been isolated and studied computationally and which adopts a C_{2v} structure.)[72] Oxidative addition of H_2 was predicted to be exothermic by 34 kcal/mol (evidently an overestimate; see above). The pathway for oxidative addition was calculated to proceed without any barrier via an initial end-on approach of H_2. The H−H distance does not elongate and the H_2 does not swing to a sideways orientation until the Ru−H distance is close to its final value. The ΔSCF (SCF = self-consistent field) method was used to calculate the lowest energy transitions of [$Ru(PH_3)_4$] and [$Rh(PH_3)_4$]$^+$ and gave energies as 13 900 and 26 200 cm^{-1}, very accurately reproducing the experimental values for the dmpe compounds of 13 800 and 25 600 cm^{-1}, respectively. These calculations support the $4d_{z^2} \rightarrow 5p_z$ assignment of the low-energy band of [$Ru(dmpe)_2$].[71] Details of the photochemistry of related $M(H)_2P_4$ and $M(H)_2P_3(CO)$ complexes (M = Fe, Ru, Os; P = phosphine) are given in section 4.5.2.

The most thorough theoretical treatments address the photochemical reductive elimination of H_2 from $Fe(H)_2(CO)_4$ and the competing dissociation of CO. The theoretical work is linked to the matrix-isolation photochemistry of $Fe(H)_2(CO)_4$, which showed exclusive loss of H_2 and also showed that the reaction could be partially reversed by long-wavelength irradiation.[73] A simplified orbital approach examines the bonding and antibonding orbitals involved in the $Fe(H)_2$ interaction (Scheme 6) and suggests that reaction occurs by population of

DOI: 10.1021/acs.chemrev.6b00204
Chem. Rev. 2016, 116, 8506−8544

Scheme 6. Simplified Bonding and Antibonding Orbital Overlap Diagrams for a Metal Dihydride (Adapted with Permission from Ref 75; Copyright 2000 Elsevier)

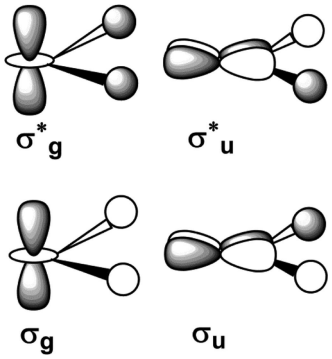

the orbital that is Fe−H antibonding and H−H bonding, labeled σ_g* in Scheme 6. According to CASSCF/CCI (CCI = contracted configuration interaction) calculations, the main contributions to the absorption spectrum relevant to H_2 dissociation are $^1A_1 \rightarrow {}^1B_1$ and $^1A_1 \rightarrow {}^1A_1$ transitions, which both correspond to d-σ_g* excitation. The upper states of these transitions are dissociative with respect to H_2 elimination. According to wave-packet analysis, H_2 elimination occurs within 40 fs.[74,75] There is no evidence for intersystem crossing. The dissociation of H_2 is predicted to dominate over CO dissociation throughout the UV absorption region. Although this sounds simple, there are numerous close-lying states, such that a multiconfigurational approach is necessary to describe the photodissociation dynamics. In more recent work, calculation of the absorption energies has been refined.[76,77]

2.2.2. Photoisomerization. Photoisomerization of an octahedral metal dihydride complex may occur via photoinduced reductive elimination of H_2 or via photoinduced loss of another ligand. The example of $Ru(H)_2(NHC)(CO)(PPh_3)_2$ (NHC = N-heterocyclic carbene) illustrates these processes (Figure 2).[78]

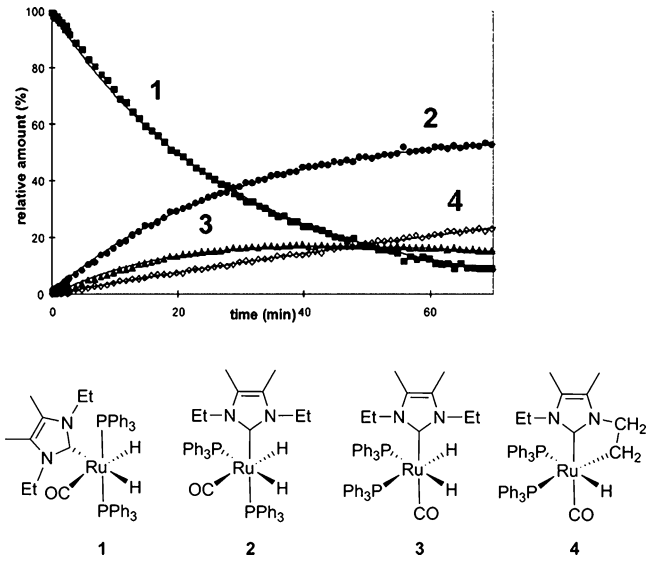

Figure 2. Time profile for conversion of **1** (■) into isomers **2** (●), **3** (▬), and **4** (♦) over 130 min upon photolysis at 223 K (observed points and fitted lines with the dominant pathways indicated). Reproduced with permission from ref 78. Copyright 2006 American Chemical Society.

The photochemical reaction was studied by in situ laser photolysis (325 nm, continuous wave) within the probehead of an NMR spectrometer at 223 K and demonstrates initial conversion of the stable isomer **1** to new isomers **2**, **3**, and cyclometalation product **4**. The role of H_2 loss was demonstrated by irradiating under a *para*-H_2 atmosphere, resulting in formation of enhanced spectra of **2** and **3**. The competing loss of PPh_3 was evident from a photochemical reaction in the presence of pyridine that yielded a substitution product. A combination of kinetic analysis and DFT calculations revealed the complete pathway for isomerization involving both H_2 and PPh_3 loss.

A particularly interesting example of photoisomerization concerns $CpMn(H)_2(dfepe)$ (dfepe = $(C_2F_5)_2PCH_2CH_2P(C_2F_5)_2$) that exists as an equilibrium mixture of the dihydride isomer with *transoid* diphosphine and the dihydrogen isomer with *cisoid* diphosphine. Photolysis at 10 °C results in complete conversion to the dihydrogen complex. When left in the dark, the original equilibrium mixture is slowly restored.[79] A related phenomenon has been observed on irradiation of $CpRe(H)_2(CO)_2$ in a methylcyclohexane glass at 10 K followed by warming to 200 K, but neither the distinction between dihydride and dihydrogen isomers nor the photoisomerization is so complete.[80] This behavior may be compared to that of $CpRe(H)_2(PPh_3)_2$ (next section).

2.2.3. Photoinduced Hydrogen Migration. Photodissociation is not the only photoprocess involving the hydride ligands that has been observed for metal dihydrides. Loss of one or both PPh_3 ligands was observed when $CpRe(H)_2(PPh_3)_2$ was photolyzed and a variety of substitution products were synthesized in the presence of phosphines, tetrahydrofuran (THF), and C_2H_4. The complex also showed photocatalytic activity (λ > 345 nm irradiating into edge of absorption band at 328 nm) for the conversion of C_2H_4 and benzene into ethylbenzene, ethane, 1-butane, and butane.[81] Additionally, it catalyzes photoinduced H/D exchange between deuterated solvents and arene or alkane substrates including methane itself.[82] An extensive series of isotope-labeling studies led to the conclusion that the photochemical mechanism does not involve $[CpRe(H)_2(PPh_3)]$ or $[CpRe(PPh_3)_2]$ as intermediates but involves metal-to-ring hydrogen migration to form (η^4-C_5H_6)-$ReH(PPh_3)_2$. This compound undergoes a further migration to form $[(\eta^3\text{-}C_5H_7)Re(PPh_3)_2]$, which is the active species for H/D exchange.[83]

2.2.4. Photoinduced Electron Transfer, Charge Transfer (CT) Adducts, and Photosensitization. The first report of the photochemistry of $Ru(H)_2(dmpe)_2$ included the demonstration of the photoreaction with tetracyanoethylene (TCNE) in benzene yielding $Ru(dmpe)_2\{C_2(CN)_3\}(CN)$. The authors detected the $TCNE^-$ radical by EPR and UV−vis spectroscopy and proposed two successive photochemical steps, the first to form $[M(dmpe)_2^+ \cdot TCNE^-]$ and the second to convert this charge-transfer adduct to $Ru(dmpe)_2\{C_2(CN)_3\}(CN)$.[58] There was no mention of ground-state adducts. Related experiments on $Cp_2W(H)_2$ yielded somewhat different results;[84] ground-state donor−acceptor adducts were observed with absorption bands in the region 480 nm (dimethylfumarate, K_{eq} = 0.08 M^{-1}) to 538 nm (maleic anhydride, K_{eq} = 0.2 M^{-1}), where K_{eq} is the formation constant of the adduct. The charge-transfer transition energies correlate with the electron affinity of the activated alkenes. Irradiation of the maleic anhydride adduct into the tail of the CT band (>550 nm) resulted in formation of the $Cp_2W(\eta^2\text{-}CC\text{-}\{C_2H_2(CO)_2O\}$ together with succinic anhydride. A similar

DOI: 10.1021/acs.chemrev.6b00204
Chem. Rev. 2016, 116, 8506−8544

Scheme 7. Solution Photochemistry of $Mo(H)_4(dppe)_2$; Ph Groups on the dppe Ligand Are Not Shown in the Products

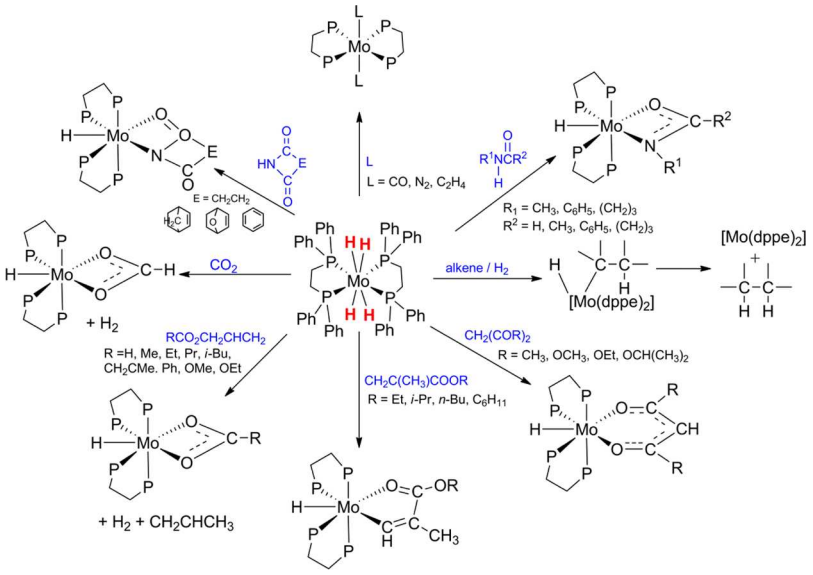

reaction occurred with fumaronitrile. These reactions evidently proceed by a very different photochemical pathway from those described in section 2.2.1 and must involve the excited state of the CT adduct.

The examples described so far absorb predominantly or exclusively in the UV region. It is therefore highly desirable to sensitize metal hydrides by using visible light absorbers. Such photosensitization has been achieved only rarely but is illustrated by the case of $[Co(H)_2(bpy)(PEt_2Ph)_2]^+$, which has an absorption tailing into the visible and undergoes photoinduced H_2 loss in methanol solution with 405 nm radiation (quantum yield = 0.14). Addition of $Fe(bpy)_2(CN)_2$ allows the photolysis to be performed with a similar quantum yield but at much longer wavelength (577 nm).[85] The mechanism does not seem to have been investigated further but may well involve photoinduced electron transfer and hence be related to the charge-transfer photochemistry described above.

An alternative approach is to use photoelectrolysis to deliver the electron to the metal hydride complex. This method is discussed in more detail in the Photocatalysis section in the context of the $[Mo(H)_2(O_2CMe)(dppe)_2]^+$ as the electron acceptor.[86]

2.3. Metal Polyhydride Complexes

Metal polyhydride complexes offer the possibility of either photoinduced H loss or H_2 loss, in addition to photodissociation of other ligands. The tetrahydride, $Mo(H)_4(dppe)_2$, provides a well-studied example of an emissive hydride complex: it absorbs at 380 nm (26 000 cm^{-1}) and emits at 580 nm (17 300 cm^{-1}) in a 2-MeTHF glass at 77 K with an emission lifetime of 87 μs, leading to the assignment of the emissive state as a spin triplet.[87] The emission yield is enhanced in the deuterated analogue, $Mo(D)_4(dppe)_2$. The photolysis (366 nm) of $Mo(H)_4(dppe)_2$ under N_2 results in conversion to *trans*-$[Mo(N_2)_2(dppe)_2]$ in high yield. Similarly, the corresponding reactions with CO or C_2H_4 give $Mo(L)_2(dppe)_2$ (L = CO, C_2H_4).[87,88] In the presence of H_2, $Mo(H)_4(dppe)_2$ acts as a photocatalyst for reduction of alkenes. Photolysis under CO_2 takes a different course, yielding the insertion product $MoH(O_2CH)(dppe)_2$,[89] while reaction with alkyl methacrylates yielded seven-coordinate $MoH(\kappa^2\text{-}CHCMeCO_2R)(dppe)_2$ by C−H activation.[90] A related reaction with allyl carboxylates yielded hydrido carboxylate complexes, releasing propene and H_2. These reactions are thought to involve initial coordination of the allyl group.[91] β-Dicarbonyl compounds such as 2,4-pentanedione react to form molybdenum hydrido dionato complexes; the authors interpret this as an O−H oxidative addition from the enol form. Photoinduced oxidative addition reactions of N−H bonds with succinimide and *N*-alkyl acetamide and related compounds were observed, yielding metalacycles.[92,93] In spite of this extensive preparative chemistry (Scheme 7), the photogenerated intermediate $[Mo(H)_2(dppe)_2]$ has not been characterized, and there remains a question of whether this intermediate undergoes a second reductive elimination to form $[Mo(dppe)_2]$ or whether the products result from reaction of $Mo(H)_2(L)(dppe)$ (photochemical or thermal). In contrast to the behavior of $Cp_2W(H)_2$, most of these reactions can also be effected by thermal reaction of $Mo(H)_4(dppe)_2$. They are reviewed in a perspective article.[21] This photoreactivity is also related to some photocatalytic reactions (section 2.6).

In a reminder of the possibility of photochemical loss of ligands other than hydrogen, even if chelating, it has recently been demonstrated that irradiation of $W(H)_4(dppe)_2$ under hydrogen results in the formation of a photostationary state between $W(H)_4(dppe)_2$ and $W(H)_6(dppe)(\kappa^1\text{-dppe})$.[94]

2.4. Metal Dihydrogen Complexes

The majority of dihydrogen complexes are thermally labile with respect to H_2 loss, meaning that photochemical loss usually becomes significant only at low temperatures. A clear demonstration of photochemical loss of H_2 from a dihydrogen complex came from the reaction of chromium hexacarbonyl in H_2-doped argon matrices at 4−12 K. UV photolysis caused generation of $[Cr(CO)_5]$, which reacted on long-wavelength photolysis to form $Cr(H_2)(CO)_5$. Irradiation at 365 nm into the absorption band of $Cr(H_2)(CO)_5$ caused conversion back to $[Cr(CO)_5]$.[95] Similarly, irradiation of $CpMH(CO)_3$ (M = Mo, W) in H_2-doped argon matrices generates $CpMH(H_2)(CO)_2$, which is itself photosensitive, losing H_2 on 350 nm irradiation.[96] In these reactions the dihydrogen ligand behaves similarly to other two-electron donor ligands in its photolability under long-wavelength irradiation. Metal dihydrogen complexes may also be

DOI: 10.1021/acs.chemrev.6b00204
Chem. Rev. 2016, 116, 8506−8544

generated by metal vapor methods in conjunction with matrix isolation. For example, $Fe(H)_2(H_2)_3$ has been formed by co-condensation of iron atoms with pure hydrogen at 4.5 K and proved to be photolabile.[97] The photochemical loss of H_2 from two $Rh(H_2)(PCP)$ (PCP = $(2,6\text{-}C_6H_3)(CH_2P\textit{t}Bu_2)_2$) complexes at room temperature has been used to monitor transient spectra and kinetics of [Rh(PCP)] intermediates (Scheme 8). Thus, the

Scheme 8. Photochemical Loss of H_2 from the Dihydrogen Complex $Rh(H_2)(PCP)$ (Reproduced with Permission from Ref 98; Copyright 2013 American Chemical Society)

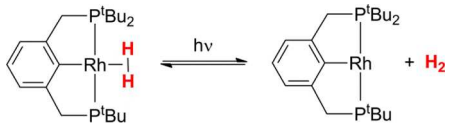

photodissociation of the η^2-H_2 ligand can prove useful, even though $Rh(H_2)(PCP)$ equilibrates with other ligands very readily.[98] An example of photocatalysis,[99] probably involving photolysis of dihydrogen complexes, is summarized in section 2.6.

2.5. Bridging Metal Hydrides

The photochemistry of dinuclear and polynuclear complexes offers approaches to photochemical generation of hydrogen with visible light rather than UV radiation. Recent work has also highlighted the importance of bridging hydrides in bioinorganic chemistry. This section illustrates key principles for bridging hydrides. The first example to be studied was $[Pt_2(H)_2(\mu\text{-}H)(dppm)_2]^+$ (dppm = $Ph_2PCH_2PPh_2$), which contains two terminal and one bridging hydride supported by two bridging diphosphine ligands.[100] Irradiation in CH_3CN leads to conversion to $Pt_2H(dppm)_2(CH_3CN)$ with a single terminal hydride with a quantum yield of 0.62 at 366 nm. This reaction has a far higher quantum yield than that for irradiation of $[Pt_2(H)_2Cl(dppm)_2]^+$, which has one hydride on each platinum. There are some dinuclear complexes that also undergo loss of H_2, among them dirhodium complexes containing parallel terminal rhodium−hydride bonds studied for hydrogen production. The diplatinum complex can be considered as a model for the photochemical H_2 release from these dinuclear rhodium complexes that are postulated to convert to HRh(μ-H)Rh isomers before losing H_2.[101] σ−σ^* excitation of these $d^8\cdots d^8$ rhodium dimers generates predominantly H_2 even in the presence of THF as a trap. Crossover experiments with mixtures of $[Rh_2(H)_2]$ and $[Rh_2(D)_2]$ generate mainly H_2 and D_2 (Scheme 9).

Scheme 9. General Scheme for H_2 Elimination from a Dinuclear Metal Species (Reproduced with Permission from Ref 101; Copyright 2005 American Chemical Society)

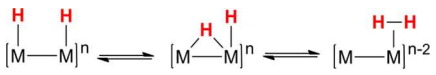

Much more recently, the photochemistry of $(Cp^*Ru)_2(\mu\text{-}H)_4$ has been examined. This complex absorbs at 371 nm (ε = 2200 $dm^3\ mol^{-1}\ cm^{-1}$) and was photochemically inert in THF, but reacted on irradiation at 365 nm with methyl ketones to form $(Cp^*Ru)_2(\mu\text{-}H)_2(\mu\text{-}\eta^4\text{-}CH_2C(O)CHR) + 2H_2$ where the bridging ligand is described as oxatrimethylenemethane.[12] The authors propose that the reaction proceeds via an exciplex, although no further evidence is provided. Photoreaction of CO_2-saturated THF solutions yielded the trihydrido formato complex $(Cp^*Ru)_2(\mu\text{-}H)_3(\mu\text{-}\kappa^2\text{-}OCHO)$ (Scheme 10). However, the corresponding reaction of $(Cp^{\ddagger}Ru)_2(\mu\text{-}H)_4$ where $Cp^{\ddagger}$ = η^5-1,2,4-$C_5H_2t\text{-}Bu_3$ yielded $(Cp^{\ddagger}Ru)_2(\mu\text{-}O)(\mu\text{-}CO)$ with bridging oxo and carbonyl ligands.[11] An interesting feature of these reactions with CO_2 is that there is no H_2 loss but there is reaction at the hydride ligands.

UV irradiation of *trans*-$[Fe_2Cp_2(\mu\text{-}H)(\mu\text{-}PPh_2)(CO)_2]$ showed three photochemical pathways according to the following conditions: photoisomerization to the cis-form, introduction of a new phosphine ligand by reaction with PR_2H with concomitant P−H cleavage, loss of H_2, and CO substitution. Because isomerization is not suppressed by added CO or PR_2H, the authors postulate isomerization by reversible opening of the hydride bridge. The other pathways of the trans-complex are initiated by CO loss; the photochemistry of the cis-complex is also dominated by CO loss.[102,103] Related trans−cis photoisomerization has been reported for *trans*-$[Fe_2Cp_2(\mu\text{-}H)(\mu\text{-}PR^*_2)(CO)_2]$ where PR^*_2 is an optically active phosphine.[104,105] More recently, the high-spin Fe(II) complex $[(\beta\text{-diketiminate})\text{-}Fe(\mu\text{-}H)]_2$ was found to reductively eliminate H_2 photochemically in the presence of N_2 to yield $[(\beta\text{-diketiminate})FeNNFe(\beta\text{-diketiminate})]$.[106]

Nitrogenase generates dihydrogen at the same time as ammonia. Recently, an intermediate has been generated from a mutant in which a reduced form of the cofactor is stabilized, which is thought to store two molecules of hydrogen as two bridging hydrides and two protonated bridging sulfur atoms in a 4Fe arrangement (Scheme 11). Low-temperature (<20 K) irradiation of this form within an EPR cavity results in reversible elimination of H_2.[8] The photochemical reductive elimination exhibits a large kinetic isotope effect (KIE ≈ 10) that is temperature-independent, indicating that there is a barrier in this step that is overcome by a tunneling mechanism. The reverse oxidative addition step is induced by heating and shows a KIE of ∼5.4 at 193 K. There are no examples of photochemical reductive elimination of H_2 from small molecules that are closely comparable.

2.6. Photocatalysis

Photocatalysis can encompass many types of catalysis, and it is important to distinguish the different types where possible, even though the term is often used loosely. It may not be possible to identify to which class a reaction belongs without additional mechanistic information, especially the quantum yield. We follow Wrighton[107] in our definitions with modifications and additions by Hennig[108] and ourselves.

(a) Photoinduced catalysis refers to the situation where the photochemical reaction generates an active species that participates in thermal catalytic reactions. The quantum yield may exceed unity and the overall free energy of the catalyzed reaction must be negative.

(b) In photoassisted catalysis, at least one photochemical reaction lies within the catalytic cycle and the quantum yield cannot exceed unity. Catalytic reactions with overall positive free energy must belong to this class, although those that are exergonic could also belong to it.

(c) Photosensitized catalytic reactions involve excitation of the photosensitizer that transfers (i) its excitation energy (photoinduced energy transfer) or (ii) an electron (photoinduced electron transfer to another species

DOI: 10.1021/acs.chemrev.6b00204
Chem. Rev. 2016, 116, 8506−8544

Scheme 10. Photoreactivity of $(Cp^*Ru)_2(\mu\text{-}H)_4$ (Reproduced with Permission from Refs 11 and 12; Copyright 2014 American Chemical Society and 2013 John Wiley and Sons, Respectively)

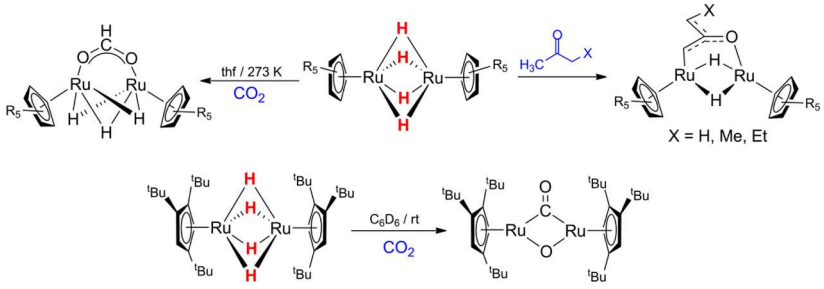

Scheme 11. Photochemical Reductive Elimination of H_2 from Cofactor of Nitrogenase (Reproduced with Permission from Ref 8; Copyright 2016 American Chemical Society)

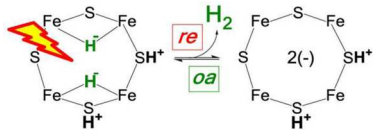

allowing entry to the catalytic cycle). The resulting mechanism could belong to either class a or class b.

(d) Photoelectrocatalysis combines the use of electrolysis and photochemistry. The light absorber may be a photoelectrode such as a semiconductor or a species in the electrolyte solution. In photoelectrocatalysis, additional energy may be provided to overcome a thermodynamic or kinetic barrier via an electrical bias.

2.6.1. Photoinduced Catalysis. A clear-cut example of photoinduced catalysis is provided by the tungsten monohydride $CpWH(CO)_3$, which undergoes CO substitution by PBu_3 on UV irradiation (311 nm) without dimerization, with quantum yields up to at least 30. A radical chain initiated by W−H bond homolysis was given as the primary mechanism; the 17e-radical substitutes much faster than the 18e-complex, yielding $CpW(CO)_2(PBu_3)$, which abstracts H from $CpWH(CO)_3$. The quantum yield becomes much higher on addition of a few percent of $[CpW(CO)_3]_2$, reaching values of at least 1000.[109]

2.6.2. Photoassisted Catalysis. The range of examples of photoassisted catalysis involving metal hydrides is well illustrated in Esswein and Nocera's review.[16] One of the major goals is, of course, to produce H_2 from water, a process that is very successfully catalyzed by hydrogenases. The mimic of [FeFe]-hydrogenase $[Fe_2(CO)_4(dppv)(\mu\text{-}pdt)(\mu\text{-}H)]BF_4$ (dppv = cis-$Ph_2PCH{=}CHPPh_2$, pdt = propane dithiolate) generates H_2 on irradiation of CH_2Cl_2 solutions containing $[H(OEt_2)]BF_4$ or HOTf. Addition of octamethylferrocene inhibits catalyst decomposition, but the turnover numbers are <10.[18]

In an effort to develop a light-driven energy conversion catalyst, Heyduk and Nocera reported a two-electron mixed-valence Rh compound as photocatalyst for H_2 evolution from the reduction of hydrohalic acid.[110] A few years later the same group showed that an analogous two-electron mixed-valent complex $Rh_2^{0,II}(tfepma)_2(CNAd)_2Cl_2$ (tfepma = $CH_3N[P(OCH_2CF_3)_2]_2$ and CNAd = 1-adamantylisonitrile) could photolytically split HCl with H_2 production continuing for 177 h in THF solution. A rhodium monohydride−chloride dimer formed during the catalytic cycle was the photoactive species that generated H_2 and a dichloride Rh dimer (Scheme 12).[111]

Scheme 12. Photocatalytic Cycle for HCl Splitting; P = $P(OCH_2CF_3)_2$ (Reproduced with Permission from Ref 111; Copyright 2012 Royal Society of Chemistry)

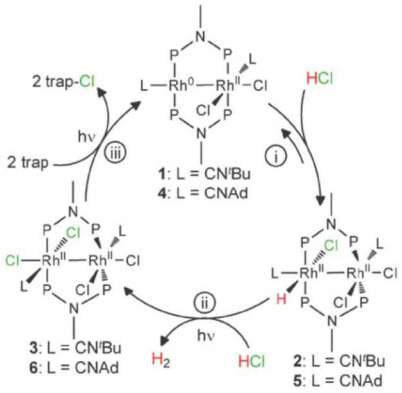

The photocatalytic reaction of aqueous formate to $CO_2 + H_2$ is catalyzed by [Cp*Ir(bpy)Cl]Cl or its 4,4′-bpy$(OMe)_2$ analogue with irradiation by blue light. The catalyst is active over the range pH 5−10 and there is a kinetic isotope effect of 2.6; there is no pressure inhibition up to H_2 pressures of 4 atm. The light absorber is proposed to be the hydride $[Cp^*IrH(bpy)]^+$, and the cycle involves conversion of the hydride to the hydroxide complex by hydride transfer (see section 2.1.4), thereby releasing H_2. The hydroxide complex is converted to the formate complex that loses CO_2, regenerating the hydride (Scheme 13). The optimum results were obtained in a pressure vessel (3 M aqueous sodium formate solution at pH 8, 0.37 mM methoxy catalyst, 296 K, λ_{ex} 443 nm, initial TOF > 50 h^{-1}, TON > 500 over 30 h, TOF = turnover frequency, TON = turnover number) giving 5 atm pressure.[112]

The rhodium porphyrin complex Rh^I(tetrakis(4-methoxyphenyl)porphyrin) reacts photocatalytically in the presence of silanes $SiHR_3$ in THF/H_2O solutions to generate silanols. Because the rhodium iodide complex reacts immediately with silanes to form rhodium hydrides, it is postulated that the photoactive species is [RhH(porphyrin)], which undergoes Rh−H homolysis. The full photocatalytic mechanism is shown in Scheme 14.[113]

There are also a number of catalytic reactions that depend on metal hydrides as absorbers to generate coordinatively unsaturated species for hydrogenation/dehydrogenation, hydrosilylation, etc. Two recent examples are illustrated here, one for arene borylation and the other for conversion of silanes to silanols. In keeping with the photosensitivity of *cis*-$[Fe(H)_2(dmpe)_2]$, it may also be used as a photocatalyst. The borylation of arenes by HBpin (pin = pinacolate 1,2-$O_2C_2Me_4$)

DOI: 10.1021/acs.chemrev.6b00204
Chem. Rev. 2016, 116, 8506−8544

Scheme 13. Proposed Catalytic Cycle for Photochemical Dehydrogenation of Formic Acid by $[Cp^*IrH(bpy)]^+$ (Reproduced with Permission from Ref 112; Copyright 2015 American Chemical Society)

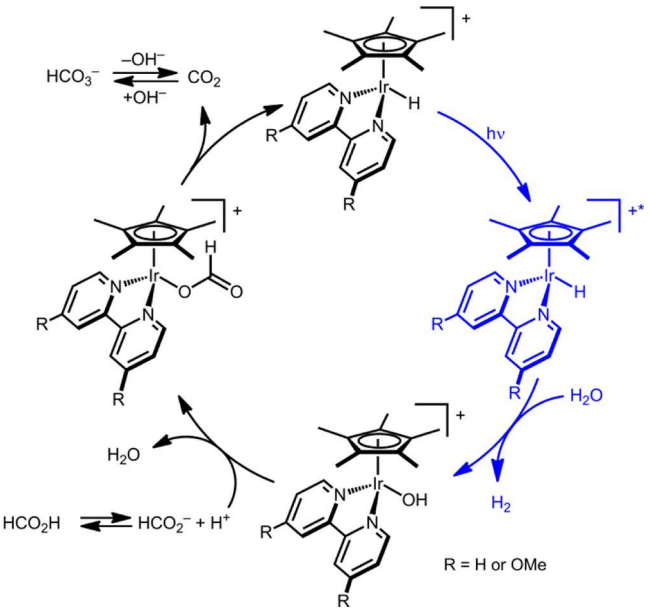

Scheme 14. Proposed Mechanism of Catalytic Hydrolysis of Silanes by Rhodium Porphyrin (Reproduced with Permission from Ref 113; Copyright 2015 American Chemical Society)

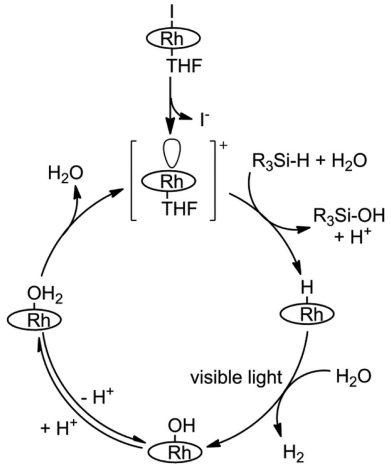

proceeds with 5 mol % catalyst and 350 nm radiation, although the performance of *cis*-$[Fe(Me)_2(dmpe)_2]$ is better. Stoichiometrically, both generate cis and trans isomers of $FeH(dmpe)_2(Bpin)$. The boryl hydride complex is also photocatalytically active. It seems likely that more than one species acts as a light absorber in the catalytic reaction.[114] The dppe complex *cis*-$[Fe(H)_2(dppe)_2]$ was inactive for borylation but showed activity as a precatalyst for the photolytic hydrosilylation of aldehydes and ketones.[115] The mechanistic details are unclear, so we cannot be certain whether these reactions represent photoinduced catalysis or photoassisted catalysis.

2.6.3. Photosensitized Catalysis. There are many examples of photosensitized catalysis in which metal hydrides are postulated in the catalytic cycle, although usually they are not the immediate electron acceptors. The principles are set out in other reviews[13,16] but are illustrated schematically in Figure 3.

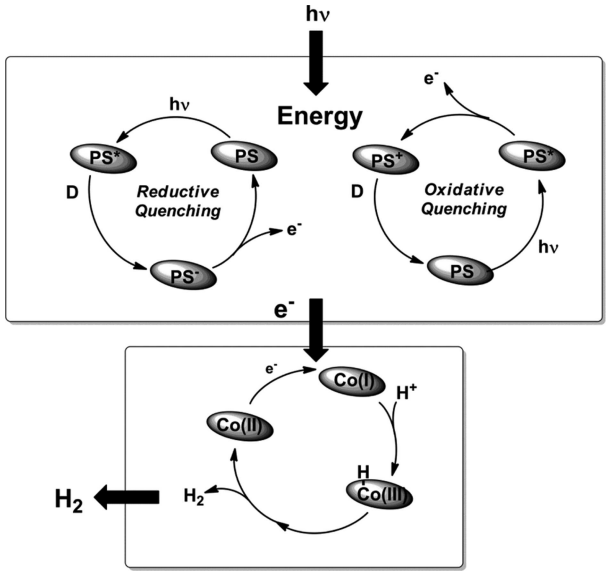

Figure 3. General scheme for photosensitized catalysis of hydrogen evolution by cobalt complexes; PS = photosensitizer, D = donor. Adapted with permission from ref 13. Copyright 2011 John Wiley and Sons.

2.6.4. Photoelectrocatalysis. An alternative strategy is to use photoelectrocatalysis, such that light is absorbed by the electrode. Following studies of its electrochemistry, $[Mo(H)_2(\kappa^2\text{-}O_2CMe)(dppe)]^+$ was investigated in CH_3CN with added acetic acid with a *p*-type silicon photoelectrode. Photocatalysis is sustained for >65 h, giving turnover numbers greater than 120. The maximum efficiency of conversion of photon energy to chemical energy is 2.8%. The proposed mechanism is shown in Scheme 15.[86]

Photoelectrocatalytic conversion of water to H_2 was also investigated with $[Cp^*Ir(bpy)Cl]Cl$ as catalyst. The reaction was investigated by examining the electrochemistry and the photochemistry in turn. Controlled potential electrolysis generates the hydride $[Cp^*Ir(bpy)H]^+$ (Figure 4); the resulting hydride was

Scheme 15. Proposed Mechanism of Photoelectrocatalysis of H_2 Production by $[Mo(H)(O_2CMe)(dppe)]^+$; The dppe Ligands Are Omitted (Reproduced with Permission from Ref 86; Copyright 2012 John Wiley and Sons)

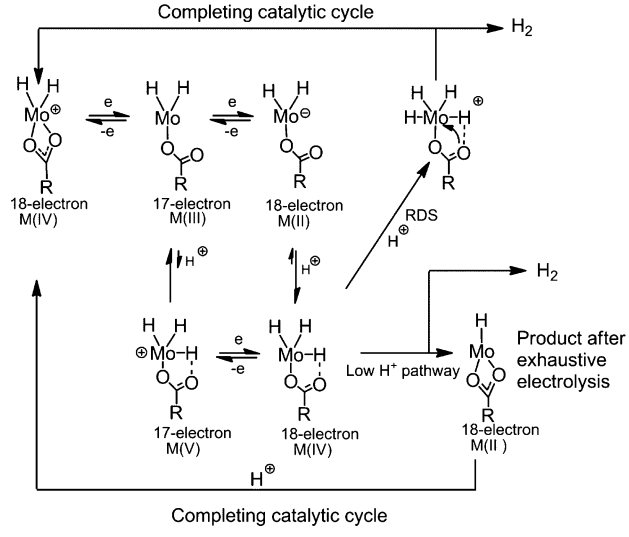

DOI: 10.1021/acs.chemrev.6b00204
Chem. Rev. 2016, 116, 8506−8544

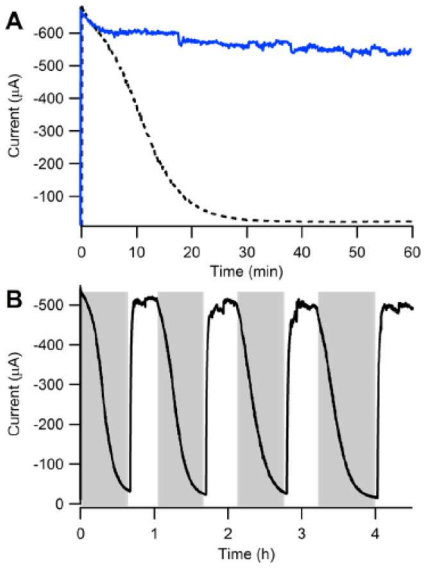

Figure 4. (A) Controlled potential electrolysis at −1 V vs NHE of [Cp*Ir(bpy)Cl]Cl in 0.1 M phosphate buffer at pH 7 in the dark (dashed black) and under 460 nm irradiation (solid blue). (B) Same but at −0.9 V with light off (gray) and light on (white). Reproduced with permission from ref 19. Copyright 2014 American Chemical Society.

photolyzed, generating H_2 and the initial iridium chloride cation. Full photoelectrocatalysis involves the iridium hydride acting as light absorber and catalyst, not the electrode. The performance was improved with 4,4′-bpy$(CO_2H)_2$ giving the following results with 460 nm radiation: rate constant 0.1 s^{-1} at 100 mV overpotential buffered at pH 7. The external quantum efficiency was ca. 10%. Again, the catalysis depends on excited-state hydricity with a similar photocycle to that for the formate reaction.[19]

3. SPECIALIST PHOTOCHEMICAL METHODS FOR REACTIVE INTERMEDIATES AND MECHANISM

Photochemistry is exceptionally well-suited to the study of highly reactive molecules and can reveal their electronic and molecular structure as well as their reactivity in far more detail than conventional thermal methods. When a metal dihydride complex is irradiated in the presence of dissolved hydrogen, a reversible degenerate reaction is set up in which the hydrides are removed photochemically and reformed thermally. Time-resolved spectroscopy allows detection of reaction intermediates and measurement of the rates of their reaction with H_2. Alternatively, the rate of oxidative addition of other element−hydrogen (E−H) bonds may be determined (Scheme 16). The application of such methods to metal hydride photochemistry is of particular relevance to catalytic reactions that involve hydrogenation or hydroformylation and also to reactions involving the oxidative addition of E−H bonds. The principal detection methods for

Scheme 16. General Scheme for the Photoinduced Reductive Elimination of H_2 and Kinetics of H_2 or EH Oxidative Addition

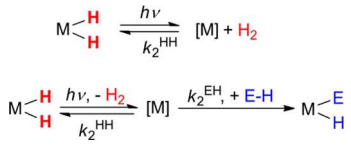

time-resolved spectroscopy of relevance to metal hydrides are UV−vis and IR spectroscopy, but time-resolved NMR spectroscopy is beginning to make a mark in conjunction with *para*-hydrogen enhancement. Examples of the use of time-resolved spectroscopy on the photochemistry of $Ru(H)_2(dmpe)_2$ have already been described (section 2.2.1).

Matrix-isolation methods[24,25,116−119] have seen particular success in two different approaches, the photochemistry of stable metal hydride complexes embedded in low-temperature matrices and the formation and photochemical reactivity of very small molecules by co-condensation of metal atoms with hydrogen sources together with noble gases. For some reaction intermediates such as $[Ru(dmpe)_2]$, matrix isolation and time-resolved spectroscopy have proved to be complementary methods (section 2.2.1). For others, matrix photochemistry of metal hydrides is unique; it remains the only method of direct study. Examples include rhenocene[52,54,120] generated by photolysis of Cp_2ReH and $(H)_2Mo{=}(CH_2)$ generated by photolysis of the metal vapor product $HMo(CH_3)$ (see section 4.3).[121]

Photochemistry of stable hydride complexes in matrices has yielded extensive spectroscopic information about reaction intermediates such as $[Cp_2W]$ and $[Ru(dmpe)_2]$ as well as information about the photochemical processes (section 2.2.1).[23,24] The condition for isolation of stable molecules such as $Cp_2W(H)_2$ in matrices is that they may be sublimed or vaporized with minimal decomposition so that they may be co-condensed with noble gases or more reactive matrices such as N_2, CH_4, or CO. They may then be examined by UV−vis, IR, laser-induced fluorescence (LIF), resonance Raman, EPR, and magnetic circular dichroism (MCD) spectroscopy with only slight perturbation or spectroscopic interference from the matrix material. The matrix is irradiated after deposition with conventional sources or with low power lasers. Often, the coordinatively unsaturated species generated on initial photolysis exhibit a long-wavelength absorption band and will recombine on selective irradiation into this band. Although pure H_2 cannot be condensed under high vacuum at the typical operating temperatures of 8−20 K, substantial proportions of H_2 can be incorporated into an argon matrix. If the temperature is lowered to 4 K, however, pure H_2 can be condensed successfully.[122] Several studies of metal hydride complexes have also been reported using hydrocarbon matrices at 77 K in conjunction with IR spectroscopy for compounds that cannot be sublimed but are soluble in hydrocarbons.[123]

Co-condensation of metal vapor with mixtures of hydrogen sources and noble gases has proved to be an effective method for studying binary metal hydride complexes and small molecules with M−H bonds, including their photochemistry. The metal vapor may be generated by effusion from an oven, or nowadays more often by laser ablation. The hydrogen source may be H_2 itself or alternatives such as methane or hydrogen chloride, which give access to species such as $HM(CH_3)$ or HM(Cl), respectively.[121,124] Often, photolysis of the matrix-isolated metal atoms is required to induce reaction in the matrix. Early work has been reviewed previously.[25,116] The methods are illustrated by the reactions of molybdenum atoms with methane at 8 K (2% in Ar); the products are identified by IR spectroscopy with extensive isotope labeling, assisted by DFT calculations.[121] Long-wavelength photolysis converts the initially generated $HMo(CH_3)$ to $(H)_2Mo{=}(CH_2)$, which is converted in turn to $(H)_3Mo{\equiv}(CH)$; short-wavelength photolysis reverses the process. In many of the papers reviewed here, photochemistry

DOI: 10.1021/acs.chemrev.6b00204
Chem. Rev. 2016, 116, 8506−8544

is used simply as a means of grouping bands and assisting in assignment. It is important to note that there is some radiation generated in the laser ablation process, so the initial spectra may have resulted in part from photochemical reactions.

3.1. Spectroscopic Methods for Time-Resolved Spectroscopy and Matrix Isolation

In this section, we illustrate the application of different spectroscopic methods in conjunction with time-resolved spectroscopy and matrix isolation, placing emphasis on opportunities with new and improved techniques, such as time-resolved IR spectroscopy and NMR with *para*-hydrogen enhancement.[125]

3.1.1. IR Spectroscopy. Metal hydride stretching vibrations range from ca. 2200 cm^{-1} for some terminal platinum hydride complexes[126] to ca. 1400 cm^{-1} for some terminal titanium hydrides,[127] with much lower frequencies for bridging metal hydrides. Metal hydride stretching frequencies exhibit a very strong dependence on the metal as well as on the ligand environment. The frequencies typically increase from first to second to third row of the transition metals, as illustrated by the M−H stretching frequencies of $HM(CH_3)$: M = V, 1534 cm^{-1}; M = Nb, 1611 cm^{-1}; M = Ta, 1726 cm^{-1}.[128] The increases in M−H stretching frequencies of related $Cp_2M(H)_n$ complexes from left to right as well as down a transition metal group have been noted.[129] Information about ligand effects on the IR spectra of rhodium hydrides has also been collected.[130] There is usually very little difference between symmetric and antisymmetric stretching modes of *cis*-$M(H)_2$ groups. There would be opportunities to parametrize M−H stretching frequencies, especially with improved DFT methods, as little has been done since 1986.[129] Infrared spectra showing M−H stretching bands of metal hydrides have proved important in following the evolution of reactions in low-temperature matrices, but they are often complicated by the presence of multiple conformers or matrix sites.[59,63,131,132]

Matrix IR spectra can also reveal many other aspects of the photoreactions because they can be recorded across the full frequency range, for example, showing the vibrations of $(H)_2Mo{=}(CH_2)$ or the characteristics of a parallel ring metallocene.[121,131] Of particular importance is the sensitivity of CO stretching vibrations of metal carbonyls to a change in oxidation state. For example, the ν(CO) band of $CpIr(H)_2(CO)$ appears at 2021.6 cm^{-1} in argon matrices. On photolysis, $CpIr(H)_2(CO)$ undergoes reductive elimination generating [CpIr(CO)] with a ν(CO) band at 1954.4 cm^{-1}, a shift of 67 cm^{-1} resulting from the change from Ir^{III} to Ir^{I}.[133] This complex does not undergo photochemical CO loss at all. In contrast to the behavior in argon matrices, photolysis in methane matrices revealed a product band at 2006.6, shifted only 11 cm^{-1} from the position of $CpIr(H)_2(CO)$ in the same matrix that is readily assigned as an Ir^{III} product, $CpIrH(CH_3)(CO)$.

Time-resolved IR spectroscopy has played a part in understanding the photochemistry of metal hydrides in solution, but M−H stretching modes have not been detected because of their low absorption coefficients. Instead, time-resolved IR studies have focused on CO-stretching modes of metal carbonyl hydrides. Ultrafast IR spectroscopy of $Ru(H)_2(PPh_3)_3(CO)$ established that reductive elimination of H_2 occurs within 6 ps of the initial laser pulse, by observing the 98 cm^{-1} shift in the ν(CO) band from 1941 cm^{-1} for the precursor to 1843 cm^{-1} in the $[Ru(PPh_3)_3(CO)]$ transient.[134] The recombination of $[Ru(PPh_3)_3(CO)]$ with H_2 could be followed by time-resolved IR spectroscopy and time-resolved absorption. There have been major improvements in ultrafast IR spectroscopy in recent years, as is illustrated by the study of the hydrogenase analogue containing a bridging hydride, $[Fe_2(\mu\text{-H})(CO)_4(dppv)(\mu\text{-pdt})]^+$. Excitation at 572 nm resulted in formation of a product with three ν(CO) bands that was formed within <1 ps and exhibited a lifetime of ca. 140 ps (Figure 5). This species was

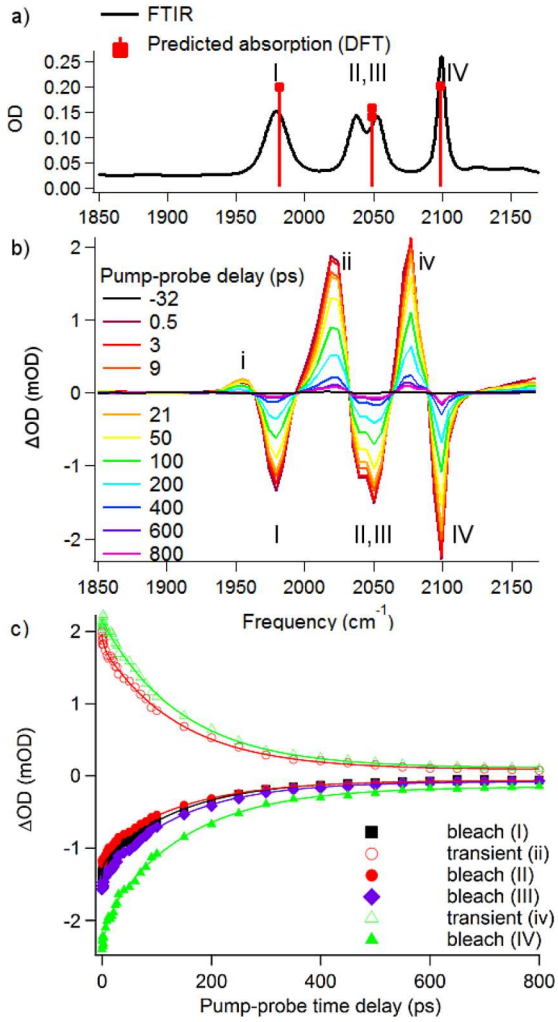

Figure 5. Time-resolved IR study of $[Fe_2(\mu\text{-H})(CO)_4(dppv)(\mu\text{-pdt})]^+$. (a) Fourier transform infrared (FTIR) spectrum solution in CH_2Cl_2 (10 mM). Red squares and droplines represent the DFT-calculated absorption frequencies. (b) Time-resolved infrared (TRIR) (λ_{ex} 572 nm) difference spectra at a range of pump−probe delay times (ps). (c) Time dependence of the amplitudes of peaks in TRIR spectra. Solid lines display fits of an exponential function. Reproduced from ref 135. Copyright 2014 American Chemical Society.

distinguished from hot bands of the precursor with the aid of IR pump−IR probe experiments. The product was assigned as a CO-loss species with the aid of DFT calculations.[135] This result was at odds with the observation of photoinduced H_2 loss observed previously.[18] With the improvements in sensitivity of time-resolved IR spectroscopy, it may soon be possible to follow ν(M−H) bands in solution in favorable cases.

3.1.2. UV−Vis Absorption and Emission Spectroscopy and Allied Methods. In this section, we are concerned with the use of UV−vis absorption spectroscopy and related techniques for the characterization of reaction intermediates derived from

DOI: 10.1021/acs.chemrev.6b00204
Chem. Rev. 2016, 116, 8506−8544

metal hydride complexes. Matrix isolation has the benefit of providing UV−vis and full-range IR spectra, measured with conventional high-resolution spectrometers. UV−vis and IR spectra may be measured under the same conditions to aid assignment. The method also benefits from access to variable-wavelength photochemistry applied to the reaction intermediates. On the other hand, it is not possible to determine the kinetics of reaction of the intermediates, and moreover, matrix isolation does not stabilize excited states. In time-resolved absorption studies, both the spectra and kinetics of the reaction intermediates and excited states are accessible. The kinetics may be determined continuously, as illustrated by the transient decay of $[Ru(BPE)_2]$ derived from $Ru(H)_2(BPE)_2$ (Figure 6, BPE = 1,2-bis(2,5-dimethylphospholano)ethane), and the spectra are derived point-by-point.[136] Alternatively, spectra are derived continuously and kinetic decays by point-to-point methods. In practice, it has only proved possible to detect electronic excited states of metal hydrides in exceptional cases, such as $Mo(H)_4(dppe)_2$ (section 2.3) and $Cp^*IrH(bpy)^+$ (section 2.1.4), because most excited states undergo dissociation within the instrumental response time.

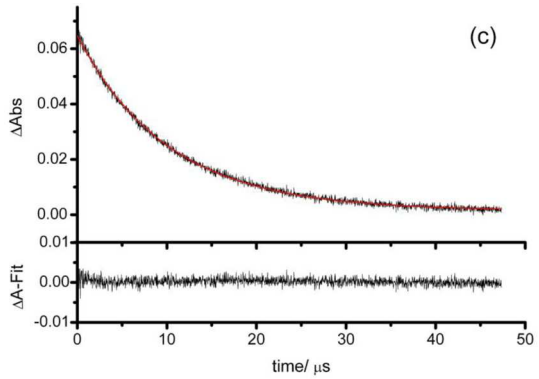

Figure 6. (Above) Transient decay after photolysis of $Ru(H)_2(BPE)_2$ (BPE = 1,2-bis(2,5-dimethylphospholano)ethane) under hydrogen recorded at 500 nm (black line). The fitted exponential decay is shown in red. (Below) Difference between the experimental data and the fitted line. Reproduced with permission from ref 136. Copyright 2012 American Chemical Society.

The major absorption features of most metal mononuclear metal hydride complexes lie in the UV−vis part of the spectrum. In contrast, many coordinatively unsaturated intermediates exhibit rich visible absorption bands. This point is illustrated by the spectra of $Os(H)_2(dmpe)_2$, which is colorless and exhibits broad, featureless UV spectra. On the other hand, the matrix photoproduct $[Os(dmpe)_2]$ shows several absorption bands in the visible and one band in the near-IR at 798 nm.[68] The transient absorption spectrum of $[Os(dmpe)_2]$ measured in solution at 294 K 100 ns after the laser flash is remarkably similar to the methane matrix spectra measured at 12 K (Figure 7), demonstrating the complementarity of the methods. The visible absorption peaks can be used to measure reaction kinetics (Figure 8). In the absence of matrix spectra, evidence for the nature of the reaction intermediate may be obtained by using multiple precursors as illustrated by the transient photochemistry of $Rh(H_2)(PCP)$ and related complexes (Scheme 8).[98] Ultrafast transient absorption spectroscopy has been used very effectively to monitor the formation of the triplet excited state of $[Cp^*IrH(bpy)]^+$ and its subsequent deprotonation.[10]

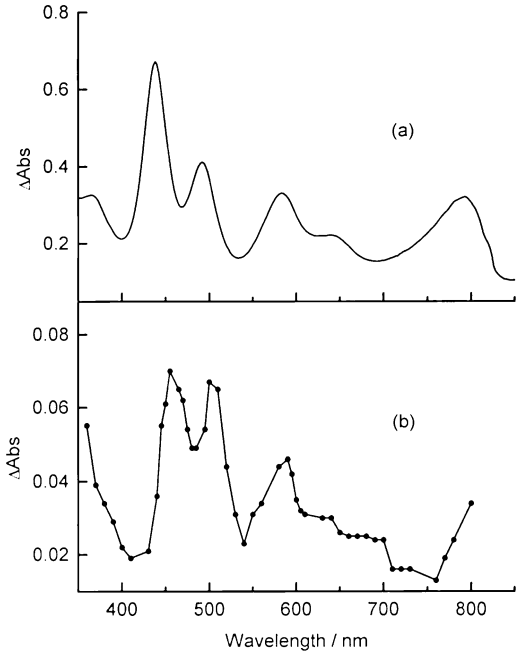

Figure 7. Visible spectra of $[Os(dmpe)_2]$ (a) in CH_4 matrix at 12 K and (b) in cyclohexane solution at 294 K by transient absorption spectroscopy measured 100 ns after laser flash (λ_{ex} 266 nm). Reproduced with permission from ref 68. Copyright 1998 American Chemical Society.

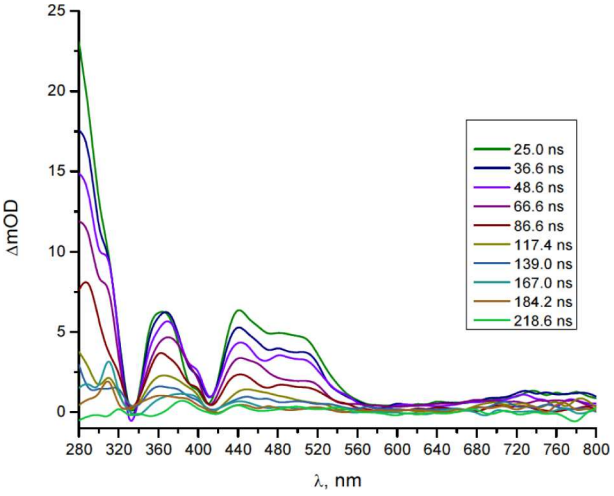

Figure 8. UV−vis transient absorption spectra obtained at specified time delays after 355 nm laser flash photolysis of $Rh(H_2)(PCP)$ in *n*-heptane under H_2 at 298 K (see also Scheme 8). Reproduced with permission from ref 98. Copyright 2013 American Chemical Society.

Matrix isolation also allows the measurement of emission and magnetic circular dichroism. The low temperature combined with the low dielectric host can lead to exceptionally sharp absorption and emission spectra for matrix-isolated molecules, as exemplified by rhenocene. The photolysis of Cp_2ReH in argon or nitrogen matrices leads to Re−H homolysis and formation of $[Cp_2Re]$, which exhibits very prominent emission spectrum due to ligand-to-metal charge transfer with an emission lifetime of ca. 72 ± 1 ns in solid nitrogen (Figure 9). Both the fluorescence spectrum and the corresponding excitation spectrum are fully vibrationally resolved with progressions in the symmetric Cp−Re−Cp stretching mode.[120] The magnetic properties of the same

DOI: 10.1021/acs.chemrev.6b00204
Chem. Rev. 2016, 116, 8506−8544

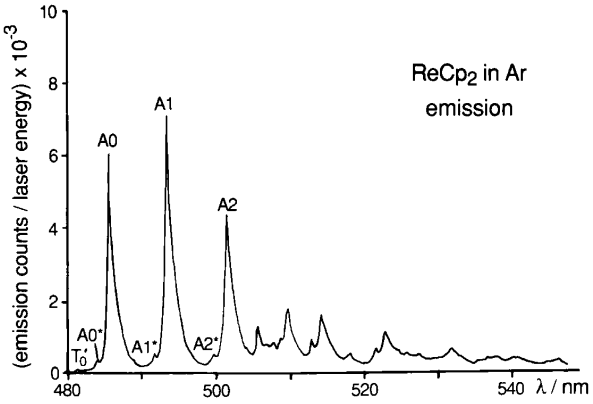

Figure 9. Laser-induced fluorescence spectrum of [Cp_2Re] obtained following UV photolysis of Cp_2ReH in an argon matrix at 12 K excited with λ_{ex} = 470.0 nm. A0, A1, and A2 refer to members of the vibrational progression in ν(Cp−Re−Cp). Reproduced with permission from ref 120. Copyright 1995 American Chemical Society.

molecules were determined by MCD in nitrogen matrices, leading to a value of $g_{\parallel}$ of 5.3 ± 0.4, consistent with a $^2E_1$ ground state.[52]

3.2. NMR Spectroscopy and *para*-Hydrogen Enhancement

The photochemical hydrogen cycle (Scheme 16) lends itself to the use of ^{1}H NMR spectroscopy for the study of metal hydrides. Dissolved dihydrogen itself may be detected by NMR spectroscopy (δ 4.45 in C_6D_6) and readily distinguished from HD by the prominent coupling (J_{HD} = 42 Hz). Photochemical reactions may be followed effectively by use of in situ methods where the sample is irradiated within the probehead either by white light from an arc lamp or by monochromatic laser irradiation. Examples include the photoisomerization of $Ru(H_2)(CO)(NHC)(PPh_3)_2$ (section 2.2.2)[78] or the generation of a photostationary state between $W(H)_4(dppe)_2$ and $W(H)_6(dppe)(\kappa^1\text{-dppe})$ by low-temperature irradiation under H_2.[94] The photochemical kinetics of reaction of $Tp'Rh(H)_2(PMe_3)$ (Tp′ = tris(3,5-dimethyl-1-pyrazolyl)borate) with HBpin and with $PhSiH_3$ were determined by laser photolysis within the probe, demonstrating that the reaction is zero order with respect to substrate concentration.[137] Competition reactions with two substrates revealed the relative rates of reaction of the [$Tp'Rh(PMe_3)$] intermediate with different substrates.

The ^{1}H NMR spectra obtained through the photochemical hydrogen cycle can be enhanced by the use of *para*-hydrogen if certain conditions are met. Hydrogen has two nuclear spin isomers, ortho and para; *para*-hydrogen is the antisymmetric nuclear spin isomer of H_2 (nuclear spin function $\alpha\beta - \beta\alpha$), which is a nuclear spin singlet and therefore NMR-silent.[125] Nevertheless, if it undergoes oxidative addition to a metal complex in a concerted manner to generate a metal dihydride such that the two hydride nuclei are chemically or magnetically inequivalent, the spectrum may be strongly enhanced. The "hyperpolarized" NMR spectrum formed in this way typically shows an absorption-emission (or emission-absorption) profile as a consequence of the overpopulation of the nuclear spin states formed in the addition process. The principle is illustrated by the example of $Ru(H)_2(PPh_3)_3(CO)$ in Figure 10. This *para*-hydrogen induced polarization (PHIP) effect may be optimized by use of a 45° *rf* pulse leading to signal enhancements of several thousand. The enhancement may also be transmitted through to

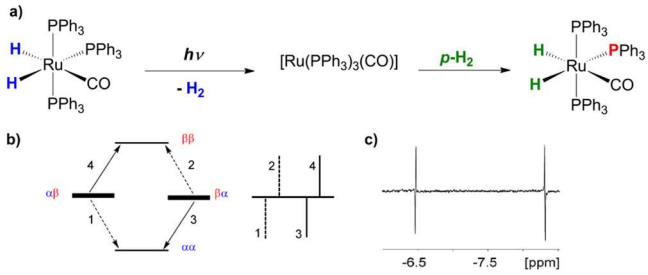

Figure 10. (a) $Ru(H)_2(PPh_3)_3(CO)$ as example of incorporation of *p*-H_2 into a metal dihydride complex by photochemical reductive elimination and susbequent thermal oxidative addition of *p*-H_2. (b) Energy level diagram for nuclear spin states for two coupled ^{1}H nuclei, showing overpopulation (thick bars) of $\alpha\beta$ and $\beta\alpha$ states as a consequence of incorporation of *p*-H_2. (c) $^1H\{^{31}P\}$ NMR spectrum in the hydride region for $Ru(H)_2(PPh_3)_3(CO)$ after addition of *p*-H_2, showing *p*-H_2 enhancement and emission-absorption pattern. Reproduced from ref 7. Copyright 2014 American Chemical Society.

organic hydrogenation products. It may last long enough to obtain COSY spectra, and the polarization may be transmitted through to heteronuclei.

This approach has been demonstrated in several examples including the photoisomerization of $Ru(H)_2(CO)(NHC)(PPh_3)_2$ (Figure 2). Here photolysis in situ under *para*-H_2 results in the immediate formation of two new isomers with enhanced hydride resonances, one with chemically inequivalent hydrides and the other with magnetically inequivalent hydride resonances.[78] In another striking example, in situ laser irradiation of $Ru(H)_2(Duphos)_2$ (Duphos = 1,2-bis(2,5-dimethylphospholano)benzene) in the presence of *para*-H_2 results in strong enhancement of the hydride resonances of the magnetically inequivalent hydrides and also simplification of the hydride signals resulting from the overpopulation of selected energy levels. Transfer of polarization to phosphorus enhances the signal from the ^{31}P nuclei trans to hydride.[136] This PHIP enhancement is characteristic of concerted oxidative addition of H_2. However, the absence of PHIP enhancement should not be taken as evidence of a nonconcerted pathway because the enhancement may be prevented by rapid nuclear spin relaxation associated with an electronic triplet-state intermediate found for iron complexes or with a dihydrogen complex as intermediate.[138] There are several examples of photodissociation of CO or N_2 under *para*-H_2 from metal carbonyls and metal dinitrogen complexes generating hydride complexes with enhanced NMR signals.[94,138,139] It is not yet clear whether these reactions also involve photochemical hydrogen cycling through light absorption by the dihydride complexes.

Most recently, the photochemistries of $Ru(H)_2(PPh_3)_3(CO)$ and $Ru(H)_2(dppe)_2$ in solution under a *para*-H_2 atmosphere have been investigated in laser pump−NMR probe experiments (Figure 11, above) in which a single pulse of a laser (355 nm) initiates dissociation of H_2.[7] Photodissociation of H_2 and reaction with *para*-H_2 result in the formation of both dihydride complexes in selected nuclear spin states, greatly increasing the sensitivity of NMR detection (Figure 10). Indeed, $Ru(H)_2(dppe)_2$ is now detected with a single 90° *rf* pulse, showing a very simplified spectrum in the hydride region with a greatly enhanced signal. Use of variable delays between the laser pulse and the *rf* pulse on the millisecond time scale reveals oscillations in the magnetization. For $Ru(H)_2(PPh_3)_3(CO)$, the oscillation frequency corresponds to the chemical shift difference between the inequivalent hydride resonances. For $Ru(H)_2(dppe)_2$, the

DOI: 10.1021/acs.chemrev.6b00204
Chem. Rev. 2016, 116, 8506−8544

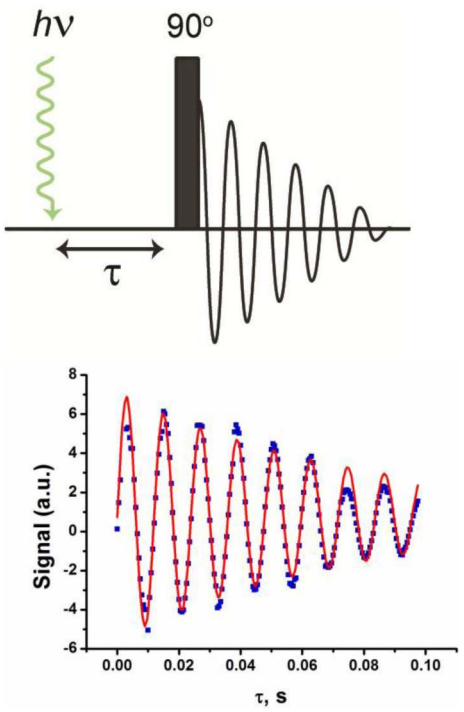

Figure 11. (Above) NMR pump−probe sequence used in the PHIP study. (Below) Integral of the hyperpolarized hydride signal of $Ru(H)_2(dppe)_2$ in a series of ^1H pump−probe NMR experiments acquired with increasing values of the pump−probe delay. Red line is a fit to a decaying sine-wave of 83.7 ± 0.1 Hz. Reproduced from ref 7. Copyright 2014 American Chemical Society.

hydrides are chemically equivalent but magnetically inequivalent and the oscillation frequency of 83 ± 5 Hz corresponds to the difference between the P−H spin−spin coupling constants $|J_{PHtrans} - J_{PHcis}|$ (Figure 11, below). Such oscillations have not been observed previously because the phase coherence of the spin states is lost. This method demonstrates that it is possible to use a laser pulse to generate NMR coherence, rather than one of the usual *rf* pulse sequences. Moreover, it reveals the connection between the oscillations in the *x*−*y* coherence and the coupling constants in a molecule exhibiting magnetically equivalent hydrides.

3.3. Computational Methods

Computational methods play a very important role in understanding photochemical reactions of metal hydrides.[25] The rapid advance of DFT theory means that it is straightforward to calculate the *ground-state* structures of reactants, intermediates, and products. We see such methods in use, for instance, in the identification of products in metal atom chemistry described in section 3.1.[121] In these applications, calculated IR spectra are of particular importance. One of the limitations of these methods is that they provide harmonic frequencies, although anharmonicity is likely to be significant in any vibrational modes involving M−H bonds. Methods are available for calculating anharmonic corrections with DFT theory, although they have not been applied to metal hydrides as far as we are aware.[140,141] When we move to calculating UV/vis spectra of metal hydrides, time-dependent DFT methods are appropriate and it is also possible to include the effects of spin−orbit coupling on the spectra, as illustrated for $HM(CO)_5$ (M = Mn, Re).[32] Such calculations clearly identify the order of excited states for vertical transitions. For example, the time-dependent density functional theory (TD-DFT) calculations on $HRe(CO)_5$ show two close-lying spin-allowed transitions to ^1E states at lowest energy, one of which is predominantly Re(5d) → π*(CO) in character, while the other is principally Re(5d) → σ*(Re−H).[32] Some authors go further and use complete active space or coupled cluster methods to calculate the spectra in order to account more effectively for configuration interaction and electron correlation.[142] A very recent comparative study of these methods applied to transition metal carbonyls, albeit not metal hydrides, found exceptional performance for TD-CAM-B3LYP (time-dependent Coulomb-attenuating method), which is a relatively low-cost method.[143] The requirements for modeling photodissociation are considerably more stringent because bond cleavage necessarily involves dynamic change of geometry and the relative energies of states are liable to change markedly during the process. Nevertheless, TD-DFT has proved to be very successful, notably in modeling the photodissociation of CO from metal hexacarbonyls via excitation into a ^{1}MLCT state and passage into a singlet ligand field state as it moves through an avoided crossing during dissociation.[144,145] A recent review surveys applications of time-dependent DFT to the photochemistry of transition metal complexes.[146] These and more demanding multiconfiguration methods have been compared in the context of transition-metal excited states.[147] A very striking advance is the coupling of molecular dynamics methods with TD-DFT to simulate photodissociation of H_2; this approach has been demonstrated for ruthenium dihydrides with a two-dimensional potential energy surface.[70] The importance of more sophisticated methods is apparent when looking at the details of the dissociation process, both in metal hydrides and metal carbonyls where there may be conical intersections.[22,75,148,149]

4. METAL HYDRIDE PHOTOCHEMISTRY BY TRANSITION METAL GROUP

In this section, we summarize a full range of metal hydride photochemistry, ordered primarily by transition metal group. The majority of the examples are to be found in groups 6−9, and for these groups, we subdivide into mono-, di-, and polyhydrides. In most sections, we arrange the examples by element within the group.

4.1. Group 4 Metals

Very few examples of photoactive complexes are reported for Ti, Zr, and Hf hydride species. Titanium atoms co-condensed with H_2 in Ar matrices formed the hydride species $Ti(H)_2$ and $Ti(H)_4$ under visible light, which decomposed under UV irradiation.[127] When the laser ablation method was employed with methane, $TiH(CH_3)$ was formed, which isomerized to (CH_2)═$Ti(H)_2$ on near-UV irradiation and was identified by isotopic labeling in conjunction with DFT calculations; the reaction was reversed with visible radiation.[150] Related experiments were reported on (CH_2)═$Zr(H)_2$ and (CH_2)═$Hf(H)_2$.[151,152] Matrix-isolation IR spectroscopy identified $Ti(O)(CH_4)$ as the product of co-condensing TiO with methane. This rearranged to $TiH(CH_3)$-(O) photochemically; the latter was capable of isomerization under UV light to yield the $TiH(CH_2)(OH)$ carbene complex. When a CH_4 molecule added spontaneously to the $TiH(CH_2)$-(OH) complex, a dimethyl $TiH(CH_3)_2(OH)$ was formed that could also be obtained via UV photorearrangement of the $TiH(O)(CH_3)(CH_4)$ species.[153]

The first complexes of group 4 to be investigated photochemically were $Cp^*_2Zr(H)_2$ and $Cp^*_2ZrH(R)$ (R = alkyl or aryl); the dihydride underwent slow H_2 photoejection with near-

DOI: 10.1021/acs.chemrev.6b00204
Chem. Rev. 2016, 116, 8506−8544

UV radiation and the fragment formed inserted into the C−H bond of benzene. Similar reactivity is shown by the alkyl hydride analogue but in this case alkane reductive elimination was observed upon irradiation. The quantum yield of Cp^*_2ZrH(alkyl) was higher than that of $Cp^*_2Zr(H)_2$. Crossover and isotopic labeling demonstrated that the reductive elimination occurs by an intramolecular mechanism.[35] Photolysis of $(\eta^5$-$C_5Me_4H)_2ZrH$(aryl) was exploited in a preparative way to form the zirconocene dinitrogen complex $[\{(\eta^5$-$C_5Me_4H)_2Zr\}_2(\mu^2,\eta^2,\eta^2$-$N_2)]$ through arene reductive elimination.[154]

4.2. Group 5 Metals

The photochemistry of group 5 is also very limited. Investigations of the metal atom chemistry have been carried out on the three metals in the presence of CH_4 in excess argon. All of the metals formed hydride complexes by CH_4 activation; the Nb and Ta products were found to convert to higher-order products of the formula $(CH_3)_2M(H)_2$ upon further photolysis.[128]

Both $Cp_2Nb(H)_3$ and $Cp_2Ta(H)_3$ complexes were irradiated in aromatic solvents and found to yield the photogenerated intermediates $[Cp_2MH]$ (M = Nb, Ta) as a consequence of H_2 photoejection. The monohydrides $Cp_2MH(CO)$ (M = Nb, Ta) were also investigated photochemically and were found to follow the same reactivity.[155] The unsaturated species displayed reactivity toward CO, H_2, or PEt_3 to yield the substitution products and also proved able to insert into aromatic C−H bonds and catalyze H/D exchange. The PEt_3 substitution product was obtained just with the second-row metal (Nb) but not with third-row metal (Ta).[155] Similar behavior was observed for group 6 (section 4.3). Low-temperature matrix (Ar, N_2) studies followed; the identity of the transient $[Cp_2MH]$ (M = Nb, Ta) formed from H_2 loss as a primary photoprocess was confirmed by IR and UV−vis spectroscopy for photoreactions starting both from the trihydride and the carbonyl−hydride species. In the latter case, a small amount of the $17e^-$ complex $[Cp_2M(CO)]$ was also observed, suggesting that a minor amount of M−H homolysis took place.[156]

More recently the complex $\{(Me_2Si)_2(\eta^5$-$C_5H_4)_2\}Nb(H)_3$ was prepared and found to be very unstable both in solution and in solid state. However, irradiation in benzene-d_6 converted it to the dimeric analogue $[(Me_2Si)_2\{\mu$-$(\eta^1{:}\eta^5$-$C_5H_3)\}(\eta^5$-$C_5H_4)NbH]_2$; H_2 photoelimination was proposed as the primary photoprocess.[157]

4.3. Group 6 Metals

The hydrides of the group 6 metals provide several of the paradigms, especially for autocatalytic M−H homolysis, for H_2 elimination from $Cp_2M(H)_2$ (M = Mo, W), and for the effect of constraining cyclopentadienyl rings with a link between them (the *ansa* effect).

4.3.1. Group 6 Monohydrides. The main photochemical process in the solution photochemistry of the anionic $[M_2(\mu$-$H)(CO)_{10}]^-$ (M = Cr, W) was shown to be CO loss, and the M−H−M bonding network was not involved in the photochemistry.[158] The $CrH(CO)_5^-$ anion was reported to produce the radical $Cr(CO)_5^-$ as a damage product of γ-radiation, suggesting M−H bond homolysis.[159] The photochemistry of $CpCrH(CO)_3$ was studied in gas matrices at 12 K, and CO photoejection postulated as the initial step of the photoreaction at wavelengths between 290 and 370 nm; reversibility was observed on irradiation at $\lambda > 370$ nm. Photolysis in CO matrices led to the formation of the HCO radical, indicating Cr−H cleavage under these conditions. Solution photochemistry at room temperature formed the dimer $[Cp_2Cr(CO)_2]_2$ along with CO and H_2 production.[160] The irradiation of $(\eta^5$-$C_5H_4PPh_2)$-$CrH(CO)_3$ with broadband photolysis was employed as a preparative method to obtain the dimer $[(\mu,\eta^5$−$C_5H_4PPh_2)Cr$-$(CO)_2]_2$, but competition between decarbonylation and dehydrogenation afforded a mixture of products.[161]

The molybdenum hydride $CpMoH(CO)_3$ showed the same behavior in matrix photochemistry as the Cr analogue, but it proved less photoactive in solution photochemistry. The major product after prolonged photolysis was characterized as $[CpMo(CO)_3]_2$ derived from dehydrogenation; a minor product arisen from decarbonylation was also detected.[160,162] Further investigations on the same complex in C_2H_4-doped CH_4 matrices were performed to elucidate the hydroformylation mechanism. The $16e^-$-intermediate, $CpMo(CO)_2H$, was observed together with the cis and trans isomers of the ethylene adduct; secondary photolysis of this species led to olefin insertion to form $CpMo(CO)_2(C_2H_5)$.[162,163] Photolysis of $CpMoH(CO)_3$ and $(\eta^5$-$C_5R_5)MoH(CO)_3$ (R = H, Me) in H_2-containing matrices yielded cis and trans isomers of $(\eta^5$-$C_5R_5)MoH(H_2)(CO)_2$ identified by IR analysis. All the steps in the formation of these products showed reversibility on changing the photolysis wavelength.[96] When D_2 was employed, H/D exchange was observed for the Cp complex through an isotopic shift of the $CpMoD(CO)_2$ bands.[164] The photochemical synthesis of the Mo dimer $[(\mu,\eta^5$-$C_5H_4PPh_2)Mo(CO)_2]_2$ from $(\eta^5$-$C_5H_4PPh_2)$-$MoH(CO)_3$ proceeded cleanly.[161] The photoreaction of $Cp^*MoH(\eta^6$-$C_5Me_4CH_2)$ is described together with that of $Cp^*_2Mo(H)_2$ below.

Experiments on the reactions of Mo atoms in matrices with CH_4 in excess Ar formed the hydride species $(CH_3)MoH$, $(CH_2){=}Mo(H)_2$, and $(CH){=}Mo(H)_3$. These compounds were found to reversibly interconvert by α-H transfer when irradiated with visible or UV light.[121] Photoreversibility was also determined for methylidene and methylidyne complexes of the type $(CH_2){=}MoHX$ and $(CH){=}Mo(H)_2X$ (X = F, Cl, Br, I) formed in similar experiments in the presence of methyl halides.[165] The reactivity of molybdenum atoms toward hydrogen is discussed under group 6 polyhydrides.

The tungsten monohydride, $CpWH(CO)_3$, undergoes CO substitution by PBu_3 on UV irradiation (311 nm) in a photoinduced catalysis reaction (section 3).[109] Following this first publication, numerous investigations on the photochemical behavior of this complex were undertaken in Ar, N_2, and CH_4 matrices containing $CpWH(CO)_3$ and $Cp^*WH(CO)_3$, and the intermediate formed from CO loss was trapped. Addition of two-electron donor ligands (L = N_2, C_2H_4) to the matrices led to $CpWH(CO)_2L$. As observed for Cr and Mo, CO matrix photochemistry led to the identification of the HCO radical indicating W−H bond cleavage.[162,163] Solution photochemistry of tungsten complexes proved to be the least efficient of the group; in addition to the products obtained for the Cr and Mo analogues, a dinuclear complex $[CpW(CO)_2(\mu$-$H)]_2$ was formed.[160,162] Solution photochemistry in the presence of ethylene also proved to be very similar; the olefin adduct *trans*-$[CpWH(CO)_2(C_2H_4)]$ was found to be photoactive and converted to the cis form before affording the insertion product $CpW(CO)_2(C_2H_5)$. Similar behavior was observed in ethylene-doped matrices.[162] Different results from the molybdenum analogues were obtained when H_2 matrices were investigated: both Cp and Cp* complexes afforded the dihydrogen adduct postulated to form via the CO loss intermediate $[CpWH(CO)_2]$,

DOI: 10.1021/acs.chemrev.6b00204
Chem. Rev. 2016, 116, 8506−8544

but unlike $CpMoH(H_2)(CO)_2$, they did not photoeject H_2 upon further photolysis but instead oxidatively added H_2 to yield $CpW(H)_3(CO)$.[96] $Cp_2WH(CH_3)$ also proved to be photoactive, ejecting CH_4 upon broadband photolysis in low-temperature Ar matrices to form $[Cp_2W]$.[131] The photoreaction of $Cp^*WH(\eta^6\text{-}C_5Me_4CH_2)$ is described together with that of $Cp^*_2W(H)_2$ below. The bimetallic species $Cp^*(CO)_2W(\mu\text{-}SiMe_2)(\mu\text{-}H)Re(CO)_2Cp^*$ was used to prepare silylene-bridged W−Re complexes through photoinitiation.[166] More recently, the dimeric compound $Cp_2W_2(H)(\mu\text{-}PCy_2)(CO)_2$ exhibited photoactivity in the presence of various metal carbonyl complexes (metal = Ru, Cr, Mo, W) to yield heterometallic compounds with either W_2M or W_2M_2 metal cores.[167] Reactions of methyl halides with W atoms generated (CH_2)═WHX and (CH)≡$W(H)_2X$ that showed photoreversibility by the use of either visible or UV light as mentioned earlier for the Mo analogues.[165]

4.3.2. Group 6 Dihydrides and Dihydrogen Complexes. There are no examples of chromium dihydride complexes investigated photochemically, but there are examples of photochemistry of dihydrogen adducts. The dihydrogen complex $Cr(H_2)(CO)_5$ was formed from UV photolysis of $Cr(CO)_6$ in H_2-doped Xe matrices. The reaction proved to be reversible under visible light irradiation (section 2.4). Short-wavelength photolysis led to CO loss and formation of $Cr(H_2)_2(CO)_4$.[95] Co-condensation of Cr metal and H_2 in Kr and Ar matrices produced the dihydrogen adduct $Cr(H_2)$. When H_2 was in excess, the latter was converted to the trihydride $Cr(H)_3$ by photolysis (520−580 nm).[168]

The scenario for molybdenum and tungsten is much richer than that for chromium, and there are close parallels in the behavior of the two elements. It is dominated by the photochemistry of $Cp_2M(H)_2$ (M = Mo, W) and their derivatives. The absorption spectrum of $Cp_2Mo(H)_2$ in solution shows bands at 270 and 310 nm. The gas-phase electronic absorption spectrum of $Cp_2Mo(H)_2$ gave a clearly defined Rydberg band, confirming that the HOMO is nonbonding.[49] The photoactivity of $Cp_2Mo(H)_2$ led to H_2 elimination in the primary photochemical step (quantum yield at 366 nm = 0.1 ± 0.02) to yield the transient unsaturated species $[Cp_2Mo]$ that was trapped in the presence of CO, C_2H_2, and PR_3 to form the respective adducts.[50,169] The photochemical reaction in C_6H_6 resulted in dimerization,[170] while irradiation in the presence of thiophene formed the C−H activated product Cp_2MoH(2-thienyl), selectively.[48] Reactions in the presence of hydridosilanes produced the silyl hydride complexes $Cp_2MoH(SiR_3)$ in very good yields through a reductive elimination/oxidative addition process; similar behavior was observed for the Cp* analogue.[55,56] Thus, molybdenocene inserts into Si−H bonds, but the only C−H bonds that prove reactive are those of thiophene and its own precursor $Cp_2Mo(H)_2$. The reactions in the presence of activated alkenes formed a series of electron donor−acceptor complexes with charge-transfer bands in the visible region. Irradiation into the charge-transfer band led to products; for example, $Cp_2MoH(CHCNCH_2CN)$ was formed on photolysis at >550 nm with fumaronitrile.[84] A more detailed explanation of this mechanism is given in section 2.2.4. The formation of clusters was achieved by photolysis of the $Cp_2Mo(H)_2$ in the presence of metal carbonyl dimers generating a series of homo and heterometallic complexes.[57]

UV photolysis of $Cp_2Mo(H)_2$ in an argon matrix at 10 K led to the formation of the metallocene $[Cp_2Mo]$, characterized by IR and UV/vis spectroscopy. The photoelimination of H_2 was described as concerted due to lack of detection of the HCO radical in CO matrices.[131,171] Photogeneration of the metallocene in matrices was exploited to generate the $[Cp_2Mo]$ fragment for optical determination of magnetization behavior; like $[Cp_2W]$, it has a triplet ground state.[52] Molybdenocene exhibits an LMCT absorption (origin at 420 nm) and laser-induced fluorescence from the same electronic state.[53,54] UV−vis transient photochemistry agreed with the matrix investigations; a transient species was detected that decayed in ca. 10 μs by reaction with CO or the parent complex and was assigned to $[Cp_2Mo]$.[172]

Photolysis of $Cp^*_2Mo(H)_2$ in pentane caused loss of H_2 and intramolecular C−H bond activation to form $Cp^*MoH(\eta^6\text{-}C_5Me_4CH_2)$, which in turn lost H_2 again to form $Cp^*Mo\{\eta^7\text{-}C_5Me_3(CH_2)_2\}$. The first product can be considered as having a tetramethylfulvene ligand or a "tucked-in" tetramethylcyclopentadienyl group with one coordinated alkyl ligand, while the second may be described an allyldiene or as doubly tucked-in (Scheme 17).[173] The irradiation of Cp'_2MoH_2 (Cp′ = η^5-$C_5H_4CH_3$) in H_2O/CH_3CN mixture afforded Cp'_2MoO and H_2 gas (2 equiv) quantitatively. The mechanism was proposed to start with H_2 reductive elimination to form the unsaturated fragment, which could then undergo H_2O activation and release the second equivalent of H_2.[174] The *ansa*-bridged molybdenocene dihydride $(\eta^5\text{-}C_5H_4)CMe_2(\eta^5\text{-}C_5H_4)Mo(H)_2$ proved to be photoactive when irradiated in C_6H_6 solutions, yielding the phenyl hydride product (Scheme 18). Thus, this *ansa*-bridged molybdenocene is capable of activating benzene C−H bonds whereas molybdenocene is not.[175] This observation illustrates the change in reactivity resulting from the bridge between the cyclopentadienyl rings, which is named the *ansa* effect. An investigation of the selectivity between the activation of C−H versus C−chalcogen bonds of furan, thiophene, and selenophene bonds was reported, exploiting the photochemical ability of *ansa*-$[Me_2Si(C_5Me_4)_2]Mo(H)_2$ to eliminate H_2 to form the *ansa*-metallocene. The reactivity toward the different substrates was found to be quite diverse: C−S insertion with thiophene, C−H insertion at both positions with furan but only at the 3-position with benzofuran, and C−Se insertion with selenophene (Scheme 18).[176,177] These experiments illustrate the strong effects of the *ansa* geometry. The metallocene 1,1-disilamolybdenocenophane was synthesized by the photochemical reaction of the dihydride analogue and H_2 reductive elimination with intramolecular Si−Si oxidative addition (Scheme 18).[178,179]

Scheme 17. Photolysis of $Cp^*_2M(H)_2$ (M = Mo, W, Re^+)

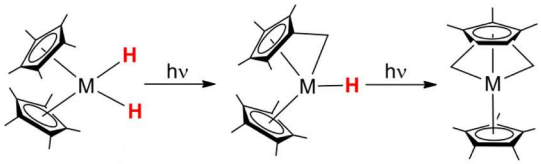

Dinuclear−dihydride complexes have also been the subject of photochemical investigations; $[\{CpMoH\}_2(\mu\text{-}\eta^5\text{-}C_5H_4\text{-}\eta^5\text{-}C_5H_4]$ converted into *cis*- and *trans*-$[\{Mo(\eta^5\text{-}C_5H_5)H\}_2(\mu\text{-}\sigma\text{:}\eta^5\text{-}C_5H_4)_2]$ and eventually yielded the $[\{Mo(\eta\text{-}C_5H_5)\}_2(\mu\text{-}\sigma\text{:}\eta^5\text{-}C_5H_4)_2]$. A mechanism was proposed for the generation of this latter complex where the first photochemical step induced a ring shift from η^5 to η^3, followed by hydride migration reminiscent of Scheme 3, allowing photoinduced H_2 elimination and ring shift back to η^5 coordination to afford the final product.[180] The cyclopentadienyl bridged complex [MoH-

DOI: 10.1021/acs.chemrev.6b00204
Chem. Rev. 2016, 116, 8506−8544

Scheme 18. Photoreactivity of *ansa*-Molybdenocene Complexes

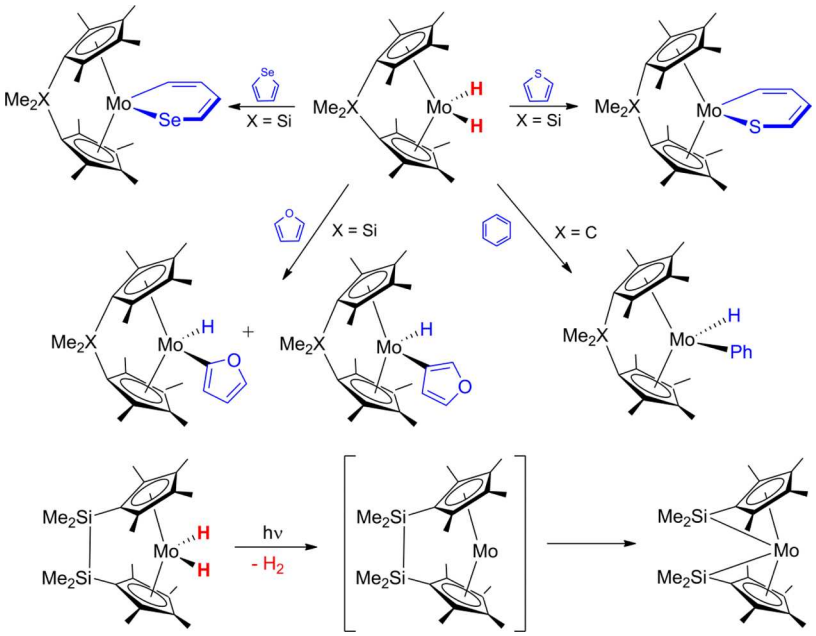

$(CO)_3]_2(\eta^5\text{-}\eta^5\text{-}C_5H_4CH_2C_5H_4)$ was stable in solution if kept in the dark but was reported to lose hydrogen if exposed to ambient light.[181] More recently, the quadruply bonded complex $[Mo_2(H)_2\{HC(N\text{-}2,6\text{-}{}^iPr_2C_6H_3)_2\}_2(THF)_2]$ was also found to be photoactive in arene solution, yielding products with $\eta^2\text{-}\eta^2$ bridging arenes. The product contains a d^5:d^5 MoMo quintuple bond that forms the interaction with the arene, as demonstrated by DFT calculations. Free H_2 was detected, confirming H_2 photoelimination as the primary photochemical step.[182]

The photochemistry of $Cp_2W(H)_2$ is summarized in section 2.2.1 and Scheme 4, and therefore a brief résumé will be given here. Photolysis of $Cp_2W(H)_2$ at 366 nm forms the transient tungstenocene by H_2 elimination with much lower quantum yield than the molybdenum analogue. Tungstenocene has never been observed in solution, only in matrices. It is capable of activating C−H bonds of arenes[2,44,183] and Me_4Si[44,45] but not alkanes. The same fragment was able to insert into MeOH to yield $Cp_2WH(OMe)$ and $Cp_2W(Me)(OMe)$ in a 1:5 ratio.[46] Photoreaction with ethyl acetate yielded $Cp_2WH(OCOEt)$, whereas reaction with carboxylic acids generated $Cp_2W(OCOR)_2$ (R= H, Me, Et, CH_2═CMe).[44,47] With thiophene, C−S bond cleavage was achieved as a primary photoproduct; prolonged irradiation converted the latter into the C−H insertion product $Cp_2WH(2\text{-thienyl})$.[48] A number of mono- and bis(silyl) complexes of W were obtained in good yields by photolysis at 350 nm of $Cp_2W(H)_2$ in hydridosilanes; Cp* derivatives were also prepared by the same method.[55,56] In the absence of substrates, dimers are formed resulting from activation of C−H bonds of the cyclopentadienyl groups.[170] The reaction of $Cp_2W(H)_2$ in the presence of M−M bonded complexes led to the formation of heterometallic clusters, but the presence of CO groups in the reagents made it unclear whether the photochemistry proceeds by H_2 reductive elimination from the tungsten precursor or CO loss from one of the dimers.[57] The photochemistry of the charge-transfer adducts of $Cp_2W(H)_2$ was summarized in section 2.2.4.[84]

Studies of the photochemistry of $Cp_2W(H)_2$ in low-temperature matrices[131,171] confirmed the formation of the $[Cp_2W]$ fragment by H_2 photoinduced concerted elimination; $[Cp_2W]$ was characterized by IR and UV/vis absorption, laser-induced fluorescence,[53,54] and magnetic circular dichroism[52,184] (see section 2.2.1 for details).

Irradiation of $Cp^*_2W(H)_2$ in pentane proceeded by loss of H_2 in two steps like the molybdenum analogue to generate $Cp^*WH(\eta^6\text{-}C_5Me_4CH_2)$ and $Cp^*W\{\eta^7\text{-}C_5Me_3(CH_2)_2\}$. When starting with $Cp^*_2W(D)_2$ no deuterium is incorporated into the solvent, consistent with $[Cp^*_2W]$ as the intermediate in the first stage of reaction.[173] The *ansa*-bridged tungsten dihydride $\{(\eta\text{-}C_5H_4)CMe_2(\eta\text{-}C_5H_4)\}W(H)_2$ is not photosensitive, unlike its molybdenum analogue.[175] The adduct $(i\text{-}C_3H_7C_5H_4)_2W(H)_2$-9,10-phenanthrenequinone was found to display a long-wavelength charge-transfer absorption at λ_{max} = 530 nm; irradiation into this band was claimed to result in H_2 transfer to the diol, but no evidence was presented.[185]

4.3.3. Group 6 Polyhydrides. In this section, we will treat analogous molybdenum and tungsten compounds together because of their close relationship. $Mo(H)_4$ was formed from the photochemical reaction of co-condensed H_2 and Mo atoms in Kr and Ar matrices at 12 K with $\lambda > 400$ nm; photoreversibility was obtained on irradiating at shorter wavelengths (320−380 nm) where $Mo(H)_4$ liberated H_2 and regenerated the dihydride species.[168] Similar experiments were also performed with H_2-doped noble gas matrices at 3.5 K and MoH, $Mo(H)_2$, $Mo(H)_4$, and $Mo(H)_6$ were obtained and found to interconvert photochemically.[186] The structures of $Mo(H)_2$, $Mo(H)_4$, and $Mo(H)_6$ are assigned as belonging to C_{2v}, T_d, and C_{3v} (trigonal prismatic) point groups, respectively, on the basis of the spectra and DFT calculations. Reaction of W atoms with H_2 in Ne matrices generated WH, $W(H)_2$, $W(H)_3$, $W(H)_4$, and $W(H)_6$ that were distinguished by wavelength-dependent photochemistry in addition to annealing, H_2 concentration, and isotopic shifts.[187] Observation of six fundamental vibrations, including four W−H stretching bands, provided good evidence for the C_{3v} trigonal prismatic structure of $W(H)_6$, consistent with the early predictions for d^0 ML_6.[188] Co-condensation of tungsten atoms with pure H_2 generated a species assigned as $W(H)_4(H_2)_4$ which was partially destroyed by UV photolysis.[189]

DOI: 10.1021/acs.chemrev.6b00204
Chem. Rev. 2016, 116, 8506−8544

The reactivity and features of $Mo(H)_4(dppe)_2$ have been already discussed in section 2.3.[21,87,88] Studies on $W(H)_4(dppe)_2$ took place in parallel with the molybdenum ones. The complex exhibited visible light emission if photoexcited at 77 K in 2-methyltetrahydrofuran, emission lifetime (absorption λ_{max} 400 nm, emission λ_{max} 590 nm, lifetime ca. 13 μs, compared to 87 μs for the Mo analogue). Stoichiometric reduction of alkenes was achieved when $M(H)_4(dppe)_2$ (M = Mo, W) was irradiated in the presence of such substrates; this process became catalytic when H_2 was added in excess.[87] Hydrogen loss was the sole photochemical process observed until very recently when H_2 addition and phosphine dechelation to form $W(H)_6(dppe)(\kappa^1$-dppe) was reported. In this investigation, *para*-H_2 was employed to improve NMR sensitivity (section 3.2).[94] Photocatalytic reduction of molecular nitrogen to ammonia and hydrazine has been demonstrated with $W(H)_4(dppe)_2$, $W(H)_4(PPh_2Me)_4$, and $W(H)_4(etp)(PPh_3)$ (etp = $PhP(CH_2CH_2PPh_2)_2$) as catalysts; light in this case was responsible for the H_2 elimination, which creates a free vacant site for the dinitrogen to coordinate.[190] Studies on $W(H)_4(PRPh_2)_4$ (R = CD_3, C_2D_5) also established H_2 loss as the primary photochemical step; the unsaturated species formed underwent intramolecular C−D insertion to form a metal−carbon bond with subsequent HD photoelimination.[191] Finally, the clusters $[\{(Cp''Y)_4(\mu\text{-}H)_7\}(\mu\text{-}H)_4MCp^*(PMe_3)]$ (M = Mo, W, Cp'' = η^5-C_5Me_4H) were found to undergo PMe_3 loss under UV irradiation.[192]

4.4. Group 7 Metals

The photochemistry of group 7 metals has been particularly valuable for M−H homolysis of monohydrides and for the photochemical interplay of dihydride with dihydrogen complexes.

4.4.1. Group 7 Monohydrides. Hydrido manganese pentacarbonyl was the first hydride complex to be investigated photochemically, but the original 1969 publication on photolysis in Ar matrices at 15 K only recognized CO loss to form $MnH(CO)_4$.[26] Many studies followed that uncovered more insights into the photoreactivity. Use of CO matrices at 10−20 K revealed that Mn−H bond homolysis was also obtained to yield HCO and the $[Mn(CO)_5]$ fragment.[27,193] This result was validated by Ar-matrix EPR where both $Mn(CO)_5$ and the H radical were detected; the analysis of the hyperfine splitting constants of Mn led to the conclusion that the lone electron occupies a metal-centered orbital ($3d_z^2$) mixed with the $4p_z$ and 4*s*.[28] In a complementary experiment, γ-irradiation of $MnH(CO)_5$ in krypton generated $KrMn(CO)_5$ revealed through Kr-superhyperfine coupling.[194] Prolonged irradiation in Ar matrices at 193 nm proceeded along both the photochemical pathways, but the quantum yield for the homolysis process was much lower than that for CO photoejection. A photoisomerization was detected under these conditions where $[MnH(CO)_4]$ could rearrange from a C_s geometry to a C_{4v}.[29] DFT calculations computed the C_s structure to be the most stable and the C_{4v} structure to be only 3 kcal/mol higher in energy.[195] The theoretical work on the photochemistry of $MnH(CO)_5$ is described in section 2.1. In a more preparative approach, the photochemistry of $MnH(CO)_5$ was exploited to synthesize new species; photolysis in impregnated polyethylene films under a pressure of CO generated $Mn_2(CO)_{10}$ and H_2.[196] $MnH(CO)_5$ underwent multiple CO photodissociation to form the phosphine-substituted product in the presence of excess phosphine.[197] *cis*-$[MnH(CO)_4(PPh_3)]$ was found to be active in the photocatalytic hydrogenation and isomerization of alkenes,[198] while a series of disilanyl Mn compounds of the formula $Cp^*MnH(SiR_2SiR_2H)(CO)_2$ underwent photochemical decomposition by reductive elimination of disilane; interestingly, $Cp^*MnH(SiPh_2SiPh_2H)(CO)_2$ showed some H_2 evolution ascribed to 1,2-H_2 elimination.[199] The charge-transfer photochemistry of $MnH(CO)_3$(diazabutadiene) has been compared computationally to that of its alkyl and rhenium analogues.[200]

The scenario for the photochemistry of rhenium monohydrides is slightly more diverse. Earlier studies focused on the photochemistry of Cp_2ReH and $Cp_2{}^*ReH$ in Ar and CO matrices. Cp_2ReH produced the rhenocene fragment, HCO, and a monocarbonyl species; deuteration experiments confirmed that the Re−H bond was cleaved homolytically.[201] Later results identified a competing photochemical pathway that involved partial ring decoordination plus concomitant ligand addition to yield $CpReH(\eta^3\text{-}C_5H_5)(L)$ (L = CO, N_2).[202] Rhenocene was generated photochemically in Ar matrices, allowing magnetic circular dichroism and laser-induced fluorescence investigations to be undertaken (see section 3.1.2).[54,120,203] Photolysis of $Cp_2{}^*ReH$ could be carried out on a preparative scale (section 2.1); matrix investigations of $[Cp_2{}^*Re]$ were compared to those for $[Cp_2Re]$.[6,54] The low-lying excited states for $ReH(CO)_5$ were calculated and assigned to the MLCT 5d to π^*_{CO} excitations, with significant differences from its first-row analogue.[204] Rhenium monohydrides containing carbonyl ligands have also been of use in photochemistry, a series of $ReH(CO)_{5-y}L_y$ (L = $P(OEt)_3$,$PPh(OEt)_2$, $PPh_2(OEt)$, or $PPh_2(OMe)$) were prepared from photolysis of $ReH(CO)_5$ in the presence of phosphites; in these cases, CO acted as the photolabile ligand.[205] Similarly, *cis,mer*-$[ReH(CO)_2(PPh(OMe)_2)_3]$ was prepared photochemically from $ReH(CO)_3(L)$ (L = $PPh_2OCH_2CH_2OPPh_2$) with excess phosphonite.[206] Photolysis of $(\eta^6\text{-}C_6H_6)ReH(PPh_3)_2$ results in loss of PPh_3.[207] Photolysis of $Cp^*(CO)_2W(\mu\text{-}SiMe_2)(\mu\text{-}H)Re(CO)_2Cp^*$ afforded an isomeric mixture of heterobimetallic complexes $Cp^*(CO)_2HW(\mu\text{-}\eta^1,\eta^2\text{-}SiMeCH_2)ReH(CO)_2Cp^*$.[166] The complexes with a bridging hydride and a bridging pyridyl $Re_2(CO)_7(L)(\mu\text{-}H)(\mu$-pyR) (L = CO, 4-benzoylpyridine; pyR = pyridyl, 4-benzoylpyridyl) provide rare examples of metal carbonyl hydrides designed to possess long-lived emissive triplet excited states. Detailed absorption, emission, and transient absorption spectra are reported. Extensive studies of excited-state reactivity toward amines and phosphines are consistent with quenching by electron transfer to the complexes, while reactivity with methylpyridinium salts results from electron transfer in the opposite direction.[208]

4.4.2. Group 7 Dihydrides and Dihydrogen Complexes. When we move the search into dihydrides, examples of photoactive species of group 7 are more scarce. The photochemical behavior of the dihydride cations, $[Cp^*{}_2Re(H)_2]^+$, parallels that of the neutral analogues of molybdenum and tungsten (Scheme 17).[173] The dihydride $CpMn(H)_2$(dfepe) was found to exist in a thermal equilibrium with its dihydrogen analogue; full conversion to the dihydrogen adduct was observed if the solution mixture was photolyzed (see section 2.2.2).[79] Studies of *trans*-$[Cp^*Re(H)_2(CO)_2]$ in cyclohexane solution at 298 K under an atmosphere of H_2, methane, or argon or in liquid Xe at 200 K under H_2 showed that it photoisomerizes to the cisoid analogue. There was no incorporation of deuterium under a D_2 atmosphere. Matrix photochemistry at 12 K in the presence of ^{13}CO established that photoisomerization took place intramolecularly; prolonged photolysis afforded fragments

DOI: 10.1021/acs.chemrev.6b00204
Chem. Rev. 2016, 116, 8506−8544

Scheme 19. Photoreactivity of $Fe(H)_2(dmpe)_2$ in Solution; Me Groups on the dmpe Ligand Are Not Shown in the Products

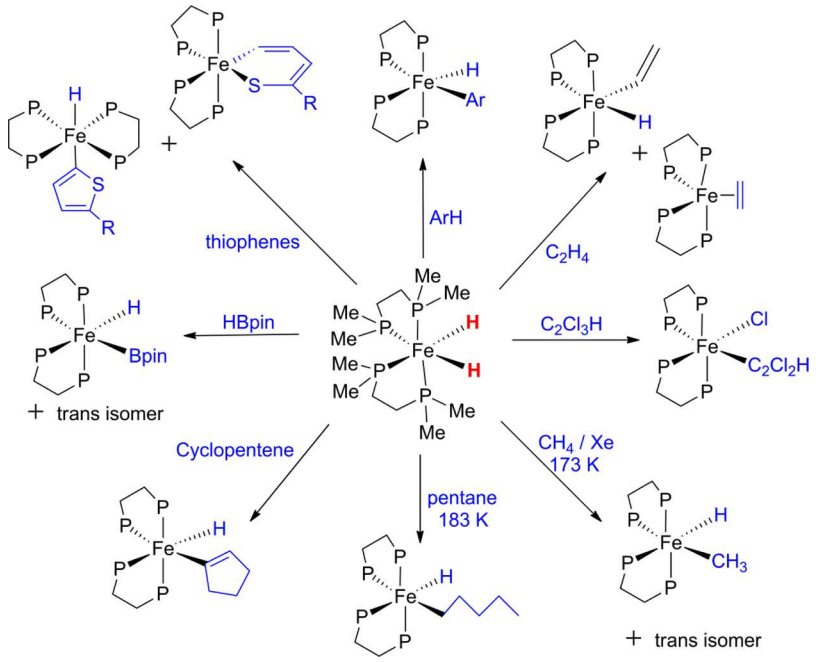

from both H_2 and CO loss.[209] The Cp analogue, $CpRe(H)_2(CO)_2$, exists as a 98:2 equilibrium mixture of transoid and cisoid isomers. However, the cisoid species may be generated as the kinetic product of reaction and itself may have dihydrogen and dihydride isomers. Photolysis of *trans*-$[CpRe(H)_2(CO)_2]$ in methylcyclohexane glasses at 77 K leads to a photostationary state with a 40:60 transoid/cisoid mixture that reverts slowly to the transoid complex on melting.[80] The photochemistry of $CpRe(H)_2(PPh_3)_2$ is described in section 2.2.3.[81−83]

4.4.3. Group 7 Polyhydrides. Polyhydride species have also offered examples in photochemistry, both for Mn and Re metal centers. The clusters $M_3(H)_3(CO)_{12}$ (M = Mn, Re) were investigated under UV irradiation. The photoreaction of the Re complex in degassed solutions yielded the dimer $Re_2(H)_2(CO)_8$ quantitatively; if a CO atmosphere was added, $ReH(CO)_5$ was detected in addition. The reaction of the manganese analogue proceeded less cleanly than the Re one. The photochemical mechanism was partially elucidated.[210] $Re(H)_3(dppe)_2$ afforded an example of cleaner photochemistry; H_2 photoejection to form the unsaturated complex $ReH(dppe)_2$ was identified as the primary photoprocess, and the transient was trapped by the use of CO, N_2, and C_2H_4.[211] Furthermore, the rhenium fragment was found to be capable of CO_2 insertion and intramolecular C−H activation of phenyls.[212] The same type of photochemistry was established for $Mn(H)_3(dmpe)_2$.[213] A similar photochemical path was followed when the bidentate phosphine was replaced with the monodentate one, PMe_2Ph, whereas phosphine loss appeared to be the major photochemical step in studies of $Re(H)_5L_3$ (L = PMe_2Ph, $PMePh_2$, PPh_3).[214] The tetrahydride $CpRe(H)_4(PPh_3)$ showed preferential loss of H_2 upon photolysis while PPh_3 loss occurred thermally.[81] The tetranuclear cluster $Re_4(\mu\text{-}H)_4(CO)_{16}$ reacted photochemically to yield the unsaturated dimer $Re_2(\mu\text{-}H)_2(CO)_8$,[215] and the heteronuclear compound $Pt_2Re_2(CO)_7(P^tBu_3)_2(\mu\text{-}H)_4$ photoejected H_2 to form $Pt_2Re_2(CO)_7(P^tBu_3)_2(\mu\text{-}H)_2$.[216]

4.5. Group 8 Metals

Iron, ruthenium, and osmium belong to one of the richest groups in examples of photoactive metal hydrides. The majority of the studies involve dihydrides with cis geometry at the metal center. Reductive elimination of H_2 is usually the primary photochemical process, but dissociation of a different ligand has also been reported. These studies have enabled detailed comparison of how reactivity varies with the structure of the transient $16e^-$ intermediate. The group also offers some of the best examples of photochemistry of bridging hydrides.

4.5.1. Group 8 Monohydrides. Little is reported about the photochemistry of iron monohydride complexes. The photochemistry of $FeHCo_3(CO)_{12}$ and $FeHCo_3(CO)_{10}(PPh_3)_2$ was explored in the context of declusterification but proved to be inconclusive.[217] The monohydride bridged dimers $Cp_2Fe_2(\mu\text{-}H)(\mu\text{-}PR_2)(CO)_2$[102−105] are discussed in section 2.5.

The biomimic of the active site of [Fe−Fe]-hydrogenases, $[Fe_2(\mu\text{-}H)(pdt)(CO)_4(dppv)]^+$, was discovered to be an effective photocatalyst for the H_2 evolution reaction, affording four turnovers in the presence of triflic acid.[18] However, the primary photoprocess was demonstrated to be CO loss (see section 3.1.1).[135]

As with iron, the photochemistry of ruthenium monohydride species is far less investigated than that of the dihydrides. It often proceeds through the loss of a two-electron donor ligand, mostly CO, followed by catalytic activity shown by the unsaturated metal−hydride intermediate formed. $RuHCl(CO)(PPh_3)_3$ was reported to lose CO under ultraviolet irradiation to form $[RuHCl(PPh_3)_3]$, a potent hydrogenation catalyst, with concomitant formation of $RuHCl(CO)_2(PPh_3)_2$.[218] Interestingly, the dicarbonyl analogue $RuHCl(CO)_2(PPh_3)_2$ did not show any photoinduced ligand-elimination reaction but underwent reversible photoisomerization according to UV and IR spectra.[219] Irradiation of $CpRuH(CO)_2$ in frozen nujol yielded [CpRuH(CO)], again displaying CO photodissociation.[123] Surprisingly, it was observed that triethylsilane reductive elimination competes with CO photorelease in $RuH(SiEt_3)$-

DOI: 10.1021/acs.chemrev.6b00204
Chem. Rev. 2016, 116, 8506−8544

$(CO)_3(PPh_3)$, for which the authors postulated an excited state similar to that of Ru−H_2 species due to the parallel to the corresponding oxidative addition reaction. The viability of changing the R group on the silane offered an additional way to tune the reactivity in comparison to molecular H_2 (see section 2.1.2).[36]

Irradiation of Cp*OsH$(CO)_2$ in the presence of H_2 delivered the photoproduct Cp*Os$(H)_3(CO)$ formed from CO loss.[220] In agreement with these observations, the photolysis of CpOsH$(CO)_2$ in frozen nujol yielded the CO-loss fragment and a species that was speculated to be either the [CpOs$(CO)_2$] radical or a compound where the hydrogen atom had migrated onto the Cp ring.[123] Photolysis of the mesitylene complex (η^6-$C_6H_3Me_3$)-OsH$(CO)(CH_3)$ in an argon matrix resulted in loss of methane identified by its IR bands and formation of [(η^6-$C_6H_3Me_3$)Os-(CO)] (see below for the photochemistry of the dihydride complex).[221] The stannylene complex Cp*OsH{SnH(trip)}-($PiPr_3$) (trip =2,4,6-triisopropylphenyl) was reported to convert slowly to the metallostannylene complex Cp*Os$(H)_2${Sn(trip)}-($PiPr_3$) under ambient light through a radical mechanism.[222] The 2-trihydrofuranyl complex OsH$(PP_3)(C_4H_7O)$ (PP_3 = P-$(CH_2CH_2PPh_2)_3$) reacted photochemically to lose tetrahydrofuran and form the product of cyclometalation of one of the phenyl rings of PP_3 (see section 4.5.2 for Os$(H)_2(PP_3)$).[66]

4.5.2. Group 8 Dihydrides. Iron dihydride complexes have attracted the photochemical community since the early 1980s for both fundamental mechanistic studies and applications in the activation of strong bonds. The main skeleton of photoactive Fe species involves either an Fe-carbonyl or an Fe-phosphine scaffold where the two *cis*-hydrides are the photolabile ligands. Sweany first reported the matrix isolation of Fe$(H)_2(CO)_4$ and formation of [Fe$(CO)_4$], which arose from photoinduced H_2 reductive elimination from the parent complex Fe$(H)_2(CO)_4$; CO loss was not observed. The reverse reaction, H_2 oxidative addition, was also induced photochemically in matrices.[73] The theoretical description of the photochemical reaction is described in section 2.2.1.

Iron phosphine dihydride complexes have proved to be more effective in small-molecule activation than iron carbonyl dihydrides. Fe$(H)_2(drpe)_2$ (drpe = dmpe, depe, dppe; depe = $Et_2PCH_2CH_2PEt_2$) are well-known as good activators of sp^2 C−H bonds of alkenes,[223,224] the much stronger sp^3 C−H bonds of alkanes,[225] and C−S bonds of thiophenes[226] (Scheme 19). The activation of such strong bonds was achieved at low temperature and involved photolysis of the dihydride parent complex to reductively eliminate molecular hydrogen and form the unsaturated intermediate capable of insertion into the C−X bonds (X = H, S). The activation of the C−H bonds of methane in liquefied xenon through photolysis of Fe$(H)_2(dmpe)_2$ was also reported.[227] Elimination of H_2 from this complex was found to be predominantly intramolecular on the basis of lack of deuterium scrambling.[58] Intramolecular C−H activation to form a metalacycle was detected in the presence of bulkier phosphine ligands.[228] Fe$(H)_2(dppe)_2$ showed activity as a precatalyst for the photolytic hydrosilylation of aldehydes and ketones.[115] The dmpe analogue, Fe$(H)_2(dmpe)_2$, showed photochemical activity in dechlorination reactions of chlorinated ethylenes.[229] The kinetics and actinometry of the hydrodechlorination of trichloroethylene and dichloroethylene with Fe$(H)_2(dmpe)_2$ in excess were investigated in detail (Figure 12). More importantly, Fe$(H)_2(dmpe)_2$ is an active photocatalyst for the C−H borylation of arenes (see section 2.6).[114]

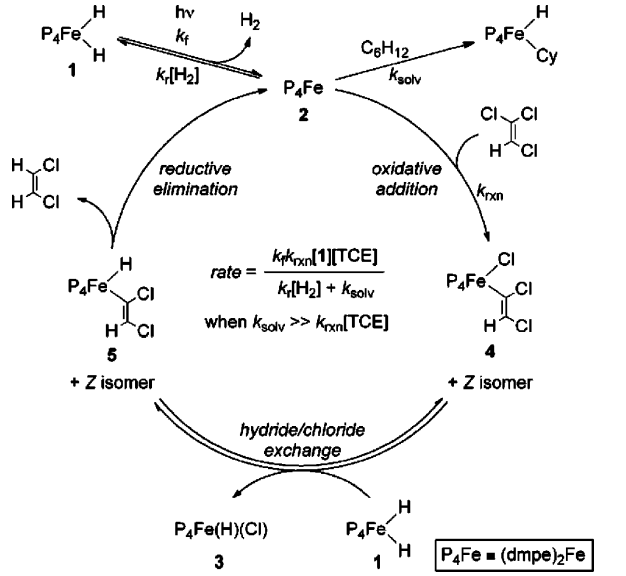

Figure 12. Proposed mechanism and corresponding rate law for the photochemical conversion of trichloroethylene to *cis*-dichloroethylene. Reproduced with permission from ref 229. Copyright 2013 Royal Society of Chemistry.

Clearer insights into the photochemical process were obtained by transient UV−vis spectroscopy and low-temperature matrix photochemistry.[63] The [Fe$(dmpe)_2$] intermediate was observed directly by both methods, and its reactivity was examined. The key finding was the formation of a single unsaturated transient [Fe$(dmpe)_2$] that differed significantly from the Ru analogue in its spectroscopic features and reactivity (see below and Figure 13).

Although both [Fe$(dmpe)_2$] and [Ru$(dmpe)_2$] react with CO with a second-order rate constant close to the diffusion limit, the reactivity toward hydrogen was found to be very different. The rate constant for reaction of [Fe$(dmpe)_2$] with H_2 in solution was

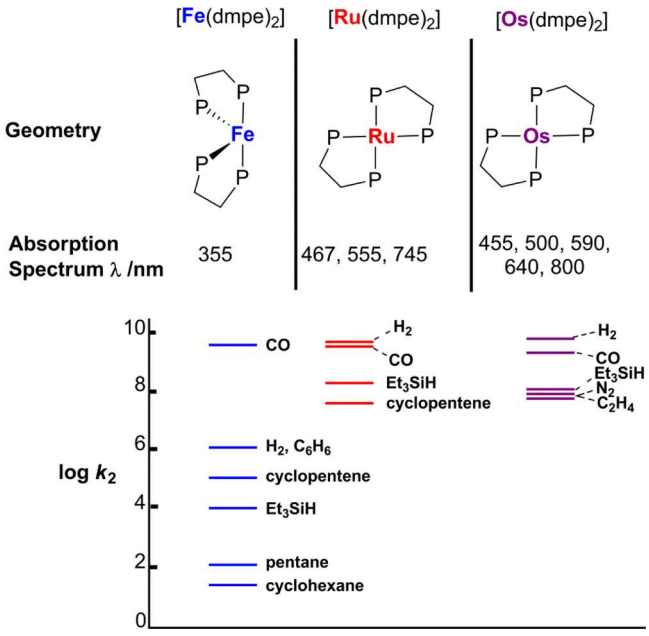

Figure 13. Comparison between spectral features and rates of reactions for group 8 metal MP_4 intermediates (M = Fe, Ru, Os).[59,63,68]

DOI: 10.1021/acs.chemrev.6b00204
Chem. Rev. 2016, 116, 8506−8544

a factor of 7500 smaller than that of $[Ru(dmpe)_2]$, and it reacted with arenes and alkanes, unlike $[Ru(dmpe)_2]$. The UV−vis absorption spectrum was also markedly different, with the long-wavelength visible absorption bands absent from the spectrum of $[Fe(dmpe)_2]$, leaving only a near-UV band. These differences were rationalized in terms of a different geometry for the two species, and a C_{2v} geometry with a triplet ground state was suggested for $[Fe(dmpe)_2]$ by analogy with $[Fe(CO)_4]$.[63] Rate constants were also reported for the coordination or oxidative addition reactions of $[Fe(dmpe)_2]$ with benzene, toluene, alkenes, nitrogen, and triethylsilane. Notably, $[Fe(dmpe)_2]$ exhibited little kinetic discrimination.[63] The enthalpies of activation for the reactions with triethylsilane (Table 1) highlight the differences between Fe and Ru. There is also a contrast in the reactivity in low-temperature matrices because $[Fe(dmpe)_2]$ reacted with methane to form $FeH(CH_3)(dmpe)_2$ whereas no corresponding reaction was observed for $[Ru(dmpe)_2]$.

Density functional calculations predicted a more stable singlet configuration for the Ru complex with a D_{2d} geometry, while the Fe species was computed to be slightly more stable in its triplet state with a C_{2v} geometry.[71] Later calculations confirmed that Fe^0P_4 complexes have a C_{2v} geometry with a triplet ground state. The triplet singlet energy gap changes in the order $[Fe(PH_3)_4]$ > $[Fe(dpe)_2]$ > $[Fe(dmpe)_2]$. In the case of $[Fe(dmpe)_2]$, the triplet state was calculated to be more stable than the singlet by 52.5 kJ/mol. The reaction with hydrogen was analyzed by the minimum energy crossing point method, accounting for the slower rate of reaction of $[Fe(dmpe)_2]$ with H_2 compared to $[Ru(dmpe)_2]$.[230,231]

Irradiation of iron atoms in molecular H_2/noble gas matrices at 12 K generated $Fe(H)_2$.[232−234] The results suggested that H_2 oxidative addition to the metal center had a small degree of H−H stretching in an early transition state and no activation barrier to insertion. The process followed a "simple" concerted insertion into the Fe metal. The insertion product was investigated by 440 nm photoexcitation at 12 K and found to be converted back to Fe atoms; the reverse reaction was described as a concerted reductive elimination with no activation barrier (Scheme 20).

Scheme 20. Photochemistry of Fe + H_2 in Matrices (Adapted with Permission from Ref 232; Copyright 1984 American Chemical Society)

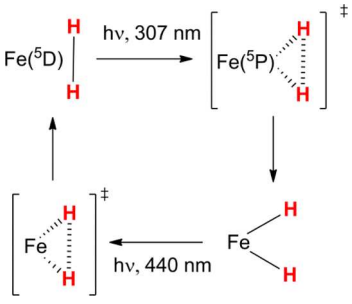

Both H_2 insertion and its microscopic reverse were reported to happen with no detectable formation of FeH or $Fe(H)_x$ (x > 3) or hydrogen atom abstraction products. This work represented the first example of ligand-free H_2 reductive elimination from a metal center. Studies of the kinetic isotope effect (KIE) for oxidative addition at low temperature in Xe yielded a k_H/k_D isotope ratio of 5.6. Although this seems large, it translates into a k_H/k_D ratio of ∼1.1 at ambient temperature, indicating a small degree of H−H stretching and low activation barrier for insertion.[232,233] Later studies of Fe in H_2/Ar and Fe/Kr reported laser-induced fluorescence excitation spectra and IR spectra. The authors suggest that $Fe(H)_2$ is formed from an $Fe(H_2)$ exciplex with broadened and shifted absorptions. Isotopic substitution indicated an H−Fe−H angle exceeding 170° and enabled measurement of KIEs for forward and reverse reactions. The KIE for the formation of $Fe(H)_2$ was measured as 7 in Ar but 86 in Kr, and the KIE for the reverse reaction was ca. 3 in both matrices.[234] Later studies with laser ablation sources of Fe are barely concerned with the photochemistry.[235]

The photoreactions of the high-spin Fe(II) complex with bridging hydride ligands[106] $[(\beta\text{-diketiminate})Fe(\mu\text{-}H)]_2$ and the photochemistry of nitrogenase[8] are covered in section 2.5.

Ruthenium dihydride complexes also show a wide variety of examples in photochemistry. Unlike its monohydride analogues, $Ru(H)_2(CO)(PPh_3)_3$ underwent H_2 reductive elimination when exposed to ultraviolet irradiation. Photoelimination of CO did not occur, as confirmed by the GC analysis of the gases produced. The transient was trapped when it was exposed to a CO atmosphere during photolysis where $[Ru(CO)_3(PPh_3)_3]$ was the only product formed.[219] The transient photochemistry (Scheme 21) for this complex was investigated 20 years later by laser flash

Scheme 21. Photochemical H_2 Reductive Elimination from $Ru(H)_2(CO)(PPh_3)_3$ and Reverse Reaction (Reproduced with Permission from Ref 134; Copyright 1997 Royal Society of Chemistry)

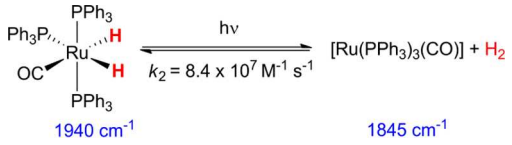

photolysis in benzene solution. The transient $[Ru(CO)(PPh_3)_3]$ reacted with an H_2 atmosphere to regenerate the dihydride species with a second-order rate constant of $k_2 = (8.4 \pm 0.4) \times 10^7$ dm^3 mol^{-1} s^{-1}. More notably, it was found by time-resolved IR experiments that H_2 reductive elimination was complete within 6 ps, implying that any geometry reorganization and bond breaking/making around the Ru center had to take place within this time (see section 3.1).[134] The dissociative photochemistry of this complex was also demonstrated by quantum dynamics calculations.[70]

A further example with a carbonyl ligand studied by steady-state and transient absorption spectroscopy is $Ru(H)_2(CO)$-(etp). The reactivity is exclusively derived from H_2 reductive elimination and shows little discrimination between incoming substrates (see also Table 1).[67] Substitution of a PPh_3 ligand with an NHC-carbene led to a drastic change in the reactivity; in situ photolysis and the use of *para*-H_2 established that photo-isomerization took place after both H_2 and PPh_3 dissociation had happened (see section 2.2.2).[78] $Ru(H)_2(CO)_2(PMe_3)_2$ was also subject to photochemical investigation in low-temperature Ar, CH_4, and Xe matrices. It also loses hydrogen to form the 16e$^-$ unsaturated species; the reversibility of the reaction on long-wavelength (λ > 360 nm) photolysis identified $[S\cdots Ru(CO)_2(PMe_3)_2]$ (S = Ar, CH_4, Xe) as the sole coordinatively unsaturated species.[236]

Initial studies of the photochemistry of $Ru(H)_2(PMe_3)_4$ only revealed photochemical PMe_3 loss.[237] However, more extensive investigation demonstrated the competition of two photo-chemical pathways[43] in contrast to $Ru(H)_2(CO)_2(PMe_3)_2$.

DOI: 10.1021/acs.chemrev.6b00204
Chem. Rev. 2016, 116, 8506−8544

Studies by matrix isolation, and time-resolved spectroscopy, together with NMR studies of the products showed that both $[Ru(PMe_3)_4]$ and $[Ru(H)_2(PMe_3)_3]$ are formed as transients, highlighting how the parent complex could either reductively eliminate H_2 or lose the $2e^-$ donor ligand PMe_3. The transient absorption band in the near-UV observed by flash photolysis is closely matched by the matrix spectra and is assigned to $[Ru(PMe_3)_4]$. Insertion products deriving from both unsaturated species were observed in the presence of Ph_2SiH_2 with initial relative quantum yields of 1:4.5 for H_2 loss relative to PMe_3 loss (Scheme 22).[43] The triphenylphosphine analogue $Ru(H)_2(PPh_3)_4$ and the N_2 substituted species $Ru(H)_2(N_2)(PPh_3)_3$ were investigated photochemically for H_2 production from ethanol, but the photochemical process was not identified conclusively.[238] The photochemistry of $(\eta^6\text{-}C_6H_6)Ru(H)_2(PR_3)$ (R = Me, ^{i}Pr) and $(\eta^6\text{-}C_6H_6)Ru(H)_2(PHCy_2)$ appeared to be less complicated: H_2 loss was the only photoactivated pathway to the unsaturated species that proved capable of inserting into C−H bonds of arenes.[239,240]

Scheme 22. Photoreactivity of $Ru(H)_2(PMe_3)_4$ Displaying Both H_2 Reductive Elimination and PMe_3 Loss (Reproduced with Permission from Ref 43; Copyright 2000 Royal Society of Chemistry)

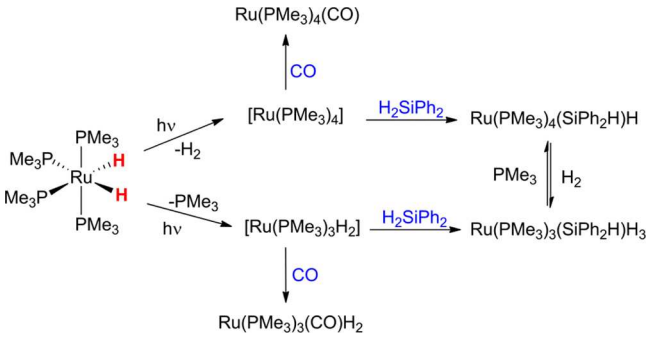

Bergamini et al. first reported the photoactivity of the $Ru(H)_2(drpe)_2$ (drpe = dmpe, dppe) type of complexes together with that of the Fe analogues. For both sets of complexes, molecular hydrogen elimination through a concerted process was found to be the sole photoprocess.[58] Details of the photochemistry and transient spectroscopy of these two complexes[7,59−61,64] are discussed in section 2.2.1. Unexpectedly, $[Ru(dmpe)_2]$ displayed very different reactivity and spectroscopic features from its Fe analogue (Figure 13). Similar complexes of the type $Ru(H)_2(drpe)_2$ (drpe = depe, dfepe, dmpm; dmpm = $Me_2PCH_2PMe_2$) were also studied by transient spectroscopy.[64,65] $Ru(depe)_2$ exhibited very similar features in its UV−vis spectra to those observed for the dmpe and dppe analogues with three major UV−vis bands. One of the bands falls at long wavelength (600−800 nm) and was assigned to an $M(d_z^2)-M(p_z)$ transition. These features, in addition to comparison of the spectra to that of $[Rh(dppe)_2]^+$, confirmed the square-planar geometry around the metal center. The $[Ru(defpe)_2]$ transient displayed a three-band UV−vis spectrum shifted further toward the blue part of the spectrum as a result of either a slight distortion from the planar structure or a stabilizing interaction of the F atom with the Ru center. Each of the effects was considered to be minor in distorting the square-planar geometry, as confirmed by the survival of the multiband UV−vis spectrum. The absorption spectrum of $[Ru(dmpm)_2]$ is also much less well resolved and blue-shifted as result of the reduction in the size of the ring.[65] The reactivity of the complexes tested with different substrates (H_2, CO, C_2H_4, silanes, and boranes) showed a sensitivity to the change of the phosphine substituent and increased in the order $[Ru(dfepe)_2] < [Ru(dppe)_2] < [Ru(depe)_2] \approx [Ru(dmpm)_2] < [Ru(dmpe)_2]$, spanning a factor of 34 000 for reaction with H_2 and 418 000 for reaction with CO.[60,64] The reactivity toward $SiHEt_3$ was used as a further standard for comparison between these complexes (Table 1). Of these complexes, only $[Ru(dmpm)_2]$ inserts into the C−H bonds of benzene, as had been shown earlier.[241] However, the kinetics of the transient's reaction with benzene were complex and interpreted in terms of a rapid pre-equilibrium step between $[Ru(dmpm)_2]$ and the arene complex $Ru(\eta^2\text{-}C_6H_6)(dmpm)_2$. The latter undergoes oxidative cleavage of benzene relatively slowly, leading to the phenyl hydride species. In line with these results, $Ru(H)_2(dfmpe)_2$ (dfmpe = $(CF_3)_2PCH_2CH_2P(CF_3)_2$) reductively eliminated H_2 if irradiated under a D_2 atmosphere to form the dideuteride analogue but showed no further reactivity toward organic C−H bonds.[242] Recently, the well-understood photochemistry of the $Ru(H)_2(dppe)_2$ was exploited in studies aimed to develop a new time-resolved method based on a laser-pump and NMR-probe setup (see section 3.2). *para*-H_2 was employed to overcome the NMR insensitivity.[7] It would be interesting to relate the reactivity of $[Ru(dppe)_2]$ to the photocatalytic experiments with $[RuCl_2(C_6H_6)]_2$ + excess dppe (see below).[99]

The photochemistry of an analogous class of Ru dihydride complexes bearing the chiral phosphines Me-BPE and Me-Duphos was also investigated. Once again, the primary photoprocess was H_2 concerted reductive elimination, as demonstrated by transient time-resolved spectroscopy. The concerted nature of this process and the H_2 oxidative readdition to the metal center was additionally established through the observation of a *para*-hydrogen enhancement of the NMR spectrum acquired after the solution was photolyzed inside the NMR probe under a *para*-H_2 atmosphere (see section 3.2). Very low temperature (180 K) photolysis in situ performed under D_2 atmosphere generated H_2 but no HD. However, repetition of the experiment at 273 K resulted in the formation of a minor amount of HD, suggesting that a secondary photoprocess could compete where the chelating phosphine unhooked from the Ru center with the subsequent formation of $[Ru(\kappa^1\text{-Duphos})(Duphos)\text{-}(H)_2(\eta^2\text{-}D_2)]$. This type of complex can undergo H/D exchange rapidly; chelate ring closing will then eliminate HD and form a Ru-hydride/deuteride complex. Kinetic studies of reactivity toward a variety of substrates were carried out. $[Ru(BPE)_2]$ reacted with H_2 with a similar rate constant to that of $[Ru(dppe)_2]$, but $[Ru(Duphos)_2]$ reacted considerably more slowly; this was explained by blocking actions of the methyl groups on the phospholane rings.[136]

The effect of introducing a more constrained unit on the Ru center such as $P(CH_2CH_2PPh_2)_3$ (PP_3) was also of interest.[66,243] The tetradentate ligand prevents the transient from adopting a square planar D_{2h} geometry and offers two additional possible arrangements: pyramidal C_{3v} or butterfly C_s. Steady-state photolysis experiments showed that, unlike the complexes with bidentate ligands, $[Ru(PP_3)]$ undergoes cyclometalation on irradiation in THF under argon but forms a stable dinitrogen complex under an N_2 atmosphere. Photolysis in benzene-doped THF yielded the metal phenyl hydride complex, while similar experiments with thiophene in THF yield the 2-thienyl hydride. As expected, laser flash photolysis demonstrated that $[Ru(PP_3)]$ showed quite different UV−vis spectra for its transient (a single

DOI: 10.1021/acs.chemrev.6b00204
Chem. Rev. 2016, 116, 8506−8544

broad absorption maximum at 390 nm) from those of $[Ru(drpe)_2]$ because of the enforced change in structure. The reactivity of $[Ru(PP_3)]$ toward H_2 was found to be much slower than that of $[Ru(dmpe)_2]$ and $[Ru(dppe)_2]$. On the other hand, $[Ru(PP_3)]$ showed a wider range of reactions, including rapid C−H activation with benzene in cyclohexane (rate constant $(1.3 \pm 0.1) \times 10^6$ M^{-1} s^{-1} with KIE 1.5 ± 0.2, compared to $[Fe(dmpe)_2]$ + benzene $(9.6 \pm 0.4) \times 10^5$ M^{-1} s^{-1}; see also Table 1); however, there was little kinetic discrimination between substrates. The reactivity toward THF is shown in Scheme 23. The two-stage kinetics of reaction of transient

Scheme 23. Comparison of $[Ru(PP_3)]$ and $[Os(PP_3)]$ Transient Photochemistry in THF

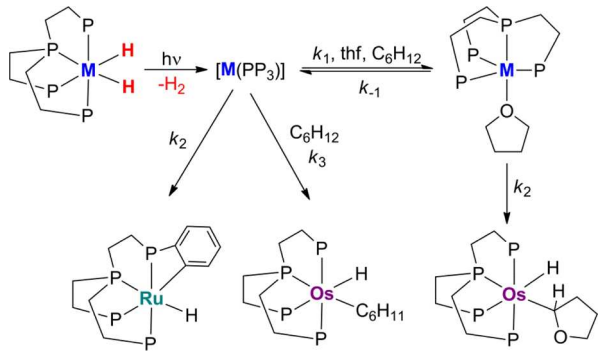

$[Ru(PP_3)]$ toward thiophene has also been reported.[243] In the most satisfactory model of the reactivity, it was postulated that $[Ru(PP_3)]$ adopts a structure with an agostic phenyl group.[66]

The use of $[RuCl_2(C_6H_6)]_2$ in the presence of a variety of phosphine ligands for the photocatalytic decomposition (380−780 nm) of formic acid·triethylamine (5:2) to hydrogen was reported.[99] The most successful phosphines were PPh_3 and dppe, giving TON of 1650 and 2800, respectively, after 3 h irradiation using 320 ppm Ru. Control experiments in the dark gave far less H_2. The catalysts work in a temperature range from 0 to 45 °C. This is a very different reaction from those described in section 2.6 because it does not require the photon energy (it is described as photoassisted, while we would use the term photoinduced catalysis). Indeed the catalyst can be activated photochemically, and the reaction then proceeds in the dark. One of the photoactive species is proposed to be a $Ru(H_2)(OCHO)(PR_3)_n$ complex.[99] Improved performance was obtained with $Fe_3(CO)_{12}$/phenanthroline/PPh_3. An analogous cycle is proposed, but evidence for hydrides, of concern for our purpose, is limited.[244]

Photoactive osmium dihydride complexes are slightly more numerous than the monohydride complexes. The first report of a photochemical reaction that involved an $Os(H)_2$ moiety aimed to prepare clusters; $Os_3(H)_2(CO)_{10}$ was irradiated in the presence of $Fe(CO)_5$ or $Ru_3(CO)_{12}$ to form a heterotetranuclear species as a consequence of CO photoelimination. The bridging dihydrides of the starting complex remained intact in the product, suggesting no reactivity toward irradiation.[245] Bergamini et al. explored the photochemistry of the $Os(H)_2(dmpe)_2$ and $Os(H)_2(dppe)_2$, analogues of the Fe and Ru mentioned previously. No substantial differences were found in the photochemical behavior at that time.[58] The photochemistry of $Os(H)_2(dmpe)_2$, explored by low-temperature matrix photochemistry, laser flash photolysis, and steady-state studies of the photolysis products, showed a strong analogy to the $[Ru(dmpe)_2]$ analogue (see section 3.1.2).[68] Notably, $[Os(dmpe)_2]$ has the lowest energy UV−vis transition of all the M^0P_4 complexes at 798 nm (Ar matrix). Unlike $[Ru(dmpe)_2]$, it undergoes C−H oxidative addition with benzene to form $OsH(Ph)(dmpe)_2$ and with ethylene to form *cis*- and *trans*-$[OsH(CH{=}CH_2)(dmpe)_2]$ without forming $Os(dmpe)_2(C_2H_4)$.

The piano-stool complex $(\eta^6\text{-}C_6H_6)Os(H)_2(CO)$ was investigated photochemically with respect to the C−H activation of saturated and aromatic hydrocarbons. The formation of the reactive species was achieved by photoelimination of H_2 with no mention of CO loss.[246] The mesitylene analogue $(\eta^6\text{-}C_6H_3Me_3)Os(H)_2(CO)$ was employed for matrix photochemistry and proved to undergo H_2 reductive elimination to yield the unsaturated fragment $[(\eta^6\text{-}C_6H_3Me_3)Os(CO)]$ upon photolysis in an Ar matrix and to form $(\eta^6\text{-}C_6H_3Me_3)OsH(CH_3)(CO)$ in a methane matrix (see section 4.5.1).[221]

The photochemistry of $Os(H)_2(PP_3)$ was studied by steady-state methods and by time-resolved absorption.[66,69,243] Transient absorption methods on $Os(H)_2(PP_3)$ complexes in the presence of hydrocarbons demonstrated that it activates the C−H bonds of primary alkanes and methane itself (rate constant $(2.6 \pm 0.4) \times 10^5$ M^{-1} s^{-1}). The transient $[Os(PP_3)]$ appeared also to react with cyclohexane, but much more slowly, thus showing kinetic selectivity for alkane C−H bonds in the order $CH_4 > 1° > 2°$, but the rate constant for benzene exceeds those for all alkanes. The alkyl products were not observed by NMR spectroscopy, principally because of the low solubility of the complex in alkanes. However, C−H activation products were identified by NMR spectroscopy with THF, benzene, and thiophene. The transient kinetics for reaction with THF and with thiophene are complicated by initial coordination of the substrate through oxygen or sulfur, respectively (Scheme 23). Unlike $[Ru(PP_3)]$ no quenching could be observed with H_2 probably because of the competing reaction with cyclohexane. Although $[Os(PP_3)]$ was quenched by N_2, no dinitrogen complex could be isolated, whereas $Ru(PP_3)(N_2)$ was isolated as a reaction product. Intramolecular photochemical C−H activation was not observed for $Os(H)_2(PP_3)$, unlike the Ru analogue: evidently the barrier for cyclometalation at Os was higher than for C−H activation of alkanes, whereas the reverse is true of $[Ru(PP_3)]$. The authors postulate that the structure of $[Os(PP_3)]$ predisposes it to C−H activation through the enforced C_{3v} or C_s structure with the additional possibility of the agostic phenyl group.[66,69,243]

4.5.3. Group 8 Polyhydrides. Iron, ruthenium, and osmium atoms formed by laser ablation have been co-condensed with pure H_2 or with Ne/H_2 mixtures at 4.5 K, allowing examination of a series of binary hydrides and hydride dihydrogen complexes. The monohydride FeH reacted with H_2 in solid neon and pure hydrogen to form $FeH(H_2)_x$; the $Fe(H)_2$ molecule was also observed experimentally and found to be capable of forming the weakly bound $Fe(H)_2(H_2)_3$ supercomplex. There is a reversible photochemical cycle linking $Fe(H)_2$ and $Fe(H)_2(H_2)_3$.[97] The behavior of Ru is similar to that of Fe with the difference that the $Ru(H)_2$ was not detected due to the large activation energy needed for atomic insertion with one H_2 molecule. The reactive RuH species formed initially reacted with hydrogen to form $Ru(H)(H_2)$ rather than a trihydrido species. Although photochemical reactions are reported, the photochemical reaction sequence is unclear.[97] The reactive OsH species combined with H_2 to form the complex $OsH(H_2)$ instead of the trihydride $Os(H)_3$, and $OsH(H_2)_x$ was also formed.[97]

DOI: 10.1021/acs.chemrev.6b00204
Chem. Rev. 2016, 116, 8506−8544

The cluster $Ru_4(H)_4(CO)_{12}$ was found to be active in catalytic isomerization and hydrogenation of alkenes when irradiated, and it was suggested that the complex $[Ru_4(H)_4(CO)_{11}]$, formed by photoejection of CO, was responsible for the reactivity.[247] The isolation of the intermediate came later by matrix photochemistry at low temperature, confirming clean loss of CO.[248]

Most of the reactions of $[Cp^*Ru]_2(\mu\text{-}H)_4$ and its analogues are described in section 2.4. It also reacted photochemically with $CpNi(CO)_2$, $CpCo(CO)_2$, and $[CpFe(CO)_2]_2$ to yield heterobimetallic clusters with different geometries. Although no mention was made of the primary photoprocess by the authors, elimination of H_2 from the tetrahydrido Ru-species is required for the observed product to be formed.[11,12,249] The only example of a polyhydride of osmium involved in a photochemical reaction is the photochemical reductive elimination of H_2 from $Cp^*Os(H)_3(CO)$ to form the dimer $[Cp^*Os(CO)]_2(\mu\text{-}H)_2$.[220]

4.6. Group 9 Metals

Group 9 metal-hydride photochemistry has played a critical role in the development of C−H bond activation and also includes some rare examples of photochemistry in aqueous solution as well as examples of equilibrated excited states.

4.6.1. Group 9 Monohydrides. The first cobalt monohydride complex reported to undergo photoreactivity was $CoH(CO)_4$; the transient $[Co(CO)_4]$ formed upon photolysis was trapped in both Ar and CO matrices and arose from metal−hydrogen bond homolysis, proposed as a primary photoprocess (eq 5).[250] A few years later, CO photoelimination was also

$$HCo(CO)_4 \xrightarrow{h\nu} H^{\bullet} + Co(CO)_4$$
$$HCo(CO)_4 \xrightarrow{h\nu} HCo(CO)_3 + CO \qquad (5)$$

detected for the same complex along with M−H bond homolysis; the relative quantum yields for M−H vs M−CO cleavage were estimated as 1:8 with 254 nm irradiation (eq 5).[251] The first calculations of electronic structure suggested that the dominant electronic transition responsible for photoactivity had mixed LF and MLCT character.[33] The photodissociation dynamics[252] for $CoH(CO)_4$ and simulation of the intersystem crossing process[253] were computed. Finally, wave packet dynamics established that competition in multiple photoprocesses had a time dependence on the sequence of the elementary events occurring between the initial absorption and the formation of the photoproducts. The Co−H homolysis can occur via population of the ^1E ($d \rightarrow \sigma^*_{Co-H}$) state as well as from triplet states (albeit, more slowly).[75] The fragment $[CoH(CO)_3]$ formed after CO loss also showed photochemical reactivity in H_2-containing matrices, forming the hydride(dihydrogen) species $CoH(H_2)(CO)_3$; the latter proved to be inert to irradiation.[254,255]

Cobalt complexes have been used extensively in photocatalytic systems for hydrogen production from water. These photosensitized reactions are thought to involve photoinduced electron transfer to cobalt and formation of cobalt hydrides by reaction with acid, but the hydrides are rarely observed directly. For details, the reader is referred to reviews.[13,14]

More direct participation of monohydrides in the photochemical process is offered by Rh-monohydrides. The first report published in 1979 showed how ultraviolet irradiation of $[RhH(NH_3)_4(OH_2)]^{2+}$ in the presence of O_2 resulted in the formation of a hydroperoxide rhodium species. The photoinitiation produces a H radical and $[Rh(NH_3)_4]^{2+}$, which acts as the chain carrier.[256] In a related example, UV photolysis of an aqueous solution of *trans*-$[RhH(14\text{-}aneN_4)]^{2+}$ (irradiating at 254 nm into absorption maximum at 288 nm) caused Rh−H homolysis, generating hydrogen atoms and Rh^{II} products *trans*-$[Rh(H_2O)(14\text{-}aneN_4)]^{2+}$ and *trans*-$[Rh(OO)(14\text{-}aneN_4)]^{2+}$ (14-aneN$_4$ = cyclo-$NH(CH_2)_3NH(CH_2)_2NH(CH_2)_3NH(CH_2)_2$) under Ar and O_2, respectively.[257] The Rh^{II} products are detected by EPR spectroscopy, and the H atoms may be detected by trapping. The 18-electron complex $RhH(CO)(PPh_3)_3$ was capable of enhanced hydrogenation of olefins under photocatalytic conditions,[258] and the triisopropylphosphine analogue $RhH(CO)(P^iPr_3)_2$ displayed photoreactivity in H_2 production in the presence of MeOH via the photoelimination of CO.[238,259] The photocatalytic reactions of a rhodium porphyrin to generate silanols and of mixed valence Rh_2 complexes to generate H_2 are summarized in section 2.6.[110,111,113]

Rhodium complexes are popular catalysts for photocatalytic reduction of protons to hydrogen. Typically, a photosensitizer transfers an electron to a rhodium complex, which subsequently picks up a proton to form a rhodium hydride. Such catalysts are the subject of a recent review.[15]

There are few examples of iridium monohydrides that undergo photochemical reaction. Clean and rapid EtOH elimination was observed on irradiation of the alkoxide hydride $Cp^*IrH(OEt)(PPh_3)$; the unsaturated fragment formed in the reaction proved to be capable of inserting into C−H bonds of arenes inter- and intramolecularly.[37] The tridentate phosphine complexes IrH(triphos)(C_2H_4) and IrH(triphos)$(CH_2{=}CHPh)$ underwent photoisomerization to form Ir^{III} vinyl dihydride complexes, which were themselves photoactive (see below).[40] In related reactions, photolysis of $CpIr(C_2H_4)_2$ in argon matrices resulted in two photoisomerization steps, first to $CpIrH(CH{=}CH_2)(C_2H_4)$ and subsequently to the vinylidene complex, $CpIr(H)_2(C{=}CH_2)$.[260] Only the first step has been observed in solution. Different behavior was observed for $IrH(CO)_2$(xantphos); despite having a large bite angle phosphine, the introduction of CO ligands led to the photodissociation of the carbonyl as the primary photochemical step, observed by photolysis under hydrogen.[260]

The ability of $[Cp^*IrH(bpy)]^+$ to undergo photochemical proton transfer and hydride transfer was discussed in section 2.1.4.[9,10] This complex, and derivatives with other polypyridine ligands, have also been used extensively for photocatalysis and photoelectrocatalysis; see section 2.6.[19,41,112] Pioneering studies of $[Cp^*IrH(NN)]^+$ (NN = bpy, phen, and several substituted derivatives of bpy) as photocatalyst for the water gas shift reaction were reported.[41] The photochemical step was identified as protonation of the hydride, and several reaction intermediates were identified spectroscopically. The activation energy was reduced by introduction of an electron-withdrawing group on the bipyridine. The global quantum yield for $[Cp^*IrCl(bpy\text{-}4,4'\text{-}(CO_2H)_2]^+$ with irradiation at 410 nm was 0.13.[41] A related derivative with terpyridine and phenylpyridine ligands, [IrH(tpy)(ppy)]$^+$, was formed as two isomers with hydride trans to N or C that exhibit very different properties in ground and excited states.[39] The N-*trans*-H isomer is emissive and is quenched by triethylamine by electron transfer, whereas the C-*trans*-H isomer is nonemissive and is not quenched in this way. Their excited-state spectra are appreciably different, as determined by transient absorption spectroscopy. Steady-state photolysis of the C-*trans*-H isomer in CD_3CN results in proton transfer and formation of Ir(tpy)(ppy) and, over longer periods, the N-*trans*-H isomer. Both isomers act as photocatalysts for CO_2 reduction in the

DOI: 10.1021/acs.chemrev.6b00204
Chem. Rev. 2016, 116, 8506−8544

presence of triethanolamine to generate CO with similar turnover numbers. It is postulated that the reaction with CO_2 occurs via a common square-pyramidal intermediate [Ir(tpy)(ppy)] with a vacancy trans to C.[39]

4.6.2. Group 9 Dihydrides and Dihydrogen Complexes. Examples of cobalt dihydride complexes involved in photochemistry are scarce. In the earliest experiments on hydride photochemistry, the cationic complexes $[Co(H)_2(NN)(PR_3)_2]^+$ (NN = bpy *or* phen, R_3 = Bu_3, Pr_3, Et_3, Et_2Ph) exhibit photoinduced reductive elimination of H_2 under vacuum, which was reversed thermally by restoring a hydrogen atmosphere; photolysis of the dideuteride under H_2 generated the dihydride (Scheme 24).[1,85] Later, $[Co(H)_2(bpy)(PEt_2Ph)_2]^+$ was shown to undergo sensitized photoelimination of H_2 with visible light in the presence of $Fe(bpy)_2(CN)_2$ (see section 2.2.3).[85]

Scheme 24. Photochemical Elimination of D_2 from $[Co(D)_2(bpy)(PEt_2Ph)_2]^+$ under H_2 Atmosphere To Form the Dihydride-Co Analogue

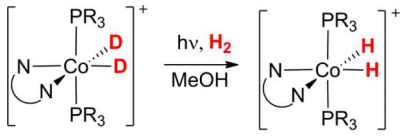

$PR_3 = PEt_2Ph$, $\phi_{408} = 0.14$

Rhodium dihydride complexes are easily accessible and have been investigated far more extensively; most of the examples have a skeleton involving a phosphine as a spectator ligand. The photochemistry of $Cp^*Rh(H)_2(PMe_3)$ was reported in seminal studies[4,261−265] that demonstrated loss of H_2 and C−H activation of arenes and alkanes (Scheme 25). For example, the

Scheme 25. Examples of Photochemistry of $Cp^*Rh(H)_2(PMe_3)$

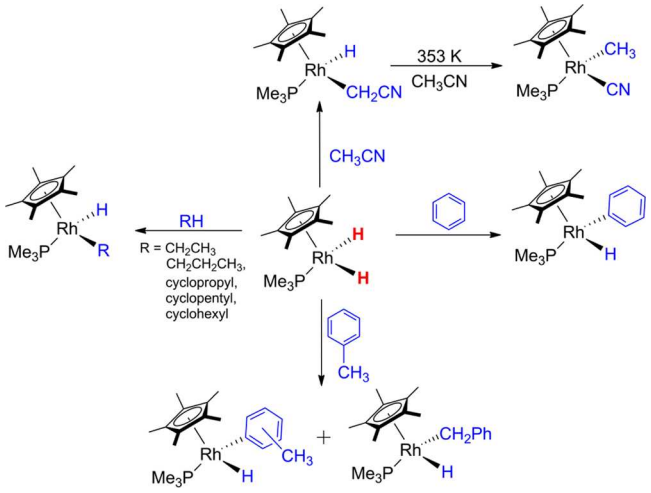

photolysis in liquid propane at low temperature yielded the propyl hydride complex. Similarly, reaction with cyclopropane generated the cyclopropyl hydride, but the latter rearranged intramolecularly to the rhodacyclobutane on warming. The rhodium dihydride exhibited substantial selectivity for primary over secondary bonds of alkanes. Careful isotope studies revealed evidence of intramolecular rearrangements of the rhodium alkyl complexes via η^2-alkane intermediates. This mechanism also allows for products of activation of secondary C−H bonds to isomerize to the preferred primary alkyl product. Strong support for the role of alkane complexes has been obtained in the intervening period.[264,266] The intramolecular competition between the benzylic and aryl protons of toluene at 228 K revealed the kinetic selectivity for aryl protons. On photoreaction with 1,3,5-$C_6H_3D_3$, the intramolecular kinetic isotope effect for arene C−H activation was measured as 1.4 ± 0.1, whereas the intermolecular competition between C_6H_6 and C_6D_6 gave a value of 1.05 ± 0.06. The competition between benzene and cyclopentane at 238 K demonstrated a 5.4:1 kinetic selectivity for benzene C−H activation. These observations proved that C−H activation of arenes did not proceed directly but proceeded via an intermediate, postulated as $CpRh(PMe_3)(\eta^2\text{-}C_6H_6)$, and led, with further measurements, to a complete free energy diagram for the alkane/arene competition at $[Cp^*Rh(PMe_3)]$.[4] A more recent photochemical study of the same complex, $Cp^*Rh(H)_2(PMe_3)$, in neat CH_3CN demonstrated the kinetic C−H activation product to be $Cp^*RhH(CH_2CN)(PMe_3)$; thermal conversion to the C−C activated complex was detected at higher temperatures (Scheme 25).[267]

Studies in low-temperature matrices revealed that a $16e^-$ fragment with a characteristic UV−vis absorption band was formed when $CpRh(H)_2(PMe_3)$ complex was irradiated and was assigned to $[CpRh(PMe_3)]$; H_2 reductive elimination, the primary photochemical process, could be partially reversed by long-wavelength photolysis. Furthermore, the transient showed reactivity in CH_4-, CO-, and N_2-doped matrices to produce the insertion/coordination products.[132]

The substitution of the Cp* with the bulkier Tp′ ligand led to three dihydride complexes that undergo photoejection of H_2 to form coordinatively unsaturated species capable of inserting into C−H bonds of arenes, $Tp'Rh(H)_2(L)$ (L = PMe_3, PMe_2Ph, $CNCH_2CMe_3$).[268,269] In addition to the phenyl hydride complex, irradiation of $Tp'Rh(H)_2(PMe_2Ph)$ yielded the cyclometalated complex $Tp'RhH(PMe_2C_6H_4)$. The selectivity for C−H activation over C−F activation and for the C−H bonds ortho to fluorine was revealed by photolysis of $Tp'Rh(H)_2(L)$ (L = PMe_3, PMe_2Ph) in fluoroarenes. This selectivity originates in the increased Rh−C bond dissociation energy, which correlates with the C−H bond dissociation energy (Figure 14).[269] Like $Cp^*RhH_2(PMe_3)$, the photoreactions of $Tp'Rh(H)_2(L)$ (L = PMe_3, PMe_2Ph) resulted in C−H bond activation of CH_3CN.[270] More recently, $Tp'Rh(H)_2(PMe_3)$ was employed in investigations on intramolecular and intermolecular selectivity between C−H and "hetero-bonds" (hetero = C−F, Si−H, B−H).[137] Notably, C−F bond activation was observed with pentafluoropyridine, but neither C−F bond activation nor arene coordination occurred with hexafluorobenzene, allowing the latter to be used as an inert solvent. There is strong intramolecular selectivity for the Si−H bond over C−H bonds in SiH_2Et_2 but lower selectivity in SiH_3Ph. The lack of dependence of the photochemical conversion on [substrate] demonstrated that this is a dissociative reaction. Irradiation with a laser within the NMR probe of C_6F_6 solutions containing two substrates allowed the intermolecular selectivity to be determined (see section 3.2). It is commonly assumed that thermal reactions of methyl hydride complexes are comparable to photochemical reactions of dihydride reactions in generating a coordinatively unsaturated intermediate. A comparison between photochemical and thermal reactivity, using $Tp'RhH(CH_3)(PMe_3)$ as a thermal precursor in the presence of a variety of substrates, was undertaken and the kinetics was studied. Interestingly, it was

DOI: 10.1021/acs.chemrev.6b00204
Chem. Rev. 2016, 116, 8506−8544

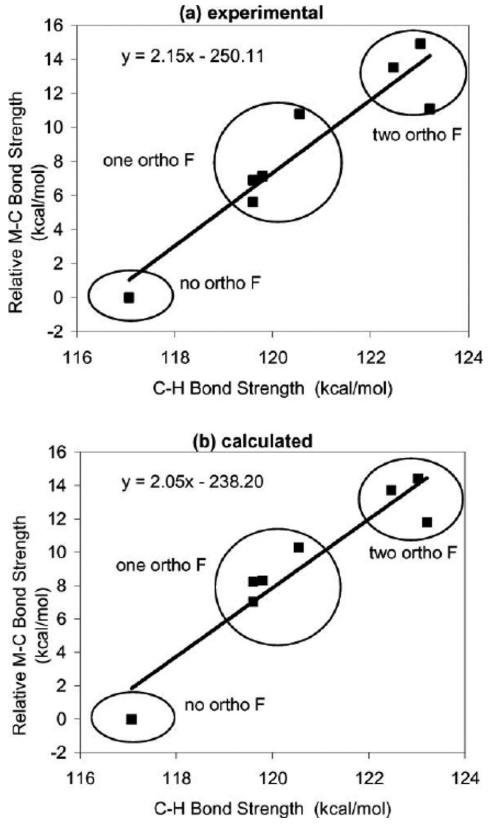

Figure 14. Plot of relative Rh−Ar^F bond strength vs calculated C−H bond strength (kcal/mol); experimental result (a) and DFT calculated result (b). Reproduced with permission from ref 269. Copyright 2010 Royal Society of Chemistry.

found that the two complexes followed different mechanisms despite forming the same final products (Figure 15).[137]

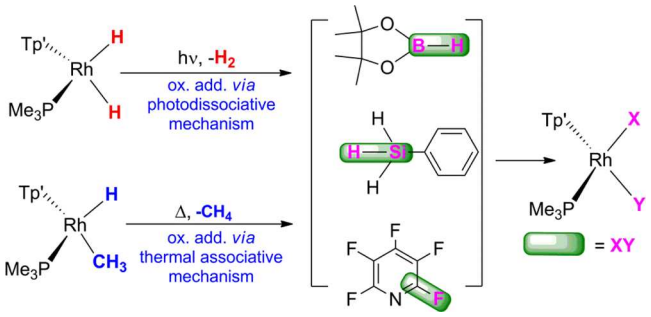

Figure 15. Reactivity of Tp′RhH$_2$(PMe$_3$) and Tp′RhH(CH$_3$)(PMe$_3$). Reproduced with permission from ref 137. Copyright 2015 American Chemical Society.

The triphenylphosphine complex Rh(H)$_2$(Cl)(PPh$_3$)$_3$ exhibited concerted reductive elimination of dihydrogen under irradiation to give Wilkinson's complex [RhCl(PPh$_3$)$_3$], as shown by flash photolysis.[271] This reactivity contrasted strongly with that of the iridium analogue (see below). Photocatalytic dehydrogenation of cyclohexane was observed on irradiation of Rh(H)$_2$(Cl)(PCy$_3$)$_2$ or of Rh(Cl)(PCy$_3$)$_2$ with optimum activity with $\lambda > 270$ nm photolysis and the same wavelength dependence for both complexes. A catalytic cycle was postulated in which cyclohexane attacks Rh(Cl)(PCy$_3$)$_2$ to form the cyclohexyl hydride; thermal β-elimination yields the cyclic alkene and Rh(H)$_2$(Cl)(PCy$_3$)$_2$ before photoelimination of H$_2$ regenerates the reactive intermediate.[272]

The photoreactivity of [CpM(CO)$_2$]$_2$ with Cp*Rh(H)$_2$(SiEt$_3$)$_2$ was exploited in the synthesis of trinuclear complexes; the fragment formed by H$_2$ elimination was capable of inserting into [CpM(CO)$_2$]$_2$ (M = Co, Ru, Ni, Fe) dimers to yield different types of metal clusters.[249] No evidence was provided that the rhodium complex was the light absorber rather than the metal carbonyl. Finally, the dimeric dihydride *syn*-[Rh^{II,II}ClH$_2$(tfepma)$_3$] (tfepma = bis[bis(trifluoroethoxy)-phosphino]methylamine, MeN(P{OCH$_2$CF$_3$}$_2$)$_2$) was shown to eliminate H$_2$ photochemically to form a short-lived blue product along with a stoichiometric amount of H$_2$. Although there is one hydride ligand on each metal, photoreaction of a mixture of Rh$_2$D$_2$ and Rh$_2$H$_2$ gave predominantly H$_2$ and D$_2$. The blue intermediate is thought to be [Rh$_2^{I,I}$(tfepma)$_3$Cl$_2$]. This process was a step in a more complicated photocycle for the production of H$_2$ in homogeneous solutions of hydrohalic acids.[101] The photochemical reactions of the dihydrogen complex Rh(H$_2$)(PCP) have been described earlier (section 2.4).[98]

The first Ir-dihydride reported to undergo photochemical H$_2$ elimination was the Vaska's dihydride adduct Ir(H)$_2$Cl(CO)(PPh$_3$)$_2$; the photochemical reaction yielded the Ir^I square-planar complex. Similar behavior was observed for the dihydride iodide analogue and for the dihydrides formed from H$_2$ addition to the cations [Ir(dppe)$_2$]$^+$ and [Ir(dppv)$_2$]$^+$.[273] The replacement of CO with PPh$_3$ afforded Ir(H)$_2$(Cl)(PPh$_3$)$_3$ and resulted in very similar photochemistry (quantum yield for loss of H$_2$ 0.56 ± 0.3); cyclometalation of the PPh$_3$ ligand was also observed in this case (Scheme 26), and the sequence could be reversed

Scheme 26. Photoreaction of Ir(H)$_2$(Cl)(PPh$_3$)$_2$ and Intramolecular Insertion into the C−H Bond of the Phosphine Phenyl Group

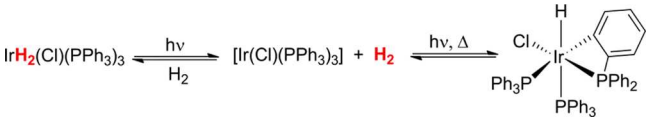

photochemically under H$_2$. Photolysis of a mixture of Ir(H)$_2$(Cl)(PPh$_3$)$_3$ and Ir(D)$_2$(Cl)(PPh$_3$)$_3$ gave only H$_2$ and D$_2$.[274] Laser flash photolysis investigations (with a 20 μs xenon arc flash lamp) on both Vaska's dihydride and the tris-PPh$_3$ analogue resulted in the observation of a common intermediate assigned to [IrCl(PPh$_3$)$_2$] formed from CO or PPh$_3$ loss, respectively. It was postulated that H$_2$ elimination would follow after the dissociation of those ligands.[271] A more modern approach with time-resolved IR spectroscopy on IrCl(CO)(PPh$_3$)$_2$ did not support this interpretation, but there has been no reexamination of the dihydride complexes.[275]

The photochemical reactivity of Cp*Ir(H)$_2$(PMe$_3$) toward alkanes, in particular cyclohexane and neopentane, heralded the age of C−H bond activation of alkanes.[276−278] With such a reactive complex, it is advantageous to find an inert solvent. Use of liquified xenon as solvent for the photoreactions at 193−198 K, followed by removal of the xenon for study by conventional methods, allowed investigation of reactions with numerous substrates. With this method, C−H oxidative addition was observed with methane and activation of secondary C−H bonds in cyclic alkanes. Whereas isopropanol and *t*-butanol reacted by C−H activation, methanol and ethanol underwent O−H

DOI: 10.1021/acs.chemrev.6b00204
Chem. Rev. 2016, 116, 8506−8544

activation.[279] Like the rhodium analogues investigated slightly later, Cp*Ir(H)$_2$(PMe$_3$) eliminates H$_2$ under irradiation to form a very reactive 16e$^-$ fragment that acts as the intermediate in these reactions.[276−278] The kinetic selectivity of the intermediate for benzene over cyclohexane was (3.5 ± 0.1):1, compared to ca. (9.1 ± 0.6):1 for the rhodium analogue. The reaction of Cp*IrH(Cl)(PMe$_3$) with a strong base appeared to give the same intermediate as obtained by photolysis of Cp*Ir(H)$_2$(PMe$_3$). However, the kinetic selectivities and kinetic isotope effects were significantly different, probably because the salt that is eliminated stays bound to iridium.[280] The reactions of (η^5-Ind)Ir(H)$_2$(PMe$_3$) with alkanes and benzene are similar to those of Cp*Ir(H)$_2$(PMe$_3$).[281] Although both Cp*Ir(H)$_2$(PPh$_3$) and Cp*Ir(H)$_2$(PMe$_3$) proved to be capable of inserting into the C−H bonds of benzene, only the PMe$_3$ complex attacked alkanes. When the reaction was run in CH$_3$CN, the PPh$_3$ complex reacted to form a cyclometalated product.

Photochemistry of CpIr(H)$_2$(PMe$_3$) in Ar matrices allowed detection of the 16e$^-$ fragment [CpIr(PMe$_3$)], confirming H$_2$ photoelimination as the primary process; the highly reactive fragment [CpIr(PMe$_3$)] inserted into the C−H bond of methane to form an Ir-methyl hydride species.[132] The analogue with phosphine replaced by CO, CpIr(H)$_2$(CO), once again underwent H$_2$ reductive elimination as the primary and only photoprocess in matrix photochemistry at 12 K. Again this complex acted as a C−H activator in methane matrices yielding CpIrH(CH$_3$)(CO). A more complicated situation was found in solution photochemistry where H/D scrambling during neopentane activation at 298 K disagreed with H$_2$ loss as the sole pathway.[133,282] In a more unusual study, the same complex was impregnated into zeolite materials and photolyzed in the presence of D$_2$, HBr, CO, C$_6$H$_6$, and alkanes. In contrast to solution photochemistry, no reactivity was detected in the presence of arenes and alkanes.[283]

An important step in the application of photochemical C−H activation was the photocatalytic dehydrogenation (λ_{ex} = 254 nm) of linear and cyclic alkanes using the complex Ir(H)$_2$(κ^2-O$_2$CCF$_3$)(PAr$_3$)$_2$ in the presence of CH$_2$=CH*t*-Bu as hydrogen acceptor. The reaction still proceeded when the hydrogen acceptor was omitted, but with reduced turnover number. The unsaturated reactive species formed via H$_2$ reductive photoelimination was postulated to react with the alkane; the resulting alkyl hydride underwent β-elimination to regenerate Ir(H)$_2$(κ^2-O$_2$CCF$_3$)(PAr$_3$)$_2$.[284,285]

The photochemical reactivity of Tp′Ir(H)$_2$(cyclooctene) with phosphites was also investigated; cyclooctene was shown to be the photolabile ligand with H$_2$ still bound to the metal center in the products. The [Tp′Ir(H)$_2$] intermediate formed initially underwent a complex series of reactions with incoming ligands and with benzene solvent.[286] The vinyl complex Ir(H)$_2$(CH=CHPh)(triphos) isomerized photochemically to two isomers of IrH(triphos)(η^2-CH$_2$=CHPh); the H$_2$-loss product Ir(H)$_2$(C≡CPh)(triphos) was also formed. The latter underwent photoisomerization to IrH(triphos)(η^2-CH=CPh) probably via a vinylidene complex. The photochemistry of Ir(H)$_2$(C$_2$H$_5$)(triphos) was less clean, producing several metal products and gases due to secondary photolysis of the species formed in solution.[40]

4.6.3. Group 9 Polyhydrides. Examples of trihydrides of group 9 involved in photochemical reactions are scarce. Rh(H)$_3$(triphos) reacted photochemically to eliminate H$_2$ and form transient [RhH(triphos)], which reacted rapidly with HBpin to form Rh(H)$_2$(Bpin)(triphos);[60] the Ir analogue also showed photoactivity in C$_6$H$_6$ to form the metal(hydride)phenyl species and H$_2$ gas.[40] Finally, the irradiation of *mer* and *fac*-[Ir(H)$_3$(PPh$_3$)$_3$] led to H$_2$ loss and cyclometalation. If the same complex was photolyzed under a hydrogen atmosphere, Ir(H)$_5$(PPh$_3$)$_2$ was the product detected, suggesting that H$_2$ loss was inhibited under these conditions, allowing loss of PPh$_3$ to be observed.[274]

4.7. Group 10 Metals

Examples of photoactive compounds become very rare as we move to the right of group 9. To our knowledge there are no palladium hydrides which have been investigated photochemically, and we have found only one example for nickel where a Ni(H$_2$)(CO)$_3$ complex underwent photodissociation of H$_2$ in H$_2$/Ar matrices.[287] Platinum offers a few more examples of photoactive mono- and dihydrides. The d^8 square-planar monohydride *trans*-[PtH(CH$_2$CN)(PPh$_3$)$_2$] was observed to isomerize to the cis-analogue on photolysis in a glass at 77 K, which underwent reductive elimination on warming. Solution photolysis (λ_{ex} 313 or 334 nm) caused reductive elimination of acetonitrile and formation of [Pt(PPh$_3$)$_2$]$_2$. Crossover experiments indicated that the reductive elimination proceeds without loss of phosphine.[288] Complexes *cis*-[PtH(SnPh$_3$)(PCy$_3$)$_2$], *cis*-[PtH(SiR$_2$R′)(PCy$_3$)$_2$] (R, R′ = H, alkyl, phenyl, OSiMe$_3$, etc.), and *cis*-[PtH(4-C$_5$NF$_4$)(PCy$_3$)$_2$] also isomerized to the trans-form under photolytic conditions.[38,289,290] The photochemistry of the dinuclear complexes [Pt$_2$(H)$_2$(μ-H)(dppm)$_2$]$^+$ and [Pt$_2$(H)$_2$(μ-Cl)(dppm)$_2$]$^+$ was summarized in section 2.5.[100] The related [{PtMe(dppm)}(μ-H)]PF$_6$ underwent photochemical reductive elimination of methane.[291]

Dissociation of H$_2$ as a primary photochemical step was also detected for a class of square-planar Pt(H)$_2$(PP) complexes (PP = (*t*-Bu)$_2$P(CH$_2$)$_2$P(*t*-Bu)$_2$, (*t*-Bu)$_2$P(CH$_2$)$_3$P(*t*-Bu)$_2$, (*t*-Bu)(Ph)P(CH$_2$)$_2$P(Ph)(*t*-Bu)); the reactive 14e$^-$ intermediates formed were capable of inserting into the C−H bonds of benzene to form PtH(Ph)(PP).[292] Finally, photoejection of H$_2$ from the cluster Pt$_2$Re$_2$(CO)$_7$(P*t*-Bu$_3$)$_2$(μ-H)$_4$ took place at room temperature; the same reactivity was achieved thermally at 97 °C.[216]

4.8. Group 11 Metals

Group 11 is even poorer in examples than group 10. Studies of atom photochemistry in cryogenic matrices were first reported for Cu; the irradiation of (CH$_3$)CuH caused fragmentation to yield Cu, CH$_3$, CuH, CuCH$_3$, and H.[233] Similar studies were performed on all the group 11 elements with the laser-ablation method of generating the atoms; methane activation afforded the C−H activated products, which were observed to fragment under further excitation.[293]

The two additional examples found are of metal clusters capable of H$_2$ ejection through light initiation; [Cu$_{20}$H$_{11}$(S$_2$P(O^{i}Pr)$_2$)$_9$] was reported to release H$_2$ upon irradiation by sunlight, but the copper product was not identifed.[294] The [Ag$_3$(H)$_2$(dppm)]$^+$ ion was studied by laser-induced dissociation of the mass-selected ion in the mass spectrometer and released H$_2$ in competition with loss of AgH as the minor pathway; deuteration experiments confirmed that the hydrogen came from hydride reductive elimination and not from the protons on the ligands. The structure, optical properties, and action spectrum were modeled by TD-DFT calculations. The ground-state structure consist of a Ag$_3$(μ-H)$_2$ unit bridged by dppm across the unique Ag−Ag bond. Additionally, molecular dynamics simulations of H$_2$ loss were performed for the ground and first excited singlet states making use of a DFT approach, but details

DOI: 10.1021/acs.chemrev.6b00204
Chem. Rev. 2016, 116, 8506−8544

of the methodology were not provided. Loss of H_2 is associated with Ag−H antibonding character and weakening of the Ag−Ag bond in the excited state.[295]

5. CONCLUSIONS AND OUTLOOK

Our survey of metal hydride photochemistry has revealed numerous examples of metal mono- and dihydrides that are photosensitive. The photochemical pathways exhibited by these two classes are strikingly different (Scheme 1 and Scheme 3). Whereas *cis*-dihydride complexes are highly likely to be photoactive with respect to H_2 reductive elimination, the photochemical behavior of monohydride complexes is less predictable. They may undergo one of several processes including M−H homolysis or, for alkyl and silyl hydride complexes, reductive elimination. Photodissociation of other ligands competes with processes involving M−H bonds in many examples but by no means in all. For example, H_2 elimination is the only process in $Ru(H)_2(CO)(etp)$ and $CpIr(H)_2(CO)$. Likewise, reductive elimination of alkanes is the only process for $Cp^*_2ZrH(alkyl)$. The selectivity of photoreaction, of great importance in synthetic chemistry, has been explored in detail in some examples, such as $Tp'Rh(H)_2(PMe_3)$. It is often assumed that *thermal* elimination of alkanes from alkyl hydrides is equivalent to *photochemical* elimination of H_2 from dihydrides—there is evidence that this is an oversimplification and the pathways differ significantly. The examples of metal hydride photochemistry are dominated by groups 6−9 of the periodic table; there are opportunities to explore the remaining groups more thoroughly. The photochemistry of metal polyhydrides and complexes with bridging hydrides is also underexplored, but there are exciting developments for bridging hydrides that are relevant to bioinorganic chemistry, in particular to hydrogenases, nitrogenase, and related enzymes. Photochemistry of paramagnetic metal hydrides has barely been explored outside the matrix environment. Another approach with opportunities for more investigation is the formation of charge-transfer complexes that are photosensitive at much longer wavelengths than their constituent components.

Applications of dissociative photochemistry in photocatalysis have been published since the early years of metal hydride photochemistry but will become more important as understanding of how to generate activity with visible radiation advances, especially for solar energy conversion. There may also be applications in hydrogen storage.

The photoprocesses mentioned so far are likely to involve dissociative excited states, but the ultrafast transient experiments that might prove this are few and far between in spite of the technical advances. Such experiments can now be associated with corresponding quantum dynamics calculations. There is more information on quantum yields, but measurements are hampered by the lack of distinctive absorption bands for the metal hydride and its product in many examples. On the other hand, transient absorption methods have been exploited extensively for group 8 metal dihydrides to determine the spectra, structure, and reactivity of the transient reactive intermediates. Transient absorption spectroscopy, often in conjunction with matrix isolation, has illuminated the structures and spectra of reaction intermediates implicated in catalysis and in activation of small molecules. The corresponding transient kinetic experiments have quantified the rates of reaction of these intermediates toward H_2, alkanes, arenes, silanes, and boranes. It is particularly striking that many of these bimolecular reactions between diamagnetic molecules have rate constants in the range 10^5−10^{10} $dm^3\ mol^{-1}\ s^{-1}$. The power of pulsed laser methods continues to develop through improvements in time-resolved infrared spectroscopy and linkage with NMR spectroscopy.

Luminescent metal hydride complexes are a rarity: we found examples containing pyridine or polypyridine ligands together with a pair of tetrahydrides $MH_4(dppe)_2$ (M = Mo, W). These complexes must have equilibrated excited states with potential for new reactions as demonstrated by the extraordinary photoinduced acidity and hydricity of $[Cp^*(H)(bpy)]^+$. Although photocatalysis with this ion was first demonstrated many years ago, its great potential is only now becoming clear. It offers a complementary approach to the standard methods employing coordinatively saturated ruthenium or iridium polypyridine complexes.

AUTHOR INFORMATION

Corresponding Authors

*E-mail: robin.perutz@york.ac.uk.
*E-mail: barbara.procacci@york.ac.uk.

Notes

The authors declare no competing financial interest.

Biographies

Robin Perutz has devoted most of his career to transition metal photochemistry. After undergraduate studies in Cambridge, he studied for his Ph.D., partly in Cambridge and partly in Newcastle-upon-Tyne under the supervision of J. J. Turner investigating metal carbonyl photochemistry in matrices. After postdoctoral work in Mülheim, he took up fixed-term positions in Edinburgh and Oxford. It was in Oxford that he was introduced to the photochemistry of $Cp_2Mo(H)_2$ and $Cp_2W(H)_2$ by M. L H. Green. In 1983 he moved to York, where he became a full professor in 1991. Another formative event was the visit of W. D. Jones to York in 1989, which started the research on $Ru(H)_2(dmpe)_2$. Nowadays, his research includes the development of new photochemical methods and the use of photochemistry to produce solar fuels. He also investigates the chemistry of C−F bond activation. He has received awards from the Royal Society of Chemistry, the Italian Chemical Society, and the French Chemical Society. He became a Fellow of the Royal Society, the U.K.'s national academy, in 2010. He has been very active in the women in science agenda for almost 15 years. He served as President of Dalton Division of the Royal Society of Chemistry. In 2015, he was elected a Fellow of the American Association for the Advancement of Science.

Barbara Procacci graduated from the Università degli Studi di Perugia in 2007. She completed her Ph.D. in 2012 at the University of York under the supervision of Professor Robin Perutz, working on photoinduced C−F, C−H, B−H, and Si−H activation by Rh and Ru complexes focusing on mechanistic investigations. She then decided to take up a position in York as a postdoctoral research fellow to work on a project jointly supervised by Professor Simon Duckett and Professor Robin Perutz. Her work is aimed to develop NMR spectroscopy as a time-resolved technique to monitor light-initiated organometallic reactions that happen on a fast time scale.

ACKNOWLEDGMENTS

We acknowledge support from EPSRC. R.N.P. is grateful to the many colleagues who have worked with him on metal hydride photochemistry. We particularly thank Professor Simon Duckett for his collaboration in *para*-hydrogen methods. We also received helpful comments on the Review from the referees and Professor Alex Miller.

DOI: 10.1021/acs.chemrev.6b00204
Chem. Rev. 2016, 116, 8506−8544

ABBREVIATIONS

14-aneN$_4$	cyclo-NH(CH$_2$)$_3$NH(CH$_2$)$_2$NH(CH$_2$)$_3$NH(CH$_2$)$_2$
bpy	2,2′-bipyridine
BPE	1,2-bis(2,5-dimethylphospholano)ethane
CASSCF	complete active space self-consistent field
CASPT2	complete active space second-order perturbation theory
CCI	contracted configuration interaction
CNAd	1-adamantylisonitrile
Cp	cyclopentadienyl, η^5-C$_5$H$_5$
Cp*	pentamethylcyclopentadienyl, η^5-C$_5$Me$_5$
Cp′	η^5-C$_5$H$_4$CH$_3$
Cp″	η^5-C$_5$Me$_4$H
Cp‡	η^5-1,2,4-C$_5$H$_2$*t*-Bu$_3$
CT	charge transfer
depe	1,2-bis(diethylphosphino)ethane
dfepe	1,2-bis(di(pentafluoroethyl)phosphino)ethane
dfmpe	1,2-bis(di(trifluoromethyl)phosphino)ethane
DFT	density functional theory
dmpe	1,2-bis(dimethylphosphino)ethane
dmpm	1,2-bis(dimethylphosphino)methane
dpe	1,2-bis(phosphino)ethane
dppe	1,2-bis(diphenylphosphino)ethane
dppm	1,2-bis(diphenylphosphino)methane
dppv	*cis*-1,2-bis(diphenylphosphino)ethene
Duphos	1,2-bis(2,5-dimethylphospholano)benzene
em	emission
etp	bis(diphenylphosphinoethyl)phenylphosphine
EPR	electron paramagnetic resonance
ex	excitation
GC	gas chromatography
HOMO	highest occupied molecular orbital
Ind	indenyl
IR	infrared
KIE	kinetic isotope effect
LF	ligand field
LIF	laser-induced fluorescence
LMCT	ligand-to-metal charge transfer
LUMO	lowest unoccupied molecular orbital
MCD	magnetic circular dichroism
MLCT	metal-to-ligand charge transfer
MRCI	multireference configuration interaction
NHC	N-heterocyclic carbene
NHE	normal hydrogen electrode
NMR	nuclear magnetic resonance
PAr$_3$	triarylphosphine
PCP	(2,6-C$_6$H$_3$)(CH$_2$P*t*Bu$_2$)$_2$
PCy$_3$	tricyclohexylphosphine
pdt	propanedithiolate
PHIP	*para*-hydrogen induced polarization
phen	1,10-phenanthroline
pin	pinacolate 1,2-O$_2$C$_2$Me$_4$
PP$_3$	tris[2-(diphenylphosphino)ethyl]phosphine
ppy	2-phenylpyridine
pyR	pyridinyl substituted by R
rf	radio frequency
SCF	self-consistent field
SOMO	singly occupied molecular orbital
TCNE	tetracyanoethylene
TD-CAM	time-dependent Coulomb-attenuating method
TD-DFT	time-dependent density functional theory
tfepma	MeN(P{OCH$_2$CF$_3$}$_2$)$_2$
THF	tetrahydrofuran
TOF	turnover frequency
TON	turnover number
tpy	2,2′:6′,2″-terpyridine
Tp′	tris(3,5-dimethyl-1-pyrazolyl)borate
Trip	2,4,6-triisopropylphenyl
triphos	MeC(CH$_2$PPh$_2$)$_3$
UV	ultraviolet

REFERENCES

(1) Camus, A.; Cocevar, C.; Mestroni, G. Cobalt complexes of 2,2′-bipyridine and 1,10-phenanthroline 2. Reactions with molecular-hydrogen and conjugated dienes in presence of tertiary phosphines. *J. Organomet. Chem.* **1972**, *39*, 355−364.

(2) Giannotti, C.; Green, M. L. H. Photoinduced insertion of bis-π-cyclopentadienyl tungsten into aromatic carbon-hydrogen bonds. *J. Chem. Soc., Chem. Commun.* **1972**, 1114−1115.

(3) Arndtsen, B. A.; Bergman, R. G.; Mobley, T. A.; Peterson, T. H. Selective intermolecular carbon-hydrogen bond activation by synthetic metal-complexes in homogeneous solution. *Acc. Chem. Res.* **1995**, *28*, 154−162.

(4) Jones, W. D.; Feher, F. J. Comparative reactivities of hydrocarbon C-H bonds with a transition-metal complex. *Acc. Chem. Res.* **1989**, *22*, 91−100.

(5) Jones, W. D. Isotope effects in C-H bond activation reactions by transition metals. *Acc. Chem. Res.* **2003**, *36*, 140−146.

(6) Bandy, J. A.; Cloke, F. G. N.; Copper, G.; Day, J. P.; Girling, R. B.; Graham, R. G.; Green, J. C.; Grinter, R.; Perutz, R. N. Decamethylrhenocene, (η^5-C$_5$Me$_5$)$_2$Re. *J. Am. Chem. Soc.* **1988**, *110*, 5039−5050.

(7) Torres, O.; Procacci, B.; Halse, M. E.; Adams, R. W.; Blazina, D.; Duckett, S. B.; Eguillor, B.; Green, R. A.; Perutz, R. N.; Williamson, D. C. Photochemical pump and NMR probe: Chemically created NMR coherence on a microsecond time scale. *J. Am. Chem. Soc.* **2014**, *136*, 10124−10131.

(8) Lukoyanov, D.; Khadka, N.; Yang, Z. Y.; Dean, D. R.; Seefeldt, L. C.; Hoffman, B. M. Reversible photoinduced reductive elimination of H$_2$ from the nitrogenase dihydride state, the E$_4$(4H) Janus intermediate. *J. Am. Chem. Soc.* **2016**, *138*, 1320−1327.

(9) Barrett, S. M.; Pitman, C. L.; Walden, A. G.; Miller, A. J. M. Photoswitchable hydride transfer from iridium to 1-methylnicotinamide rationalized by thermochemical cycles. *J. Am. Chem. Soc.* **2014**, *136*, 14718−14721.

(10) Suenobu, T.; Guldi, D. M.; Ogo, S.; Fukuzumi, S. Excited-state deprotonation and H/D exchange of an iridium hydride complex. *Angew. Chem., Int. Ed.* **2003**, *42*, 5492−5495.

(11) Shimogawa, R.; Takao, T.; Konishi, G.-I; Suzuki, H. Photochemical reaction of diruthenium tetrahydride-bridged complexes with carbon dioxide: Insertion of CO$_2$ into a Ru-H bond versus C═O double-bond cleavage. *Organometallics* **2014**, *33*, 5066−5069.

(12) Suzuki, H.; Shimogawa, R.; Muroi, Y.; Takao, T.; Oshima, M.; Konishi, G. Bimetallic activation of 2-alkanones through photo-induced α-hydrogen abstraction mediated by a dinuclear ruthenium tetrahydride complex. *Angew. Chem., Int. Ed.* **2013**, *52*, 1773−1776.

(13) Artero, V.; Chavarot-Kerlidou, M.; Fontecave, M. Splitting water with cobalt. *Angew. Chem., Int. Ed.* **2011**, *50*, 7238−7266.

(14) Dempsey, J. L.; Brunschwig, B. S.; Winkler, J. R.; Gray, H. B. Hydrogen evolution catalyzed by cobaloximes. *Acc. Chem. Res.* **2009**, *42*, 1995−2004.

(15) Stoll, T.; Castillo, C. E.; Kayanuma, M.; Sandroni, M.; Daniel, C.; Odobel, F.; Fortage, J.; Collomb, M. N. Photo-induced redox catalysis for proton reduction to hydrogen with homogeneous molecular systems using rhodium-based catalysts. *Coord. Chem. Rev.* **2015**, *304-305*, 20−37.

(16) Esswein, A. J.; Nocera, D. G. Hydrogen production by molecular photocatalysis. *Chem. Rev.* **2007**, *107*, 4022−4047.

(17) Lomoth, R.; Ott, S. Introducing a dark reaction to photochemistry: Photocatalytic hydrogen from [FeFe] hydrogenase active site model complexes. *Dalton Trans.* **2009**, 9952−9959.

DOI: 10.1021/acs.chemrev.6b00204
Chem. Rev. 2016, 116, 8506−8544

(18) Wang, W. G.; Rauchfuss, T. B.; Bertini, L.; Zampella, G. Unsensitized photochemical hydrogen production catalyzed by diiron hydrides. *J. Am. Chem. Soc.* **2012**, *134*, 4525−4528.
(19) Pitman, C. L.; Miller, A. J. M. Molecular photoelectrocatalysts for visible light-driven hydrogen evolution from neutral water. *ACS Catal.* **2014**, *4*, 2727−2733.
(20) Balzani, V.; Ceroni, P.; Juris, A. *Photochemistry and Photophysics, Concepts, Research and Applications*; Wiley-VCH: Weinheim, Germany, 2014.
(21) Ito, T. Oxidative addition reactions involving molybdenum polyhydrides. *Bull. Chem. Soc. Jpn.* **1999**, *72*, 2365−2377.
(22) Perutz, R. N.; Torres, O.; Vlček, A. J. Photochemistry of metal carbonyls. In *Comprehensive Inorganic Chemistry II*; Reedijk, J., Poeppelmeier, K., Eds.; Elsevier: Oxford, U.K., 2013; Vol. *8*, Ch. 8.06, pp 229−253.
(23) Grebenik, P.; Grinter, R.; Perutz, R. N. Metallocenes as reaction intermediates. *Chem. Soc. Rev.* **1988**, *17*, 453−490.
(24) Perutz, R. N. Tilden lecture - organometallic intermediates - ultimate reagents. *Chem. Soc. Rev.* **1993**, *22*, 361−369.
(25) (a) Andrews, L. Matrix infrared spectra and density functional calculations of transition metal hydrides and dihydrogen complexes. *Chem. Soc. Rev.* **2004**, *33*, 123−132. (b) Sweany, R. L. Matrix studies of transition metal hydrides. In *Transition metal hydrides*; Dedieu, A., Ed.; VCH: New York, 1992, Ch. 2, pp 65−101. (c) Daniel, C.; Veillard, A. Theoretical studies of the photochemistry of transition metal hydrides. In *Transition metal hydrides*; Dedieu, A., Ed.; VCH: New York, 1992, Ch. 7, pp 235−261.
(26) Rest, A. J.; Turner, J. J. Evidence for production of hydridotetracarbonylmanganese $HMn(CO)_4$ on reversible photolysis of hydridopentacarbonylmanganese $HMn(CO)_5$ in argon at 15° K. *J. Chem. Soc. D* **1969**, 375−376.
(27) Church, S. P.; Poliakoff, M.; Timney, J. A.; Turner, J. J. The generation in solid CO of the radical $Mn(CO)_5$. *J. Mol. Struct.* **1982**, *80*, 159−162.
(28) Symons, M. C. R.; Sweany, R. L. An electron-spin resonance study of matrix-isolated pentacarbonylmanganese(0) - formation from photolyzed pentacarbonylhydridomanganese(I). *Organometallics* **1982**, *1*, 834−836.
(29) Church, S. P.; Poliakoff, M.; Timney, J. A.; Turner, J. J. Photochemistry of matrix-isolated $HMn(CO)_5$ - evidence for 2 isomers of $HMn(CO)_4$. *Inorg. Chem.* **1983**, *22*, 3259−3266.
(30) Blakney, G. B.; Allen, W. F. Electronic spectra of some pentacarbonyl compounds of manganese and rhenium. *Inorg. Chem.* **1971**, *10*, 2763−2770.
(31) Hachey, M. R. J.; Daniel, C. The spectroscopy of $HMn(CO)_5$: A CASSCF/MRCI and CASPT2 ab initio study. *Inorg. Chem.* **1998**, *37*, 1387−1391.
(32) Brahim, H.; Daniel, C.; Rahmouni, A. Spin-orbit absorption spectroscopy of transition metal hydrides: A TD-DFT and MS-CASPT2 study of $HM(CO)_5$ (M = Mn, Re). *Int. J. Quantum Chem.* **2012**, *112*, 2085−2097.
(33) Eyermann, C. J.; Chung-Phillips, A. Electronic-structure of $HMn(CO)_5$, $H_2Fe(CO)_4$, and $HCo(CO)_4$ - molecular-orbitals, transition energies, and photoactive states. *J. Am. Chem. Soc.* **1984**, *106*, 7437−7443.
(34) Daniel, C. The photochemistry of transition-metal hydrides - a CASSCF/CCI study of the photodissociation of $HMn(CO)_5$. *J. Am. Chem. Soc.* **1992**, *114*, 1625−1631.
(35) Miller, F. D.; Sanner, R. D. Activation of benzene carbon hydrogen-bonds via photolysis or thermolysis of $(\eta^5\text{-}C_5Me_5)_2Zr(alkyl)H$ - isolation of $(\eta^5\text{-}C_5Me_5)_2Zr(C_6H_5)H$ and its conversion to a complex containing a tetramethylfulvene ligand. *Organometallics* **1988**, *7*, 818−825.
(36) Liu, D. K.; Brinkley, C. G.; Wrighton, M. S. Photochemistry of iron and ruthenium carbonyl-complexes - evidence for light-induced loss of carbon-monoxide and reductive elimination of triethylsilane from cis-mer-$HM(SiEt_3)(CO)_3(PPh_3)$. *Organometallics* **1984**, *3*, 1449−1457.
(37) Glueck, D. S.; Winslow, L. J. N.; Bergman, R. G. Iridium alkoxide and amide hydride complexes - synthesis, reactivity, and the mechanism of O-H and N-H reductive elimination. *Organometallics* **1991**, *10*, 1462−1479.
(38) Ford, P. C.; Hintze, R. E.; Petersen, J. D. Photochemistry of the heavier elements. In *Concepts of inorganic photochemistry*; Adamson, A. W., Fleischauer, P. D., Eds.; Wiley: New York, 1975; Ch. 5, pp 203−267.
(39) Garg, K.; Matsubara, Y.; Ertem, M. Z.; Lewandowska-Andralojc, A.; Sato, S.; Szalda, D. J.; Muckerman, J. T.; Fujita, E. Striking differences in properties of geometric isomers of $Ir(tpy)(ppy)H^+$: Experimental and computational studies of their hydricities, interaction with CO_2, and photochemistry. *Angew. Chem., Int. Ed.* **2015**, *54*, 14128−14132.
(40) Bianchini, C.; Barbaro, P.; Meli, A.; Peruzzini, M.; Vacca, A.; Vizza, F. Thermal and photochemical C-H bond activation reactions at iridium. π-coordination vs C-H cleavage of ethene, styrene, and phenylacetylene. *Organometallics* **1993**, *12*, 2505−2514.
(41) Ziessel, R. Photocatalysis - mechanistic studies of homogeneous photochemical water gas shift reaction catalyzed under mild conditions by novel cationic iridium(III) complexes. *J. Am. Chem. Soc.* **1993**, *115*, 118−127.
(42) Sandrini, D.; Maestri, M.; Ziessel, R. Spectroscopic behavior of a new family of mixed-ligand iridium(III) complexes. *Inorg. Chim. Acta* **1989**, *163*, 177−180.
(43) Montiel-Palma, V.; Perutz, R. N.; George, M. W.; Jina, O. S.; Sabo-Etienne, S. Two photochemical pathways in competition: Matrix isolation, time-resolved and NMR studies of cis-$Ru(PMe_3)_4(H)_2$. *Chem. Commun.* **2000**, 1175−1176.
(44) Berry, M.; Elmitt, K.; Green, M. L. H. Photoinduced insertion of tungsten into aromatic and aliphatic carbon-hydrogen bonds by bis(η-cyclopentadienyl)tungsten derivatives. *J. Chem. Soc., Dalton Trans.* **1979**, 1950−1958.
(45) Green, M. L. H.; Berry, M.; Couldwell, C.; Prout, K. Photoinduced insertion of tungsten into a C-H bond of tetramethylsilane. *New J. Chem.* **1977**, *1*, 187−188.
(46) Farrugia, L.; Green, M. L. H. Photoinduced insertion of tungsten into methanol giving a tungsten-methyl derivative. *J. Chem. Soc., Chem. Commun.* **1975**, 416b−417.
(47) Ito, T.; Nakano, T. Preparation and characterization of dicarboxylatobis(η-cyclopentadienyl)-tungsten(IV) complexes: a novel and convenient synthesis from $[W(\eta\text{-}C_5H_5)_2H_2]$ using molecular-oxygen as a hydrogen acceptor. *J. Chem. Soc., Dalton Trans.* **1987**, 1857−1860.
(48) Jones, W. D.; Chin, R. M.; Crane, T. W.; Baruch, D. M. Carbon sulfur bond-cleavage in thiophene by group-6 metallocenes. *Organometallics* **1994**, *13*, 4448−4452.
(49) Ketkov, S. Y.; Kutyreva, V. V.; Ob'edkov, A. M.; Domrachev, G. A. Gas-phase electronic absorption spectra of metallocene dihydrides $M(\eta^5\text{-}C_5H_5)_2H_2$ (M = Mo, W). *J. Organomet. Chem.* **2002**, *664*, 106−109.
(50) Geoffroy, G. L.; Bradley, M. G. Photochemistry of transition-metal hydride complexes. 3. Photoinduced elimination of molecular-hydrogen from $Mo(\eta^5\text{-}C_5H_5)_2H_2$. *Inorg. Chem.* **1978**, *17*, 2410−2414.
(51) Green, M. L. H.; O'Hare, D. The activation of carbon-hydrogen bonds. *Pure Appl. Chem.* **1985**, *57*, 1897−1910.
(52) Graham, R. G.; Grinter, R.; Perutz, R. N. Optical determination of magnetization behavior - a study of unstable metallocenes by magnetic circular-dichroism. *J. Am. Chem. Soc.* **1988**, *110*, 7036−7042.
(53) Hill, J. N.; Perutz, R. N.; Rooney, A. D. Laser-induced fluorescence of molybdenocene and tungstenocene. *J. Phys. Chem.* **1995**, *99*, 538−543.
(54) Bell, S. E. J.; Hill, J. N.; McCamley, A.; Perutz, R. N. Laser-induced fluorescence of reactive metallocenes $(\eta^5\text{-}C_5H_5)_2Re$, $(\eta^5\text{-}C_5H_5)_2W$, $(\eta^5\text{-}C_5H_5)_2Mo$ and $(\eta^5\text{-}C_5Me_5)_2Re$. *J. Phys. Chem.* **1990**, *94*, 3876−3878.
(55) Petri, S. H. A.; Neumann, B.; Stammler, H. G.; Jutzi, P. Silyl complexes of molybdenum and tungsten - synthesis, reactivity and structure. *J. Organomet. Chem.* **1998**, *553*, 317−329.
(56) Koloski, T. S.; Pestana, D. C.; Carroll, P. J.; Berry, D. H. Monobis(silyl) and bis(silyl) complexes of molybdenum and tungsten - synthesis, structures, and ^{29}Si NMR trends. *Organometallics* **1994**, *13*, 489−499.

DOI: 10.1021/acs.chemrev.6b00204
Chem. Rev. 2016, 116, 8506−8544

(57) Nakajima, T.; Mise, T.; Shimizu, I.; Wakatsuki, Y. A photochemical route to heterometallic complexes - synthesis and structural characterization of dinuclear and trinuclear complexes having a molybdenocene or tungstenocene unit. *Organometallics* **1995**, *14*, 5598−5604.
(58) Bergamini, P.; Sostero, S.; Traverso, O. Photochemistry of phosphine hydride complexes of iron group-metals. *J. Organomet. Chem.* **1986**, *299*, C11−C14.
(59) Hall, C.; Jones, W. D.; Mawby, R. J.; Osman, R.; Perutz, R. N.; Whittlesey, M. K. Matrix-isolation and transient photochemistry of $Ru(dmpe)_2H_2$ - characterization and reactivity of $Ru(dmpe)_2$ (dmpe = $Me_2PCH_2CH_2PMe_2$). *J. Am. Chem. Soc.* **1992**, *114*, 7425−7435.
(60) Callaghan, P. L.; Fernandez-Pacheco, R.; Jasim, N.; Lachaize, S.; Marder, T. B.; Perutz, R. N.; Rivalta, E.; Sabo-Etienne, S. Photochemical oxidative addition of B-H bonds at ruthenium and rhodium. *Chem. Commun.* **2004**, 242−243.
(61) Belt, S. T.; Scaiano, J. C.; Whittlesey, M. K. Determination of metal hydride and metal-ligand (L = CO, N_2) bond-energies using photoacoustic calorimetry. *J. Am. Chem. Soc.* **1993**, *115*, 1921−1925.
(62) Osman, R.; Perutz, R. N.; Rooney, A. D.; Langley, A. J. Picosecond photolysis of a metal dihydride - rapid reductive elimination of dihydrogen from $Ru(dmpe)_2H_2$ (dmpe = $(CH_3)_2PCH_2CH_2P(CH_3)_2$). *J. Phys. Chem.* **1994**, *98*, 3562−3563.
(63) Whittlesey, M. K.; Mawby, R. J.; Osman, R.; Perutz, R. N.; Field, L. D.; Wilkinson, M. P.; George, M. W. Transient and matrix photochemistry of $Fe(dmpe)_2H_2$ (dmpe = $Me_2PCH_2CH_2PMe_2$) - dynamics of C-H and H-H activation. *J. Am. Chem. Soc.* **1993**, *115*, 8627−8637.
(64) Cronin, L.; Nicasio, M. C.; Perutz, R. N.; Peters, R. G.; Roddick, D. M.; Whittlesey, M. K. Laser flash-photolysis and matrix-isolation studies of $Ru(R_2PCH_2CH_2PR_2)H_2$ (R = C_2H_5, C_6H_5, C_2F_5) - control of oxidative addition rates by phosphine substituents. *J. Am. Chem. Soc.* **1995**, *117*, 10047−10054.
(65) Nicasio, M. C.; Perutz, R. N.; Walton, P. H. Transient photochemistry, matrix isolation, and molecular structure of cis-$Ru(dmpm)_2H_2$ (dmpm = $Me_2PCH_2PMe_2$). *Organometallics* **1997**, *16*, 1410−1417.
(66) Osman, R.; Pattison, D. I.; Perutz, R. N.; Bianchini, C.; Casares, J. A.; Peruzzini, M. Photochemistry of $M(PP_3)H_2$ (M = Ru, Os; PP_3 = $P(CH_2CH_2PPH_2)_3$): Preparative, NMR, and time-resolved studies. *J. Am. Chem. Soc.* **1997**, *119*, 8459−8473.
(67) Montiel-Palma, V.; Pattison, D. I.; Perutz, R. N.; Turner, C. Photochemistry of $Ru(etp)(CO)H_2$ (etp = $PHP(CH_2CH_2PPH_2)_2$): Fast oxidative addition and coordination following exclusive dihydrogen loss. *Organometallics* **2004**, *23*, 4034−4039.
(68) Nicasio, M. C.; Perutz, R. N.; Tekkaya, A. Photochemistry of $Os(dmpe)_2H_2$: Matrix, transient solution, and NMR studies of 16-electron $Os(dmpe)_2$ (dmpe = $Me_2PCH_2CH_2PMe_2$). *Organometallics* **1998**, *17*, 5557−5564.
(69) Osman, R.; Pattison, D. I.; Perutz, R. N.; Bianchini, C.; Peruzzini, M. Pulsed-laser photolysis of $Os(PP_3)H_2$ [PP_3=$P(CH_2CH_2PPH_2)_3$]: kinetic selectivity for reaction with methane. *J. Chem. Soc., Chem. Commun.* **1994**, 513−514.
(70) Vendrell, O.; Moreno, M.; Lluch, J. M. Fast hydrogen elimination from the $Ru(PH_3)_3(CO)(H)_2$ and $Ru(PH_3)_4(H)_2$ complexes in the first singlet excited states: A diabatic quantum dynamics study. *J. Chem. Phys.* **2004**, *121*, 6258−6267.
(71) Macgregor, S. A.; Eisenstein, O.; Whittlesey, M. K.; Perutz, R. N. A theoretical study of $[M(PH_3)_4]$ (M = Ru or Fe), models for the highly reactive d^8 intermediates $[M(dmpe)_2]$ (dmpe = Me_2PCH_2-CH_2PMe_2). Zero activation energies for addition of CO and oxidative addition of H_2. *J. Chem. Soc., Dalton Trans.* **1998**, 291−300.
(72) Ogasawara, M.; Macgregor, S. A.; Streib, W. E.; Folting, K.; Eisenstein, O.; Caulton, K. G. Characterization and reactivity of an unprecedented unsaturated zero-valent ruthenium species: Isolable, yet highly reactive. *J. Am. Chem. Soc.* **1996**, *118*, 10189−10199.
(73) Sweany, R. L. Matrix photolysis of tetracarbonyldihydridoiron - evidence for oxidative addition of dihydrogen on tetracarbonyliron. *J. Am. Chem. Soc.* **1981**, *103*, 2410−2412.
(74) Heitz, M. C.; Daniel, C. Photodissociation dynamics of organometallics: Quantum simulation for the dihydride complex $H_2Fe(CO)_4$. *J. Am. Chem. Soc.* **1997**, *119*, 8269−8275.
(75) Heitz, M. C.; Guillaumont, D.; Cote-Bruand, I.; Daniel, C. Photodissociation and electronic spectroscopy of transition metal hydrides carbonyls: Quantum chemistry and wave packet dynamics. *J. Organomet. Chem.* **2000**, *609*, 66−76.
(76) Vallet, V.; Bossert, J.; Strich, A.; Daniel, C. The electronic spectroscopy of transition metal di-hydrides $H_2M(CO)_4$ (M = Fe, Os): A theoretical study based on CASSCF/MS-CASPT2 and TD-DFT. *Phys. Chem. Chem. Phys.* **2003**, *5*, 2948−2953.
(77) Vallet, V.; Strich, A.; Daniel, C. Spin-orbit effects on the electronic spectroscopy of transition metal dihydrides $H_2M(CO)_4$ (M = Fe, Os). *Chem. Phys.* **2005**, *311*, 13−18.
(78) Ampt, K. A. M.; Burling, S.; Donald, S. M. A.; Douglas, S.; Duckett, S. B.; Macgregor, S. A.; Perutz, R. N.; Whittlesey, M. K. Photochemical isomerization of N-heterocyclic carbene ruthenium hydride complexes: In situ photolysis, parahydrogen, and computational studies. *J. Am. Chem. Soc.* **2006**, *128*, 7452−7453.
(79) Merwin, R. K.; Ontko, A. C.; Houlis, J. F.; Roddick, D. M. Synthesis and characterization of CpMn(dfepe)(L) complexes (dfepe = $(C_2F_5)_2PCH_2CH_2P(C_2F_5)_2$; L = CO, H_2, N_2): An unusual example of a dihydride to dihydrogen photochemical conversion. *Polyhedron* **2004**, *23*, 2873−2878.
(80) Casey, C. P.; Tanke, R. S.; Hazin, P. N.; Kemnitz, C. R.; McMahon, R. J. Kinetic generation of *cis*-$C_5H_5(CO)_2ReH_2$ from the reaction of $C_5H_5(CO)_2Re(\mu$-H)Pt(H)$(PPh_3)_2$ with diphenylacetylene. *Inorg. Chem.* **1992**, *31*, 5474−5479.
(81) Jones, W. D.; Maguire, J. A.; Rosini, G. P. Thermal and photochemical substitution reactions of $CpRe(PPh_3)_2H_2$ and $CpRe(PPh_3)H_4$. Catalytic insertion of ethylene into the C-H bond of benzene. *Inorg. Chim. Acta* **1998**, *270*, 77−86.
(82) Jones, W. D.; Maguire, J. A. The activation of methane by rhenium - catalytic H/D exchange in alkanes with $CpRe(PPh_3)_2H_2$. *Organometallics* **1986**, *5*, 590−591.
(83) Jones, W. D.; Rosini, G. P.; Maguire, J. A. Photochemical C-H activation and ligand exchange reactions of $CpRe(PPh_3)_2H_2$. Phosphine dissociation is not involved. *Organometallics* **1999**, *18*, 1754−1760.
(84) Ko, J. J.; Bockman, T. M.; Kochi, J. K. Photoinduced hydrometalation and hydrogenation of activated olefins with molybdenum and tungsten dihydrides (Cp_2MH_2). *Organometallics* **1990**, *9*, 1833−1842.
(85) Brewer, K. J.; Murphy, W. R.; Moore, K. J.; Eberle, E. C.; Petersen, J. D. Visible-light production of molecular-hydrogen by sensitization of a cobalt dihydride complex. *Inorg. Chem.* **1986**, *25*, 2470−2472.
(86) Webster, L. R.; Ibrahim, S. K.; Wright, J. A.; Pickett, C. J. Solar fuels: Visible-light-driven generation of dihydrogen at p-type silicon electrocatalysed by molybdenum hydrides. *Chem. - Eur. J.* **2012**, *18*, 11798−11803.
(87) Graff, J. L.; Sobieralski, T. J.; Wrighton, M. S.; Geoffroy, G. L. Photophysical and photochemical behavior of tetrahydridobis(bis(1,2-diphenylphosphino)ethane)molybdenum and -tungsten: optical-emission and photoreduction of alkenes. *J. Am. Chem. Soc.* **1982**, *104*, 7526−7533.
(88) Pierantozzi, R.; Geoffroy, G. L. Photoinduced elimination of H_2 from $MoH_4(diphos)_2$ and $MoH_4(PPh_2Me)_4$. *Inorg. Chem.* **1980**, *19*, 1821−1822.
(89) Ito, T.; Matsubara, T. Insertion of carbon-dioxide into a molybdenum hydrogen-bond - photochemical formation of hydrido-formato complex of molybdenum(II). *J. Chem. Soc., Dalton Trans.* **1988**, 2241−2242.
(90) Ito, T.; Tosaka, H.; Yoshida, S.; Mita, K.; Yamamoto, A. Selective activation of olefinic C-H bonds - reaction of a hydridomolybdenum complex with methacrylic esters to form hydrido alkenyl complexes. *Organometallics* **1986**, *5*, 735−739.
(91) Ito, T.; Matsubara, T.; Yamashita, Y. Selective C-O bond-cleavage of allylic esters using $MoH_4(PH_2PCH_2CH_2PPH_2)_2$ under light irradiation to give hydridocarboxylatomolybdenum(II) complexes. *J. Chem. Soc., Dalton Trans.* **1990**, 2407−2412.

DOI: 10.1021/acs.chemrev.6b00204
Chem. Rev. 2016, 116, 8506−8544

(92) Kurishima, S.; Matsuda, N.; Tamura, N.; Ito, T. Bidentate cyclic imido complexes of molybdenum(II) - preparation, solution behavior and x-ray crystal-structure. *J. Chem. Soc., Dalton Trans.* **1991**, 1135−1141.
(93) Ito, T.; Kurishima, S.; Tanaka, M.; Osakada, K. Oxidative addition of N-substituted amides to molybdenum(II) involving N-H bond-cleavage to give (η^2-*N*-acylamido-*N,O*)hydridomolybdenum(II) complexes - X-ray molecular-structure of the 7-coordinate complex $MoH(N(COCH_3)CH_3)((C_6H_5)_2PCH_2CH_2P(C_6H_5)_2)_2$. *Organometallics* **1992**, *11*, 2333−2335.
(94) Eguillor, B.; Caldwell, P. J.; Cockett, M. C. R.; Duckett, S. B.; John, R. O.; Lynam, J. M.; Sleigh, C. J.; Wilson, I. Detection of unusual reaction intermediates during the conversion of $W(N_2)_2(dppe)_2$ to $W(H)_4(dppe)_2$ and of H_2O into H_2. *J. Am. Chem. Soc.* **2012**, *134*, 18257−18265.
(95) Sweany, R. L. Photolysis of hexacarbonylchromium in hydrogen-containing matrices - evidence of simple adducts of molecular-hydrogen. *J. Am. Chem. Soc.* **1985**, *107*, 2374−2379.
(96) Sweany, R. L. Photolysis of (cyclopentadienyl)-tricarbonylhydridometal and (pentamethylcyclopentadienyl)-tricarbonylhydridometal complexes of tungsten and molybdenum in dihydrogen-containing matrices - evidence for adducts of molecular-hydrogen. *J. Am. Chem. Soc.* **1986**, *108*, 6986−6991.
(97) Wang, X.; Andrews, L. Infrared spectra and theoretical calculations for Fe, Ru, and Os metal hydrides and dihydrogen complexes. *J. Phys. Chem. A* **2009**, *113*, 551−563.
(98) Doherty, M. D.; Grills, D. C.; Huang, K. W.; Muckerman, J. T.; Polyansky, D. E.; van Eldik, R.; Fujita, E. Kinetics and thermodynamics of small molecule binding to pincer-PCP rhodium(I) complexes. *Inorg. Chem.* **2013**, *52*, 4160−4172.
(99) Loges, B.; Boddien, A.; Junge, H.; Noyes, J. R.; Baumann, W.; Beller, M. Hydrogen generation: Catalytic acceleration and control by light. *Chem. Commun.* **2009**, 4185−4187.
(100) Foley, H. C.; Morris, R. H.; Targos, T. S.; Geoffroy, G. L. Photoinduced elimination of H_2 from $[Pt_2H_3(dppm)_2]PF_6$ and $[Pt_2H_2Cl(dppm)_2]PF_6$. *J. Am. Chem. Soc.* **1981**, *103*, 7337−7339.
(101) Esswein, A. J.; Veige, A. S.; Nocera, D. G. A photocycle for hydrogen production from two-electron mixed-valence complexes. *J. Am. Chem. Soc.* **2005**, *127*, 16641−16651.
(102) Alvarez, C. M.; Garcia, M. E.; Ruiz, M. A.; Connelly, N. G. Diphenylphosphide-bridged diiron derivatives of $Fe_2(\eta^5\text{-}C_5H_5)_2(\mu\text{-}H)(\mu\text{-}PPh_2)(CO)_2$. *Organometallics* **2004**, *23*, 4750−4758.
(103) Alvarez, C. M.; Galán, B.; García, M. E.; Riera, V.; Ruiz, M. A.; Vaissermann, J. P−C and C−H bond cleavages in the photochemical reactions of $[Fe_2(\eta^5\text{-}C_5H_5)_2(CO)_4]$ with bis(diphenylphosphino)-methane. *Organometallics* **2003**, *22*, 5504−5512.
(104) Brunner, H.; Peter, H. Optically-active transition-metal complexes 99. Photochemically induced *cis-trans*-isomerization in optically-active phosphido bridged iron complexes of the type $[CpFe(\mu\text{-}PR_2)CO)_2]$ and $[Cp_2Fe_2(\mu\text{-}H)(\mu\text{-}PR_2)(CO)_2]$. *J. Organomet. Chem.* **1990**, *393*, 411−422.
(105) Brunner, H.; Rotzer, M. Enantioselective catalysis 78. Optically-active phosphido-bridged iron complex $(\eta^5\text{-}C_5H_5)_2Fe_2(\mu\text{-}H)(\mu\text{-}PMen_2)(CO)_2$ - synthesis, isomerization, catalysis. *J. Organomet. Chem.* **1992**, *425*, 119−124.
(106) Yu, Y.; Sadique, A. R.; Smith, J. M.; Dugan, T. R.; Cowley, R. E.; Brennessel, W. W.; Flaschenriem, C. J.; Bill, E.; Cundari, T. R.; Holland, P. L. The reactivity patterns of low-coordinate iron-hydride complexes. *J. Am. Chem. Soc.* **2008**, *130*, 6624−6638.
(107) Wrighton, M. Photochemistry of metal carbonyls. *Chem. Rev.* **1974**, *74*, 401−430.
(108) Hennig, H. Homogeneous photocatalysis by transition metal complexes. *Coord. Chem. Rev.* **1999**, *182*, 101−123.
(109) Hoffman, N. W.; Brown, T. L. Thermal and photochemical substitution-reactions of tricarbonyl(cyclopentadienyl)hydrido compounds of tungsten and molybdenum. *Inorg. Chem.* **1978**, *17*, 613−617.
(110) Heyduk, A. F.; Nocera, D. G. Hydrogen produced from hydrohalic acid solutions by a two-electron mixed-valence photocatalyst. *Science* **2001**, *293*, 1639−1641.
(111) Elgrishi, N.; Teets, T. S.; Chambers, M. B.; Nocera, D. G. Stability-enhanced hydrogen-evolving dirhodium photocatalysts through ligand modification. *Chem. Commun.* **2012**, *48*, 9474−9476.
(112) Barrett, S. M.; Slattery, S. A.; Miller, A. J. M. Photochemical formic acid dehydrogenation by iridium complexes: Understanding mechanism and overcoming deactivation. *ACS Catal.* **2015**, *5*, 6320−6327.
(113) Yu, M. M.; Jing, H. Z.; Liu, X.; Fu, X. F. Visible-light-promoted generation of hydrogen from the hydrolysis of silanes catalyzed by rhodium(III) porphyrins. *Organometallics* **2015**, *34*, 5754−5758.
(114) Dombray, T.; Werncke, C. G.; Jiang, S.; Grellier, M.; Vendier, L.; Bontemps, S.; Sortais, J. B.; Sabo-Etienne, S.; Darcel, C. Iron-catalyzed C-H borylation of arenes. *J. Am. Chem. Soc.* **2015**, *137*, 4062−4065.
(115) Castro, L. C. M.; Bezier, D.; Sortais, J. B.; Darcel, C. Iron dihydride complex as the pre-catalyst for efficient hydrosilylation of aldehydes and ketones under visible light activation. *Adv. Synth. Catal.* **2011**, *353*, 1279−1284.
(116) Perutz, R. N. Photochemical reactions involving matrix-isolated atoms. *Chem. Rev.* **1985**, *85*, 77−96.
(117) Perutz, R. N. Photochemistry of small molecules in low-temperature matrices. *Chem. Rev.* **1985**, *85*, 97−127.
(118) Bondybey, V. E.; Smith, A. M.; Agreiter, J. New developments in matrix isolation spectroscopy. *Chem. Rev.* **1996**, *96*, 2113−2134.
(119) Khriachtchev, L.; Rasanen, M.; Gerber, R. B. Noble-gas hydrides: New chemistry at low temperatures. *Acc. Chem. Res.* **2009**, *42*, 183−191.
(120) Hill, J. N.; Perutz, R. N.; Rooney, A. D. Laser-induced fluorescence of rhenocene in low-temperature matrices - selective excitation and emission. *J. Phys. Chem.* **1995**, *99*, 531−537.
(121) Cho, H. G.; Andrews, L. Infrared spectra of CH_3-MoH, $CH_2{=}MoH_2$, and $CH{\equiv}MoH_3$ formed by activation of CH_4 by molybdenum atoms. *J. Am. Chem. Soc.* **2005**, *127*, 8226−8231.
(122) Wang, X.; Andrews, L.; Infante, I.; Gagliardi, L. Matrix infrared spectroscopic and computational investigation of late lanthanide metal hydride species $MH_X(H_2)_Y$ (M = Tb-Lu, x = 1−4, y = 0−3). *J. Phys. Chem. A* **2009**, *113*, 12566−12572.
(123) Bitterwolf, T. E.; Linehan, J. C.; Shade, J. E. Solution and nujol matrix photochemistry of $(\eta^5\text{-}C_5H_5)_2Os_2(CO)_4$ and nujol matrix photochemistry of $(\eta^5\text{-}C_5H_4CH_3)_2Ru_2(CO)_4$ and $(\eta^5\text{-}C_5H_5)M(CO)_2H$, where M = Ru and Os. *Organometallics* **2001**, *20*, 775−781.
(124) Macrae, V. A.; Green, J. C.; Greene, T. M.; Downs, A. J. Thermal and photolytic reactions of group 12 metal atoms in HCl-doped argon matrixes: Formation and characterization of the hydride species HMCl (M = Zn, Cd, or Hg). *J. Phys. Chem. A* **2004**, *108*, 9500−9509.
(125) Green, R. A.; Adams, R. W.; Duckett, S. B.; Mewis, R. E.; Williamson, D. C.; Green, G. G. R. The theory and practice of hyperpolarization in magnetic resonance using parahydrogen. *Prog. Nucl. Magn. Reson. Spectrosc.* **2012**, *67*, 1−48.
(126) Reinartz, S.; White, P. S.; Brookhart, M.; Templeton, J. L. Syntheses of platinum(IV) aryl dihydride complexes via arene C-H bond activation. *Organometallics* **2001**, *20*, 1709−1712.
(127) Xiao, Z. L.; Hauge, R. H.; Margrave, J. L. Reactions of vanadium and titanium with molecular-hydrogen in Kr and Ar matrices at 12 K. *J. Phys. Chem.* **1991**, *95*, 2696−2700.
(128) Cho, H. G.; Andrews, L. Methane activation by laser-ablated V, Nb, and Ta atoms: Formation of CH_3-MH, $CH_2{=}MH_2$, $CH{\equiv}MH_3$, and $(CH_3)_2MH_2$. *J. Phys. Chem. A* **2006**, *110*, 3886−3902.
(129) Girling, R. B.; Grebenik, P.; Perutz, R. N. Vibrational-spectra of terminal metal-hydrides - solution and matrix-isolation studies of $[(\eta\text{-}C_5H_5)_2MH_n]^{x+}$ (M = Re, Mo, W, Nb, Ta, n = 1−3, x = 0, 1). *Inorg. Chem.* **1986**, *25*, 31−36.
(130) Bakac, A. Photoinduced insertion of molecular oxygen into metal-hydrogen bonds. *J. Photochem. Photobiol., A* **2000**, *132*, 87−89.
(131) Chetwynd-Talbot, J.; Grebenik, P.; Perutz, R. N. Photochemical reactions of $W(\eta\text{-}C_5H_5)_2L_n$, $Mo(\eta\text{-}C_5H_5)_2L_n$, $Cr(\eta\text{-}C_5H_5)_2L_n$, $V(\eta\text{-}C_5H_5)_2$ in low temperature matrices. Detection of tungstenocene and molybdenocene. *Inorg. Chem.* **1982**, *21*, 3647−3657.
(132) Partridge, M. G.; McCamley, A.; Perutz, R. N. Photochemical generation of 16-electron $Rh(\eta^5\text{-}C_5H_5)(PMe_3)$ and $Ir(\eta^5\text{-}C_5H_5)(PMe_3)$

DOI: 10.1021/acs.chemrev.6b00204
Chem. Rev. 2016, 116, 8506−8544

in low-temperature matrices - evidence for methane activation. *J. Chem. Soc., Dalton Trans.* **1994**, 3519−3526.
(133) Bloyce, P. E.; Rest, A. J.; Whitwell, I. Photochemistry of carbonyl(η^5-cyclopentadienyl)dihydridoiridium in frozen gas matrices at ca 12 K - infrared evidence relating to C-H activation. *J. Chem. Soc., Dalton Trans.* **1990**, 813−821.
(134) Colombo, M.; George, M. W.; Moore, J. N.; Pattison, D. I.; Perutz, R. N.; Virrels, I. G.; Ye, T. Q. Ultrafast reductive elimination of hydrogen from a metal carbonyl dihydride complex; a study by time-resolved IR and visible spectroscopy. *J. Chem. Soc., Dalton Trans.* **1997**, 2857−2859.
(135) Frederix, P.; Adamczyk, K.; Wright, J. A.; Tuttle, T.; Ulijn, R. V.; Pickett, C. J.; Hunt, N. T. Investigation of the ultrafast dynamics occurring during unsensitized photocatalytic H_2 evolution by an [FeFe]-hydrogenase subsite analogue. *Organometallics* **2014**, *33*, 5888−5896.
(136) Campian, M. V.; Perutz, R. N.; Procacci, B.; Thatcher, R. J.; Torres, O.; Whitwood, A. C. Selective photochemistry at stereogenic metal and ligand centers of *cis*-Ru(diphosphine)$_2$(H)$_2$: Preparative, nmr, solid state, and laser flash studies. *J. Am. Chem. Soc.* **2012**, *134*, 3480−3497.
(137) Procacci, B.; Jiao, Y.; Evans, M. E.; Jones, W. D.; Perutz, R. N.; Whitwood, A. C. Activation of B-H, Si-H, and C-F bonds with Tp′Rh(PMe$_3$) complexes: Kinetics, mechanism, and selectivity. *J. Am. Chem. Soc.* **2015**, *137*, 1258−1272.
(138) Schott, D.; Callaghan, P.; Dunne, J.; Duckett, S. B.; Godard, C.; Goicoechea, J. M.; Harvey, J. N.; Lowe, J. P.; Mawby, R. J.; Muller, G.; Perutz, R. N.; Poli, R.; Whittlesey, M. K. The reaction of M(CO)$_3$(Ph$_2$PCH$_2$CH$_2$PPh$_2$) (M = Fe, Ru) with parahydrogen: Probing the electronic structure of reaction intermediates and the internal rearrangement mechanism for the dihydride products. *Dalton Trans.* **2004**, 3218−3224.
(139) Blazina, D.; Dunne, J. P.; Aiken, S.; Duckett, S. B.; Elkington, C.; McGrady, J. E.; Poli, R.; Walton, S. J.; Anwar, M. S.; Jones, J. A.; Carteret, H. A. Contrasting photochemical and thermal reactivity of Ru(CO)$_2$(PPh$_3$)(dppe) towards hydrogen rationalised by parahydrogen NMR and DFT studies. *Dalton Trans.* **2006**, 2072−2080.
(140) Hanson-Heine, M. W. D.; George, M. W.; Besley, N. A. Rapid anharmonic vibrational corrections derived from partial Hessian analysis. *J. Chem. Phys.* **2012**, *136*, 224102.
(141) Hanson-Heine, M. W. D.; George, M. W.; Besley, N. A. Investigating the calculation of anharmonic vibrational frequencies using force fields derived from density functional theory. *J. Phys. Chem. A* **2012**, *116*, 4417−4425.
(142) Villaume, S.; Strich, A.; Daniel, C.; Perera, S. A.; Bartlett, R. J. A coupled cluster study of the electronic spectroscopy and photochemistry of Cr(CO)$_6$. *Phys. Chem. Chem. Phys.* **2007**, *9*, 6115−6122.
(143) McKinlay, R. G.; Almeida, N. M. S.; Coe, J. P.; Paterson, M. J. Excited states of the nickel carbonyls Ni(CO) and Ni(CO)$_4$: Challenging molecules for electronic structure theory. *J. Phys. Chem. A* **2015**, *119*, 10076−10083.
(144) Rosa, A.; Baerends, E. J.; van Gisbergen, S. J. A.; van Lenthe, E.; Groeneveld, J. A.; Snijders, J. G. Electronic spectra of M(CO)$_6$ (M = Cr, Mo, W) revisited by a relativistic TDDFT approach. *J. Am. Chem. Soc.* **1999**, *121*, 10356−10365.
(145) Baerends, E. J.; Rosa, A. Metal-CO photodissociation in transition metal complexes: The role of ligand-field and charge-transfer excited states in the photochemical dissociation of metal-ligand bonds. *Coord. Chem. Rev.* **1998**, *177*, 97−125.
(146) Garino, C.; Salassa, L. The photochemistry of transition metal complexes using density functional theory. *Philos. Trans. R. Soc., A* **2013**, *371*, 20120134.
(147) Daniel, C. Photochemistry and photophysics of transition metal complexes: Quantum chemistry. *Coord. Chem. Rev.* **2015**, *282-283*, 19−32.
(148) Kosma, K.; Trushin, S. A.; Fuss, W.; Schmid, W. E.; Schneider, B. M. R. Photodissociation of group-6 hexacarbonyls: Observation of coherent oscillations in an antisymmetric (pseudorotation) vibration in Mo(CO)$_5$ and W(CO)$_5$. *Phys. Chem. Chem. Phys.* **2010**, *12*, 13197−13214.
(149) Paterson, M. J.; Hunt, P. A.; Robb, M. A.; Takahashi, O. Non-adiabatic direct dynamics study of chromium hexacarbonyl photodissociation. *J. Phys. Chem. A* **2002**, *106*, 10494−10504.
(150) Andrews, L.; Cho, H. G.; Wang, X. Reactions of methane with titanium atoms: CH$_3$TiH, CH$_2$═TiH$_2$, agostic bonding, and (CH$_3$)$_2$TiH$_2$. *Inorg. Chem.* **2005**, *44*, 4834−4842.
(151) Cho, H. G.; Wang, X. F.; Andrews, L. Reactions of methane with hafnium atoms: CH$_2$═HfH$_2$, agostic bonding, and (CH$_3$)$_2$HfH$_2$. *Organometallics* **2005**, *24*, 2854−2861.
(152) Cho, H. G.; Wang, X. F.; Andrews, L. The C-H activation of methane by laser-ablated zirconium atoms: CH$_2$═ZrH$_2$, the simplest carbene hydride complex, agostic bonding, and (CH$_3$)$_2$ZrH$_2$. *J. Am. Chem. Soc.* **2005**, *127*, 465−473.
(153) Wang, G. J.; Gong, Y.; Chen, M. H.; Zhou, M. F. Methane activation by titanium monoxide molecules: A matrix isolation infrared spectroscopic and theoretical study. *J. Am. Chem. Soc.* **2006**, *128*, 5974−5980.
(154) Margulieux, G. W.; Semproni, S. P.; Chirik, P. J. Photochemically induced reductive elimination as a route to a zirconocene complex with a strongly activated N$_2$ ligand. *Angew. Chem., Int. Ed.* **2014**, *53*, 9189−9192.
(155) Foust, D. F.; Rogers, R. D.; Rausch, M. D.; Atwood, J. L. Photoinduced reactions of (η^5-C$_5$H$_5$)$_2$MH$_3$ and (η^5-C$_5$H$_5$)$_2$M(CO)H (M = Nb, Ta) and the molecular-structure of (η^5-C$_5$H$_5$)$_2$Ta(CO)H. *J. Am. Chem. Soc.* **1982**, *104*, 5646−5650.
(156) Baynham, R. F. G.; Chetwynd-Talbot, J.; Grebenik, P.; Perutz, R. N.; Powell, M. H. A. Photochemistry of M(η^5-C$_5$H$_5$)$_2$(H)CO and M(η^5-C$_5$H$_5$)$_2$H$_3$ (M = Nb, Ta) in low-temperature matrices. *J. Organomet. Chem.* **1985**, *284*, 229−242.
(157) Braunschweig, H.; Gross, M.; Kraft, K. Synthesis and reactivity of 2-disilaniobocenophanes. *J. Organomet. Chem.* **2011**, *696*, 568−571.
(158) Darensbourg, D. J.; Incorvia, M. J. Solution photochemistry of anionic metal-carbonyl hydride derivatives - substitution and dimer disruption processes in μ-H[M(CO)$_5$]$_2^-$ (M = Cr and W). *Inorg. Chem.* **1979**, *18*, 18−22.
(159) Hynes, R. C.; Preston, K. F.; Springs, J. J.; Williams, A. J. EPR studies of M(CO)$_5^-$ radicals trapped in single-crystals of PPN$^+$HM(CO)$_5^-$. *Organometallics* **1990**, *9*, 2298−2304.
(160) Alt, H. G.; Mahmoud, K. A.; Rest, A. J. Photolysis of the cyclopentadienyl(hydrido) complexes C$_5$H$_5$M(CO)$_3$H (M = Cr, Mo, W) in matrices and in solution - characterization of C$_5$H$_5$W(CO)$_2$H$_2$ and C$_5$Me$_5$W(CO)$_2$H$_2$. *Angew. Chem., Int. Ed. Engl.* **1983**, *22*, 544−545.
(161) Brumas-Soula, B.; Dahan, F.; Poilblanc, R. Transition-metal derivatives of the functionalized cyclopentadienyl ligand. XVI. Synthesis of the bridged complexes [(μ-η^5-C$_5$H$_4$PPh$_2$)M(CO)$_2$]$_2$ (M = Cr, Mo, W). X-ray crystal structure of the dihydride derivative [(μ-η^5-C$_5$H$_4$PPh$_2$)W(CO)$_2$H]$_2$. *New J. Chem.* **1998**, *22*, 15−23.
(162) Mahmoud, K. A.; Rest, A. J.; Alt, H. G. Photochemistry of tricarbonyl (η^5-cyclopentadienyl)hydrido complexes of molybdenum and tungsten and of dicarbonyl(η^5-cyclopentadienyl)(ethylene)-hydridotungsten in solution and in frozen gas matrices at 12 K. *J. Chem. Soc., Dalton Trans.* **1984**, 187−197.
(163) Alt, H. G.; Mahmoud, K. A.; Rest, A. J. Matrix-isolation studies of hydroformylation intermediates - infrared spectroscopic evidence for stepwise substitution of ethylene into (η^5-cyclopentadienyl)tricarbonyl(hydrido)-molybdenum and (η^5-cyclopentadenyl)tri-carbonyl-(hydrido)-tungsten complex followed by insertion into the metal hydrogen-bond. *J. Organomet. Chem.* **1983**, *243*, C5−C9.
(164) Sweany, R. L. Formation of adducts of molecular-hydrogen and dicarbonyl(η^5-cyclopentadienyl)hydridomolybdenum in low-temperature matrices. *Organometallics* **1986**, *5*, 387−388.
(165) Cho, H.-G.; Andrews, L. Infrared spectra and density functional calculations of CH$_2$ = MHX and CH = MH$_2$X complexes prepared in reactions of methyl halides with Mo and W atoms. *J. Phys. Chem. A* **2006**, *110*, 13151−13162.
(166) Sakaba, H.; Ishida, K.; Horino, H. Synthesis of a silylene- and hydride-bridged Re-W heterobimetallic complex and its photolysis to form novel silenyl-bridged heterobimetallic complexes. *Chem. Lett.* **1998**, 149−150.

DOI: 10.1021/acs.chemrev.6b00204
Chem. Rev. 2016, 116, 8506−8544

(167) Alvarez, M. A.; García, M. E.; Ruiz, M. A.; Toyos, A.; Vega, M. F. Heterometallic derivatives of the unsaturated ditungsten hydride $[W_2(\eta^5\text{-}C_5H_5)_2(H)(\mu\text{-}PCy_2)(CO)_2]$. *Inorg. Chem.* **2013**, *52*, 7068−7077.
(168) Xiao, Z. L.; Hauge, R. H.; Margrave, J. L. Reactions and photochemistry of chromium and molybdenum with molecular-hydrogen at 12 K. *J. Phys. Chem.* **1992**, *96*, 636−644.
(169) Geoffroy, G. L.; Bradley, M. G. Photoinduced elimination of H_2 from $Mo(\eta^5\text{-}C_5H_5)_2H_2$ - generation of molybdenocene. *J. Organomet. Chem.* **1977**, *134*, C27−C31.
(170) Berry, M.; Davies, S. G.; Green, M. L. H. Photoinduced synthesis of binuclear molybdenocene and tungstenocene derivatives - catalytic deoxygenation of epoxides by metallocenes. *J. Chem. Soc., Chem. Commun.* **1978**, 99−100.
(171) Grebenik, P.; Downs, A. J.; Green, M. L. H.; Perutz, R. N. Infrared spectroscopic evidence for photo-chemical generation of the metallocenes $(\eta\text{-}C_5H_5)_2M$ (M = Mo or W) in low-temperature matrices. *J. Chem. Soc., Chem. Commun.* **1979**, 742−744.
(172) Perutz, R. N.; Scaiano, J. C. Transient spectroscopy and kinetics of monomeric molybdenocene $Mo(\eta\text{-}C_5H_5)_2$ in solution. *J. Chem. Soc., Chem. Commun.* **1984**, 457−458.
(173) Cloke, F. G. N.; Day, J. P.; Green, J. C.; Morley, C. P.; Swain, A. C. Bis(η-pentamethylcyclopentadienyl) complexes of molybdenum, tungsten and rhenium via metal vapor synthesis. *J. Chem. Soc., Dalton Trans.* **1991**, 789−796.
(174) Baxley, G. T.; Avey, A. A.; Aukett, T. M.; Tyler, D. R. Photoactivation of water by $Cp_2'Mo$ and photochemical studies of Cp_2MoO. Investigation of a proposed water-splitting cycle and preparation of a water-soluble molybdocene dihydride. *Inorg. Chim. Acta* **2000**, *300-302*, 102−112.
(175) Labella, L.; Chernega, A.; Green, M. L. H. Syntheses and reactions of *ansa*-2,2-bis(η-cyclopentadienyl)propane-tungsten and -molybdenum compounds. *J. Chem. Soc., Dalton Trans.* **1995**, 395−402.
(176) Churchill, D. G.; Bridgewater, B. M.; Parkin, G. Modeling aspects of hydrodesulfurization at molybdenum: Carbon-sulfur bond cleavage of thiophenes by *ansa* molybdenocene complexes. *J. Am. Chem. Soc.* **2000**, *122*, 178−179.
(177) Churchill, D. G.; Bridgewater, B. M.; Zhu, G.; Pang, K. L.; Parkin, G. Carbon-hydrogen versus carbon-chalcogen bond cleavage of furan, thiophene and selenophene by *ansa* molybdenocene complexes. *Polyhedron* **2006**, *25*, 499−512.
(178) Braunschweig, H.; Gross, M.; Radacki, K.; Rothgaengel, C. Intramolecular activation of a disila[2]molybdenocenophanedihydride: Synthesis and structure of a [1],[1]metalloarenophane. *Angew. Chem., Int. Ed.* **2008**, *47*, 9979−9981.
(179) Arnold, T.; Braunschweig, H.; Gross, M.; Kaupp, M.; Muller, R.; Radacki, K. Electronic structure and reactivity of a [1],[1]-disilamolybdenocenophane. *Chem. - Eur. J.* **2010**, *16*, 3014−3020.
(180) del Carmen Barral, M.; Green, M. L. H.; Jimenez, R. Photochemical studies on binuclear hydrido-molybdenocene compounds. *J. Chem. Soc., Dalton Trans.* **1982**, 2495−2498.
(181) Bitterwolf, T. E.; Saygh, A.; Haener, J. L.; Fierro, R.; Shade, J. E.; Rheingold, A. L.; Liable-Sands, L.; Alt, H. G. Synthesis and photolysis of $[M(CO)_3H]_2(\eta^5,\eta^5\text{-}C_5H_4CH_2C_5H_4)$, where M = Mo and W. Photochemical 'twist' rearrangement of $M_2(CO)_6(\eta^5,\eta^5\text{-}C_5H_4CH_2C_5H_4)$ to give $[M(CO)_3][M(CO)_3H](\eta^5,\eta^5{:}\eta^1\text{-}C_5H_4CH_2C_5H_3)$, where M = Mo and W. The molecular structure $[Mo(CO)_3][Mo(CO)_3Cl](\eta^5,\eta^5{:}\eta^1\text{-}C_5H_4CH_2C_5H_3)$. *Inorg. Chim. Acta* **2002**, *334*, 54−58.
(182) Carrasco, M.; Curado, N.; Alvarez, E.; Maya, C.; Peloso, R.; Poveda, M. L.; Rodriguez, A.; Ruiz, E.; Alvarez, S.; Carmona, E. Experimental and theoretical studies on arene-bridged metal-metal-bonded dimolybdenum complexes. *Chem. - Eur. J.* **2014**, *20*, 6092−6102.
(183) Elmitt, K.; Green, M. L. H.; Forder, R. A.; Jefferson, I.; Prout, K. Photoinduced insertion of tungsten into a methyl C-H bond in p-xylene and mesitylene - crystal-structure of $(\eta\text{-}C_5H_5)_2WCH_2(3,5\text{-}Me_2C_6H_3)_2$. *J. Chem. Soc., Chem. Commun.* **1974**, 747−748.
(184) Cox, P. A.; Grebenik, P.; Perutz, R. N.; Robinson, M. D.; Grinter, R.; Stern, D. R. Electronic-structure of molybdenocene and tungstenocene - detection of paramagnetism by magnetic circular-dichroism in argon matrices. *Inorg. Chem.* **1983**, *22*, 3614−3620.
(185) Kunkely, H.; Vogler, A. Photochemical hydrogen transfer from bis(i-propylcyclopentadienyl) tungsten dihydride to 9,10-phenanthrenequinone induced by outer sphere charge transfer excitation. *Inorg. Chem. Commun.* **1998**, *1*, 200−202.
(186) Wang, X. F.; Andrews, L. Matrix infrared spectra and density functional theory calculations of molybdenum hydrides. *J. Phys. Chem. A* **2005**, *109*, 9021−9027.
(187) Wang, X. F.; Andrews, L. Neon matrix infrared spectra and DFT calculations of tungsten hydrides WH_x (x = 1-4, 6). *J. Phys. Chem. A* **2002**, *106*, 6720−6729.
(188) Kang, S. K.; Albright, T. A.; Eisenstein, O. The structure of d^0 ML_6 complexes. *Inorg. Chem.* **1989**, *28*, 1611−1613.
(189) Wang, X. F.; Andrews, L.; Infante, I.; Gagliardi, L. Infrared spectra of the $WH_4(H_2)_4$ complex in solid hydrogen. *J. Am. Chem. Soc.* **2008**, *130*, 1972−1978.
(190) Dziegielewski, J. O.; Gilbortnowska, R.; Mrzigod, J.; Malecki, J. G. Hydride complexes of tungsten in photocatalytic dinitrogen reduction. *Polyhedron* **1995**, *14*, 1375−1379.
(191) Pivovarov, A. P.; Ioffe, L. M.; Gak, Y. V.; Makhaev, V. D.; Borisov, A. P.; Borod'ko, Yu. G. Intramolecular hydrogen transfer from the alkyl substituent of a phosphine ligand to a metal atom upon the irradiation of tungsten phosphine hydride complexes. *Bull. Acad. Sci. USSR, Div. Chem. Sci.* **1987**, *36*, 928−930.
(192) Shima, T.; Hou, Z. Heterometallic polyhydride complexes containing yttrium hydrides with different Cp ligands: Synthesis, structure, and hydrogen-uptake/release properties. *Chem. - Eur. J.* **2013**, *19*, 3458−3466.
(193) Church, S. P.; Poliakoff, M.; Timney, J. A.; Turner, J. J. Synthesis and characterization of the pentacarbonylmanganese(0) radical, $Mn(CO)_5$, in low-temperature matrices. *J. Am. Chem. Soc.* **1981**, *103*, 7515−7520.
(194) Fairhurst, S. A.; Morton, J. R.; Perutz, R. N.; Preston, K. F. EPR spectra of $KrMn(CO)_5$ and $KrFe(CO)_5^+$ in a krypton matrix. *Organometallics* **1984**, *3*, 1389−1391.
(195) Frigyes, D.; Fogarasi, G. Isomers of manganese tetracarbonyl hydride: A density functional study of structure and vibrational spectra. *Organometallics* **1999**, *18*, 5245−5251.
(196) Clarke, M. J.; Howdle, S. M.; Jobling, M.; Poliakoff, M. Solvent-free impregnation of dinuclear metal-complexes into polyethylene - use of supercritical CO_2 and the in-situ photochemical assembly of $Mn_2(CO)_{10}$ from $HMn(CO)_5$. *Inorg. Chem.* **1993**, *32*, 5643−5644.
(197) Albertin, G.; Antoniutti, S.; Bettiol, M.; Bordignon, E.; Busatto, F. Synthesis, characterization, and reactivity of cationic molecular hydrogen complexes of manganese(I). *Organometallics* **1997**, *16*, 4959−4969.
(198) Bogdan, P. L.; Sullivan, P. J.; Donovan, T. A.; Atwood, J. D. Photocatalysis of hydrogenation and isomerization of alkenes by *cis*-$HMn(CO)_4PPh_3$. *J. Organomet. Chem.* **1984**, *269*, C51−C54.
(199) Karch, R.; Schubert, U. Transition metal silyl complexes part 54. Hydrido disilanyl complexes $L_nM(H)SiR_2SiR_2H$ (L_nM = $MeCp(CO)_2Mn$, $Cp(CO)_2Re$, $(CO)_3(PPh_3)Fe$). *Inorg. Chim. Acta* **1997**, *259*, 151−160.
(200) Guillaumont, D.; Daniel, C. A quantum chemical investigation of the metal-to-ligand charge-transfer photochemistry. *Coord. Chem. Rev.* **1998**, *177*, 181−199.
(201) Chetwynd-Talbot, J.; Grebenik, P.; Perutz, R. N. Photochemistry of $(\eta\text{-}C_5H_5)_2ReH$ and $(\eta\text{-}C_5H_5)(\eta^2\text{-}C_5H_6)Re(CO)_2$ in low-temperature matrices - hydrogen loss and hydrogen migration. *J. Chem. Soc., Chem. Commun.* **1981**, 452−454.
(202) Chetwynd-Talbot, J.; Grebenik, P.; Perutz, R. N.; Powell, M. H. A. Photochemical studies of rhenium η-cyclopentadienyl complexes in matrices and in solution - detection of rhenocene and mechanisms of hydrogen transfer. *Inorg. Chem.* **1983**, *22*, 1675−1684.
(203) Cox, P. A.; Grebenik, P.; Perutz, R. N.; Graham, R. G.; Grinter, R. Rhenocene - magnetic circular-dichroism and laser-induced fluorescence in nitrogen matrices. *Chem. Phys. Lett.* **1984**, *108*, 415−419.

DOI: 10.1021/acs.chemrev.6b00204
Chem. Rev. 2016, 116, 8506−8544

(204) Bossert, J.; Ben Amor, N.; Strich, A.; Daniel, C. Electronic spectroscopy of $HRe(CO)_5$: A CASSCF/CASPT2 and TD-DFT study. *Chem. Phys. Lett.* **2001**, *342*, 617−624.
(205) Albertin, G.; Antoniutti, S.; Garcia-Fontan, S.; Carballo, R.; Padoan, F. Preparation, characterisation and reactivity of a series of classical and non-classical rhenium hydride complexes. *J. Chem. Soc., Dalton Trans.* **1998**, 2071−2081.
(206) Bolano, S.; Bravo, J.; Castro, J.; del Carmen Marin, M.; Garcia-Fontan, S. Synthesis, characterization and crystal structure of *cis,mer*-$ReH(CO)_2\{PPh(OMe)_2\}_3$. *Inorg. Chem. Commun.* **2009**, *12*, 916−918.
(207) Jones, W. D.; Fan, M. Activation of C-H bonds by rhenium. Catalytic intermolecuar H/D exchange with $(\eta^6\text{-}C_6H_6)Re(PPh_3)_2H$. *Organometallics* **1986**, *5*, 1057−1059.
(208) Menon, R. K.; Brown, T. L. Excited-state properties of (μ-pyridyl)(μ-hydrido)dirhenium octacarbonyl and related dirhenium carbonyl-complexes. *Inorg. Chem.* **1989**, *28*, 1370−1379.
(209) Ball, R. G.; Campen, A. K.; Graham, W. A. G.; Hamley, P. A.; Kazarian, S. G.; Ollino, M. A.; Poliakoff, M.; Rest, A. J.; Sturgeoff, L.; Whitwell, I. Synthesis, x-ray crystal structure and photochemistry of (η^5-pentamethylcyclopentadienyl) (dicarbonyl) (dihydrido)rhenium in cyclohexane and liquid xenon solutions and in low temperature media at about 12 K. *Inorg. Chim. Acta* **1997**, *259*, 137−149.
(210) Epstein, R. A.; Gaffney, T. R.; Geoffroy, G. L.; Gladfelter, W. L.; Henderson, R. S. Photoinduced fragmentation of $H_3Re_3(CO)_{12}$ and $H_3Mn_3(CO)_{12}$. *J. Am. Chem. Soc.* **1979**, *101*, 3847−3852.
(211) Roberts, D. R.; Geoffroy, G. L.; Bradley, M. G. Reversible insertion of CO_2 into the Re-H bond of photogenerated $ReH(Ph_2PCH_2CH_2PPh_2)_2$. *J. Organomet. Chem.* **1980**, *198*, C75−C78.
(212) Bradley, M. G.; Roberts, D. A.; Geoffroy, G. L. Photogeneration of reactive $ReH(diphos)_2$ - its reversible coordination of CO_2 and activation of aromatic C-H bonds. *J. Am. Chem. Soc.* **1981**, *103*, 379−384.
(213) Perthuisot, C.; Fan, M. X.; Jones, W. D. Catalytic thermal C-H activation with manganese complexes - evidence for η^2-H_2 coordination in a neutral manganese complex and its role in C-H activation. *Organometallics* **1992**, *11*, 3622−3629.
(214) Roberts, D. A.; Geoffroy, G. L. Definitive examples of polyhydride complexes which do not eliminate H_2 in the primary photochemical-reaction - photo-dissociation of PR_3 from $ReH_3(PR_3)_4$ and $ReH_5(Pr_3)_3$ complexes. *J. Organomet. Chem.* **1981**, *214*, 221−231.
(215) Bergamo, M.; Beringhelli, T.; D'Alfonso, G.; Garavaglia, L.; Mercandelli, P.; Moret, M.; Sironi, A. Hydrido-carbonyl rhenium clusters with a square geometry of the metal core. Synthesis and x-ray characterization of the novel $Re_4(\mu\text{-}H)_3(CO)_{16}^-$ anion. *J. Cluster Sci.* **2001**, *12*, 223−242.
(216) Adams, R. D.; Captain, B.; Smith, M. D.; Beddie, C.; Hall, M. B. Unsaturated platinum-rhenium cluster complexes. Synthesis, structures and reactivity. *J. Am. Chem. Soc.* **2007**, *129*, 5981−5991.
(217) Geoffroy, G. L.; Epstein, R. A. Photoinduced de-clusterification of $HCCo_3(CO)_9$, $CH_3CCo_3(CO)_9$, and $HFeCo_3(CO)_{12}$. *Inorg. Chem.* **1977**, *16*, 2795−2799.
(218) Geoffroy, G. L.; Bradley, M. G. Photochemical generation of chlorohydridotristriphenylphosphineruthenium, $RuHCl(PPh_3)_3$. *J. Chem. Soc., Chem. Commun.* **1976**, 20−21.
(219) Geoffroy, G. L.; Bradley, M. G. Photochemistry of transition-metal hydride complexes 2. $RuClH(CO)(PPh_3)_3$, $RuH_2(CO)(PPh_3)_3$, and $RuClH(CO)_2(PPh_3)_2$. *Inorg. Chem.* **1977**, *16*, 744−748.
(220) Hoyano, J. K.; Graham, W. A. G. Hydrogen-mediated photolysis of (η-C_5Me_5)$Os(CO)_2H$ - synthesis of (η-C_5Me_5)$Os(CO)H_3$ and multiply bonded diosmium compounds. *J. Am. Chem. Soc.* **1982**, *104*, 3722−3723.
(221) McCamley, A.; Perutz, R. N.; Stahl, S.; Werner, H. Intermolecular and intramolecular photochemical C-H activation in matrices and in solution with (η^6-arene)(carbonyl)osmium complexes. *Angew. Chem., Int. Ed. Engl.* **1989**, *28*, 1690−1692.
(222) Hayes, P. G.; Gribble, C. W.; Waterman, R.; Tilley, T. D. A hydrogen-substituted osmium stannylene complex: Isomerization to a metallostannylene complex via an unusual α-hydrogen migration from tin to osmium. *J. Am. Chem. Soc.* **2009**, *131*, 4606−4607.
(223) Baker, M. V.; Field, L. D. Reaction of sp^2 C-H bonds in unactivated alkenes with bis(diphosphine) complexes of iron. *J. Am. Chem. Soc.* **1986**, *108*, 7433−7434.
(224) Baker, M. V.; Field, L. D. Reaction of ethylene with a coordinatively unsaturated iron complex, $Fe(depe)_2$ - sp^2 C-H bond activation without prior formation of a π-complex. *J. Am. Chem. Soc.* **1986**, *108*, 7436−7438.
(225) Baker, M. V.; Field, L. D. Reaction of C-H bonds in alkanes with bis(diphosphine) complexes of iron. *J. Am. Chem. Soc.* **1987**, *109*, 2825−2826.
(226) Buys, I. E.; Field, L. D.; Hambley, T. W.; McQueen, A. E. D. Photochemical-reactions of cis-$Fe(H)_2(Me_2PCH_2CH_2PMe_2)_2$ with thiophenes - insertion into C-H and C-S bonds. *J. Chem. Soc., Chem. Commun.* **1994**, 557−558.
(227) Field, L. D.; George, A. V.; Messerle, B. A. Methane activation by an iron phosphine complex in liquid xenon solution. *J. Chem. Soc., Chem. Commun.* **1991**, 1339−1341.
(228) Baker, M. V.; Field, L. D. Cyclometallation reactions in the $Fe(dprpe)_2$ system [dprpe = 1,2-bis(dipropylphosphino)ethane]. *Aust. J. Chem.* **1999**, *52*, 1005−1011.
(229) Pelton, E. J.; Blank, D. A.; McNeill, K. Dechlorination of chlorinated ethylenes by a photochemically generated iron(0) complex. *Dalton Trans.* **2013**, *42*, 10121−10128.
(230) Harvey, J. N.; Poli, R. Computational study of the spin-forbidden H_2 oxidative addition to 16-electron Fe(0) complexes. *Dalton Trans.* **2003**, 4100−4106.
(231) Poli, R. Open shell organometallics: A general analysis of their electronic structure and reactivity. *J. Organomet. Chem.* **2004**, *689*, 4291−4304.
(232) Ozin, G. A.; McCaffrey, J. G. The photoreversible oxidative-addition, reductive-elimination reactions Fe+H_2 reversible-FeH_2 in low-temperature matrices. *J. Phys. Chem.* **1984**, *88*, 645−648.
(233) Ozin, G. A.; McCaffrey, J. G.; Parnis, J. M. Photochemistry of transition-metal atoms - reactions with molecular-hydrogen and methane in low-temperature matrices. *Angew. Chem., Int. Ed. Engl.* **1986**, *25*, 1072−1085.
(234) Rubinovitz, R. L.; Nixon, E. R. The photochemical Fe+H_2 reaction in Ar-matrix and Kr-matrix by irradiation in the visible region. *J. Phys. Chem.* **1986**, *90*, 1940−1944.
(235) Chertihin, G. V.; Andrews, L. Infrared-spectra of FeH, FeH_2, and FeH_3 in solid argon. *J. Phys. Chem.* **1995**, *99*, 12131−12134.
(236) Mawby, R. J.; Perutz, R. N.; Whittlesey, M. K. Matrix photochemistry of $Ru(CO)_2(PMe_3)_2H_2$ and $Ru(CO)_3(PMe_3)_2$ - formation of $Ru(CO)_2(PMe_3)_2\cdots S$ (S═Ar, CH_4, Xe). *Organometallics* **1995**, *14*, 3268−3274.
(237) (a) Burn, M. J.; Bergman, R. G. A study of the silanolysis of triphenylsilane and *p*-methoxyphenol catalyzed by $(PMe_3)_4RuH_2$ and the stoichiometric reactions of $(PMe_3)_4Ru(H)(OC_6H_4\text{-}p\text{-}X)$ (X = Me, OMe) with Ph_3SiH. *J. Organomet. Chem.* **1994**, *472*, 43−54. (b) Procopio, L. J.; Berry, D. H. Dehydrogenative coupling of trialkylsilanes mediated by ruthenium phosphine complexes - catalytic synthesis of carbosilanes. *J. Am. Chem. Soc.* **1991**, *113*, 4039−4040.
(238) Morton, D.; Cole-Hamilton, D. J.; Utuk, I. D.; Panequesosa, M.; Lopezpoveda, M. Hydrogen-production from ethanol catalyzed by group-8 metal-complexes. *J. Chem. Soc., Dalton Trans.* **1989**, 489−495.
(239) Kletzin, H.; Werner, H. Aryl(hydrido)ruthenium complexes by C-H addition - isolation of a 4-membered metallacycle as intermediate. *Angew. Chem., Int. Ed. Engl.* **1983**, *22*, 873−874.
(240) Morris, R. H.; Shiralian, M. Benzene carbon-hydrogen bond activation using $Ru(C_6Me_6)[PH(C_6H_{11})_2]H_2$. *J. Organomet. Chem.* **1984**, *260*, C47−C51.
(241) Hartwig, J. F.; Andersen, R. A.; Bergman, R. G. Alkyl, aryl, hydrido, and acetate complexes of $(dmpm)_2Ru$ [dmpm = bis-(dimethylphosphino)methane]: reductive elimination and oxidative addition of C-H bonds. *Organometallics* **1991**, *10*, 1710−1719.
(242) Field, L. D.; Wilkinson, M. P. Synthesis and reactions of dihydridobis 1,2-bis(bis(trifluoromethyl)phosphino)ethane ruthenium-(II), $RuH_2(dfmpe)_2$. *Organometallics* **1997**, *16*, 1841−1845.

DOI: 10.1021/acs.chemrev.6b00204
Chem. Rev. 2016, 116, 8506−8544

(243) Bianchini, C.; Casares, J. A.; Osman, R.; Pattison, D. I.; Peruzzini, M.; Perutz, R. N.; Zanobini, F. C-H bond cleavage in thiophenes by $P(CH_2CH_2PPh_2)_3Ru$. UV flash kinetic spectroscopy discloses the ruthenium-thiophene adduct which precedes C-H insertion. *Organometallics* **1997**, *16*, 4611−4619.
(244) Boddien, A.; Loges, B.; Gartner, F.; Torborg, C.; Fumino, K.; Junge, H.; Ludwig, R.; Beller, M. Iron-catalyzed hydrogen production from formic acid. *J. Am. Chem. Soc.* **2010**, *132*, 8924−8934.
(245) Burkhardt, E. W.; Geoffroy, G. L. Photoassisted synthesis of mixed-metal clusters - PPN $CoOs_3(CO)_{13}$, $H_2RuOs_3(CO)_{13}$, and $H_2FeOs_3(CO)_{13}$. *J. Organomet. Chem.* **1980**, *198*, 179−188.
(246) Kiel, W. A.; Ball, R. G.; Graham, W. A. G. Carbonyl-η-hexamethylbenzene complexes of osmium. Carbon-hydrogen activation by $(\eta$-$C_6Me_6)Os(CO)(H)_2$. *J. Organomet. Chem.* **1990**, *383*, 481−496.
(247) Graff, J. L.; Wrighton, M. S. Photochemistry and photocatalytic activity of a polynuclear metal carbonyl hydride: dodecacarbonyltetrahydridotetraruthenium. *J. Am. Chem. Soc.* **1980**, *102*, 2123−2125.
(248) Bentsen, J. G.; Wrighton, M. S. Photochemistry of $H_4Ru_4(CO)_{12}$ in rigid alkane matrices at low-temperature - spectroscopic detection and characterization of coordinatively unsaturated $H_4Ru_4(CO)_{11}$. *J. Am. Chem. Soc.* **1984**, *106*, 4041−4043.
(249) Nakajima, T.; Shimizu, I.; Kobayashi, K.; Wakatsuki, Y. Synthesis of triangular and tetrahedral heteronuclear metal clusters using hydride complexes of cyclopentadienylrhodium and -ruthenium as the precursors. *Organometallics* **1998**, *17*, 262−269.
(250) Sweany, R. L. Photolysis of matrix-isolated hydridotetracarbonylcobalt(I) - evidence for metal-hydrogen bond homolysis. *Inorg. Chem.* **1980**, *19*, 3512−3516.
(251) Sweany, R. L. Photolysis of matrix-isolated hydridotetracarbonylcobalt(I) - comparison of the probabilities of carbonyl loss with hydrogen-atom loss. *Inorg. Chem.* **1982**, *21*, 752−756.
(252) Daniel, C.; Heitz, M. C.; Lehr, L.; Schroder, T.; Warmuth, B. Dynamics of photochemical-reactions - simulation by quantum calculations for transition-metal hydrides. *Int. J. Quantum Chem.* **1994**, *52*, 71−88.
(253) Heitz, M. C.; Ribbing, C.; Daniel, C. Spin-orbit induced radiationless transitions in organometallics: Quantum simulation of the intersystem crossing processes in the photodissociation of $HCo(CO)_4$. *J. Chem. Phys.* **1997**, *106*, 1421−1428.
(254) Sweany, R. L. Evidence for tricarbonyltrihydridocobalt(III) - synthesis from tricarbonylhydridocobalt(I) in matrices. *J. Am. Chem. Soc.* **1982**, *104*, 3739−3740.
(255) Sweany, R. L.; Russell, F. N. Photolysis of tetracarbonylmethylcobalt(I) and tetracarbonylhydridocobalt(I) in inert-gas and hydrogen-containing matrices - the reaction of 16-electron, coordinatively unsaturated complexes with dihydrogen. *Organometallics* **1988**, *7*, 719−727.
(256) Endicott, J. F.; Wong, C. L.; Inoue, T.; Natarajan, P. Photoinduced oxygenation of trans-aquohydridotetraamminerhodium-(III) - evidence for a transition-metal chain carrier. *Inorg. Chem.* **1979**, *18*, 450−454.
(257) Bakac, A.; Thomas, L. M. Macrocyclic rhodium(III) hydrides and a monomeric rhodium(II) complex. *Inorg. Chem.* **1996**, *35*, 5880−5884.
(258) Moriyama, H.; Yabe, A.; Matsui, F. Photoenhanced homogeneous catalytic hydrogenation of olefins following XeCl excimer laser excitation of $RhH(CO)(PPh_3)_3$. *J. Mol. Catal.* **1989**, *50*, 195−202.
(259) Yoshida, T.; Okano, T.; Otsuka, S. Activation of water-molecules. 4. Generation of dihydrogen from water by rhodium(I) hydrido and rhodium(0) carbonyl-compounds. *J. Am. Chem. Soc.* **1980**, *102*, 5966−5967.
(260) (a) Bell, T. W.; Haddleton, D. M.; McCamley, A.; Partridge, M. G.; Perutz, R. N.; Willner, H. Photochemical isomerization of metal ethene to metal vinyl hydride complexes - a matrix-isolation and solution NMR-study. *J. Am. Chem. Soc.* **1990**, *112*, 9212−9226. (b) Fox, D. J.; Duckett, S. B.; Flaschenriem, C.; Brennessel, W. W.; Schneider, J.; Gunay, A.; Eisenberg, R. A model iridium hydroformylation system with the large bite angle ligand xantphos: Reactivity with parahydrogen and implications for hydroformylation catalysis. *Inorg. Chem.* **2006**, *45*, 7197−7209.
(261) (a) Jones, W. D.; Feher, F. J. The mechanism and thermodynamics of alkane and arene carbon-hydrogen bond activation in $(C_5Me_5)Rh(PMe_3)(R)H$. *J. Am. Chem. Soc.* **1984**, *106*, 1650−1663. (b) Jones, W. D.; Feher, F. J. Isotope effects in arene C-H bond activation by $(C_5Me_5)Rh(PMe_3)$. *J. Am. Chem. Soc.* **1986**, *108*, 4814−4819.
(262) Periana, R. A.; Bergman, R. G. Rapid intramolecular rearrangement of a hydridocyclopropylrhodium complex to a rhodacyclobutane - independent synthesis of the metallacycle by addition of hydride to the central carbon-atom of a cationic rhodium pi-allyl complex. *J. Am. Chem. Soc.* **1984**, *106*, 7272−7273.
(263) Periana, R. A.; Bergman, R. G. Oxidative addition of rhodium to alkane C-H bonds - enhancement in selectivity and alkyl group functionalization. *Organometallics* **1984**, *3*, 508−510.
(264) Periana, R. A.; Bergman, R. G. Isomerization of the hydridoalkylrhodium complexes formed on oxidative addition of rhodium to alkane C-H bonds - evidence for the intermediacy of η^2-alkane complexes. *J. Am. Chem. Soc.* **1986**, *108*, 7332−7346.
(265) Periana, R. A.; Bergman, R. G. C-C activation of organic small ring compounds by rearrangement of cycloalkylhydridorhodium complexes to rhodacycloalkanes - synthesis of metallacyclobutanes, including one with a tertiary M-C bond, by nucleophilic-addition to π-allyl complexes. *J. Am. Chem. Soc.* **1986**, *108*, 7346−7355.
(266) Perutz, R. N.; Sabo-Etienne, S. The sigma-cam mechanism: Sigma complexes as the basis of sigma-bond metathesis at late-transition-metal centers. *Angew. Chem., Int. Ed.* **2007**, *46*, 2578−2592.
(267) Evans, M. E.; Li, T.; Jones, W. D. C-H vs C-C bond activation of acetonitrile and benzonitrile via oxidative addition: Rhodium vs nickel and Cp* vs Tp′ (Tp′ = hydrotris(3,5-dimethylpyrazol-1-yl)borate, Cp* = η^5-pentamethylcyclopentadienyl. *J. Am. Chem. Soc.* **2010**, *132*, 16278−16284.
(268) Wick, D. D.; Jones, W. D. Synthesis, characterization, and C-H/C-C cleavage reactions of two rhodium-trispyrazolylborate dihydrides. *Inorg. Chim. Acta* **2009**, *362*, 4416−4421.
(269) Tanabe, T.; Brennessel, W. W.; Clot, E.; Eisenstein, O.; Jones, W. D. Synthesis, structure, and reductive elimination in the series $Tp'Rh(PR_3)(Ar^F)H$; determination of rhodium-carbon bond energies of fluoroaryl substituents. *Dalton Trans.* **2010**, *39*, 10495−10509.
(270) Tanabe, T.; Evans, M. E.; Brennessel, W. W.; Jones, W. D. C-H and C-CN bond activation of acetonitrile and succinonitrile by $Tp'Rh(PR_3)$. *Organometallics* **2011**, *30*, 834−843.
(271) Wink, D. A.; Ford, P. C. A flash-photolysis investigation of dihydrogen elimination from phosphine complexes of iridium(III) and rhodium(III): $H_2IrCl(CO)(PPh_3)_2$, $H_2IrCl(PPh_3)_3$, and $H_2RhCl(PPh_3)_3$. *J. Am. Chem. Soc.* **1986**, *108*, 4838−4842.
(272) Itagaki, H.; Murayama, H.; Saito, Y. Photocatalysis of $RhCl(PCy_3)_2$ for cyclohexane dehydrogenation - thermal-dissociation of C-H bond and photoelimination of H_2. *Bull. Chem. Soc. Jpn.* **1994**, *67*, 1254−1257.
(273) Geoffroy, G. L.; Hammond, G. S.; Gray, H. B. Photochemical reductive elimination of oxygen, hydrogen, and hydrogen chloride from iridium complexes. *J. Am. Chem. Soc.* **1975**, *97*, 3933−3936.
(274) Geoffroy, G. L.; Pierantozzi, R. Photochemistry of transition-metal hydride complexes. 1. Photoinduced elimination of molecular-hydrogen from $[IrClH_2(PPh_3)_3]$ and $[IrH_3(PPh_3)_3]$. *J. Am. Chem. Soc.* **1976**, *98*, 8054−8059.
(275) Schultz, R. H. Unusual behavior in the 308 nm flash photolysis of Vaska's complex. *J. Organomet. Chem.* **2003**, *688*, 1−4.
(276) Janowicz, A. H.; Bergman, R. G. C-H activation in completely saturated-hydrocarbons - direct observation of M + R-H→M(R)(H). *J. Am. Chem. Soc.* **1982**, *104*, 352−354.
(277) Bergman, R. G. Activation of alkanes with organotransition metal-complexes. *Science* **1984**, *223*, 902−908.
(278) Janowicz, A. H.; Bergman, R. G. Activation of C-H-bonds in saturated-hydrocarbons on photolysis of $(\eta^5$-$C_5Me_5)(PMe_3)IrH_2$ - relative rates of reaction of the intermediate with different types of C-H-

DOI: 10.1021/acs.chemrev.6b00204
Chem. Rev. 2016, 116, 8506−8544

bonds and functionalization of the metal-bound alkyl-groups. *J. Am. Chem. Soc.* **1983**, *105*, 3929−3939.
(279) Sponsler, M. B.; Weiller, B. H.; Stoutland, P. O.; Bergman, R. G. Liquid xenon - an effective inert solvent for C-H oxidative addition-reactions. *J. Am. Chem. Soc.* **1989**, *111*, 6841−6843.
(280) Peterson, T. H.; Golden, J. T.; Bergman, R. G. Evidence for the intervention of different C-H activating intermediates in the irradiation of (η^5-C_5Me_5)(PMe_3)IrH_2 and the reaction of (η^5-C_5Me_5)(PMe_3)Ir-(H)(Cl) with strong base. Detection and spectroscopic characterization of (η^5-C_5Me_5)(PMe_3)Ir(Li)(Cl), an intermediate in the dehydrohalogenation reaction. *J. Am. Chem. Soc.* **2001**, *123*, 455−462.
(281) Foo, T.; Bergman, R. G. Synthesis and C-H activation reactions of (η^5-indenyl) (trimethylphosphine)iridium alkyl and hydride complexes. *Organometallics* **1992**, *11*, 1801−1810.
(282) Bloyce, P. E.; Rest, A. J.; Whitwell, I.; Graham, W. A. G.; Holmes-Smith, R. Photoactivation of alkanes by carbonyl(η^5-cyclopentadienyl)-dihydridoiridium: solution and matrix-isolation studies. *J. Chem. Soc., Chem. Commun.* **1988**, 846−848.
(283) Crowfoot, L.; Ozin, G. A.; Ozkar, S. Intrazeolite carbonyl(η^5-cyclopentadienyl)dihydridoiridium(III) ($CpIr(CO)H_2$-$M_{56}Y$, where M = H, Li, Na, K, Rb, and Cs). *J. Am. Chem. Soc.* **1991**, *113*, 2033−2040.
(284) Burk, M. J.; Crabtree, R. H.; McGrath, D. V. Thermal and photochemical catalytic dehydrogenation of alkanes with $IrH_2(CF_3CO_2)(PR_3)_2$ (R = C_6H_4F-p and cyclohexyl). *J. Chem. Soc., Chem. Commun.* **1985**, 1829−1830.
(285) Gerard, H.; Eisenstein, O.; Lee, D. H.; Chen, J. Y.; Crabtree, R. H. Unifying the mechanisms for alkane dehydrogenation and alkene H/D exchange with $IrH_2(O_2CCF_3)(PAr_3)_2$: The key role of CF_3CO_2 in the "sticky" alkane route. *New J. Chem.* **2001**, *25*, 1121−1131.
(286) Ferrari, A.; Polo, E.; Ruegger, H.; Sostero, S.; Venanzi, L. M. Photochemistry of dihydrido(hydrotris(3,5-dimethylpyrazolyl)borato)-(*Z*-cyclooctene)iridium. Synthetic intermediates and mechanism of the photochemical formation of hydridophenyl(hydrotris(3,5-dimethylpyrazolyl)borato) (trimethyl phosphite)iridium. *Inorg. Chem.* **1996**, *35*, 1602−1608.
(287) Sweany, R. L.; Polito, M. A.; Moroz, A. Photolysis of tetracarbonylnickel in dihydrogen-containing matrices - evidence for the formation of a complex of molecular-hydrogen. *Organometallics* **1989**, *8*, 2305−2308.
(288) Sostero, S.; Traverso, O.; Ros, R.; Michelin, R. A. Photoinduced reductive elimination of cyanoalkanes from hydridocyanoalkyl complexes of platinum(II). *J. Organomet. Chem.* **1983**, *246*, 325−329.
(289) Clark, H. C.; Ferguson, G.; Hampden-Smith, M. J.; Ruegger, H.; Ruhl, B. L. The chemistry of platinum hydrides. Part XXX. The chemical and structural effects of steric overcrowding in the compounds *cis*- and *trans*-H[R_3Sn]$Pt(PCy_3)_2$, R = Ph, Cl. *Can. J. Chem.* **1988**, *66*, 3120−3127.
(290) Chan, D.; Duckett, S. B.; Heath, S. L.; Khazal, I. G.; Perutz, R. N.; Sabo-Etienne, S.; Timmins, P. L. Platinum bis(tricyclohexylphosphine) silyl hydride complexes. *Organometallics* **2004**, *23*, 5744−5756.
(291) Brown, M. P.; Cooper, S. J.; Frew, A. A.; Manojlovicmuir, L.; Muir, K. W.; Puddephatt, R. J.; Thomson, M. A. The di-μ-bis(diphenylphosphino)methane-μ-hydrido-bis[methylplatinum(II)]-cation: synthesis, molecular-structure, and chemical-properties. *J. Chem. Soc., Dalton Trans.* **1982**, 299−305.
(292) Boaretto, R.; Sostero, S.; Traverso, O. Photochemistry of platinum phosphine complexes. Perspective in C-H bond activation. *Inorg. Chim. Acta* **2002**, *330*, 59−62.
(293) Cho, H.-G.; Andrews, L. Infrared spectra of CH_3-MH, CH_3-M, and CH_3-MH- prepared via methane activation by laser-ablated Au, Ag, and Cu atoms. *Dalton Trans.* **2011**, *40*, 11115−11124.
(294) Dhayal, R. S.; Liao, J.-H.; Lin, Y.-R.; Liao, P.-K.; Kahlal, S.; Saillard, J.-Y.; Liu, C. W. A nanospheric polyhydrido copper cluster of elongated triangular orthobicupola array: Liberation of H_2 from solar energy. *J. Am. Chem. Soc.* **2013**, *135*, 4704−4707.
(295) Girod, M.; Krstic, M.; Antoine, R.; MacAleese, L.; Lemoine, J.; Zavras, A.; Khairallah, G. N.; Bonacic-Koutecky, V.; Dugourd, P.; O'Hair, R. A. J. Formation and characterisation of the silver hydride nanocluster cation $Ag_3H_2((Ph_2P)_2CH_2)^+$ and its release of hydrogen. *Chem. - Eur. J.* **2014**, *20*, 16626−16633.

DOI: 10.1021/acs.chemrev.6b00204
Chem. Rev. 2016, 116, 8506−8544